

A NOVEL CLASS OF TOPOISOMERASE II POISONS
CONTAINING IRON AND RUTHENIUM: ANTICANCER
ACTIVITY AND TARGETED DELIVERY

A thesis submitted for the degree of
DOCTOR OF PHILOSOPHY

by

Y. N. VASHISHT GOPAL



Department of Biochemistry
School of Life Sciences
University of Hyderabad
Hyderabad 500 046
A.P., INDIA

February 2000
Enrollment Number: 95LBPH02



University of Hyderabad

School of Life Sciences,

Department of Biochemistry

Hyderabad 500046 INDIA

DECLARATION

I hereby declare that the work presented in my thesis is entirely original and was carried out by me in the Department of Biochemistry, University of Hyderabad, under the supervision of Dr. Anand K. Kondapi. I further declare that this work has not been submitted before for the award of degree or diploma from any institution or university.

Date: 15-2-2000

Y. N. Vashisht Gopal

Dr. Anand K. Kondapi

Dr. Anand K. Kondapi

Lecturer

School of Life Sciences

University of Hyderabad

Hyderabad-500 134, India.



University of Hyderabad

School of Life Sciences,

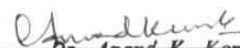
Department of Biochemistry

Hyderabad 500046 INDIA

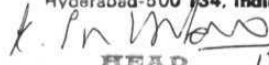
CERTIFICATE

This is to certify that this thesis entitled "*A Novel Class of Topoisomerase II Poisons containing Iron and Ruthenium: Anticancer Activity and Targeted Delivery*" submitted to the University of Hyderabad by Mr. **Y. N. Vashisht Gopal** for the degree of *Doctor of Philosophy*, is based on the studies carried out by him under my supervision. This work has not been submitted before for the award of degree or diploma from any University or institution.

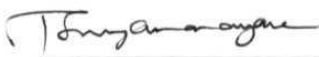
Dr. Anand K. Kondapi
supervisor


Dr. Anand K. Kondapi
Lecturer
School of Life Sciences
University of Hyderabad
Hyderabad-500 134, India.

Prof. K. Subba Rao
Head,
Department of Biochemistry


HEAD 15/2/00
Department of Biochemistry
School of Life Sciences,
University of Hyderabad,
HYDERABAD-500 134 (A.P.)

Prof. R. P. Sharma
Dean,
School of Life Sciences


15/2/00

DEAN
School of Life Sciences
University of Hyderabad
Hyderabad-500 046

Acknowledgment

*I express my deepest sense of gratitude to my research **supervisor, Dr. Anand K. Kondapi** for his guidance and foresight in making me step **into** this exciting and uncharted area of targeted drug development.*

*I wish to thank **Dr. M. Ramanadham, Dr. K. V. A. Ramaiah, Dr. N. Siva Kumar and Dr. O.H. S** hefty for the help rendered to me and letting me use their laboratory facilities. I thank **Prof. K. Subba Rao, Head, Dept. of Biochemistry, Prof. R.P. Sharma, Dean, School of Life Sciences** for providing me the **necessary** research facilities. My special thanks to the former Head, **Prof. T. Suryanarayana** for his advice.*

***I wish** to acknowledge the Council for Scientific and Industrial Research, Department of Science and Technology and the University Grants Commission for financial assistance.*

*My gratitude to **Prof. B.K. Keppler, Dept. of Inorganic Chemistry, University of Heidelberg**, for the generous gift of two metal complexes for my work. My thanks to **Prof. E.D. Jemmis, Dept. of Chemistry, University of Hyderabad**, for allowing me to use his SGI workstations for molecular modeling analysis.*

*My gratitude to **Ms. C. Subbalaxmi and Shraddha (C.C.M.B.)** for helping me with **CD. spectroscopy** studies. Without big Ram, things would have been very different for me. Small Ram too was very **helpful**. I owe a lot to **Dr. K. Srinivas, Pankaz and Ashwini**.*

*I am very grateful to **Pattabhi sir and V. enkataiah** for their help and understanding. I am also thankful to **Mr. Nageshwar Rao, Gopi kaka and Jaggu dada**. **The** animal house attendants have been very cooperative.*

*My heartfelt gratitude to **Pavan** for his never failing friendship, who was always there when I needed help. Ditto for **Gautam**, my non-blood brother. **Rajesh, rachana, udaya** for their encouragement and support in the initial period of my **Ph.D**. I am immensely thankful to **chinna sisi** for his always helpful nature.*

*I am thankful to **Jayaraju** for his help and company throughout my **Ph.D**. My new **labmates, hafeez and shivaram** are great guys to work with. **Seenu**, our lab assistant has always been a great help to me. My other labmates, the **anita, prasanna and snath** were also very helpful.*

*My friends in the school of **Life Sciences, rinay, sudhakar, local lasman, chandu, ithal, mahipal, rajagopal, baskar and ramakrishnasaoor** always came to my assistance when I needed them. My special thanks to **suresh and ravindra** for their help.*

*Last and the most, the encouragement and support of my parents has **given** me the strength to pursue research as my career.*

Vashisht.

ABBREVIATIONS

AcFccp (Acetyl Ferrocene)	1-acetyl di- π -cyclopentadiene iron (II)
ATP	adenosine triphosphate
A Tr	apotransferrin (iron or ruthenium unbound protein)
BCIP	5-bromo-4-chloro-3-indoyl phosphate
bp	base pair
Kbp	kilo base pair
BSA	bovine serum albumin
CoSAL	trans bis cobalt (III) salicylaldoxime
DacFccp (Diacetyl Ferrocene)	1,1'-diacetyl di- π -cyclopentadiene iron (II)
DMSO	dimethyl sulfoxide
DNA	deoxy ribonucleic acid
DTT	dithiothreitol
EDTA	ethylene diamine tetra acetic acid
Fccp (Ferrocene)	di- π -cyclopentadiene iron (II)
FccpOx (Ferrocene Carboxaldoxime)	1-carboxaldoxime di- π -cyclopentadiene iron (II)
FccpDox (Ferrocene Dicarboxaldoxime)	1,1'-di-carboxaldoxime di- π -cyclopentadiene iron (II)
h	hour
kDa	kilo dalton
m-AMSA	<i>N</i> -[4-(9-acridinylamino)-3-methoxy-phenyl]methanesulfonamide
mg	milligram
MgCl₂	magnesium chloride
min	minutes
M	molar
mM	millimolar
μM	micromolar
μL	microliter

NBT	nitroblue tetrazolium
PAGE	poly acrylamide gel electrophoresis
PMSF	phenyl methyl sulfonyl fluoride
SDS	sodium dodecyl sulfate
RNA	ribonucleic acid
RuBen(dmsO)	[$(\eta^6\text{-benzene})\text{dichloro}(\text{sulfinylbis(methane)-O-ruthenium (II)})$]
RuBenPyr	[$(\eta^6\text{-benzene})(\text{pyridine})\text{-N-ruthenium (II)}$]
RuBenAPy	[$(\eta^6\text{-benzene})(3\text{-amino pyridine})\text{-N}_1\text{-ruthenium (II)}$]
RuBenABa	[$(\eta^6\text{-benzene})(\text{p-amino benzoic})\text{-O-ruthenium (II)}$]
RuBenAGu	[$(\eta^6\text{-benzene})(\text{amino guanidine})\text{-N}_1\text{-ruthenium (II)}$]
RuIm	trans-imidazolium (bis imidazole) tetrachloro ruthenate (III)
RuInd	trans-indazolium (bis indazole) tetrachloro ruthenate (III)
RuSal	trans-bis salicylaldoximate ruthenium (II)
TCA	trichloro acetic acid
T_m	melting temperature
topo II	topoisomerase II
Tr	transferrin (iron or ruthenium bound protein)
TrR	transferrin receptor
tris	tris (hydroxy methyl) aminomethane
uv	ultraviolet

Contents

	page No
Chapter 1: Introduction	1-26
Chapter 2: Experimental Procedures	27-56
Chapter 3: Topoisomerase II poisoning and anticancer activity by DNA non-binding derivatives of ferrocene	57-68
Chapter 4 Topoisomerase II antagonism by two structurally distinct ruthenium compounds: Elucidation of a ligand dependent mode of action	69-80
Chapter 5: Development of novel RuBen derivatives to enhance potency of topoisomerase II poisoning	81-88
Chapter 6: Development of a transferrin mediated delivery system for the anticancer RuBen drugs	89-96
Chapter 7: Topoisomerase II poisoning by ruthenium coordination complexes: A study of structure-activity relationship	97-103
Conclusions:	104-108
References:	109-116
spectral data of synthesized complexes.	

Chapter 1

INTRODUCTION

Hippocrates, 25 centuries ago, had named malignant tumors in the human body as *karkinois* (crab) because the swollen blood vessels around the tumor mass gives it **the** appearance of a crab. Cancer has been with man all along his existence. This disease, characterized by abnormal and uncontrolled division of cells, arises due to genetic instabilities that develop over the years in the DNA of these cells. Increased life expectancy, coupled with the increase of numerous environmental pollutants and mutagens has cumulated the genetic aberrations, which increased the incidence of cancer. Inheritance of these genetic aberrations has also turned it into a potential inheritable disease.

Cancer in the world:

Cancer is the second common cause of death in the developed countries next to cardiovascular diseases. In Europe and North America, approximately one in five people die of cancer. Such is the widespread mortality of cancer that according to a WHO estimate, out of 50 million deaths annually in the world, more than 5 million are attributed to cancer, and this number is rapidly increasing.

Cancer in India:

Increase of human life span in India over the last 5 decades has also increased the incidence of cancer. Approximately, 500,000 new cases of cancer are reported every year and according to a survey conducted by the Indian Cancer Society, 1.5 million people suffer from this disease at any given point of time. Oral and Cervical cancer are the major cancers in this country.

Cancer Therapy:

Though great strides are being made in unraveling the molecular basis of carcinogenesis, this knowledge has not yet been translated into a complete and effective cure for cancer. Whatever the treatment procedure adopted, there is always a doubt of an incomplete cure or a relapse. Presently, cancers are treated by the following methods depending upon the site and stage of the disease.

1. Surgery
2. Radiation therapy
3. Chemotherapy
4. Hormonal therapy

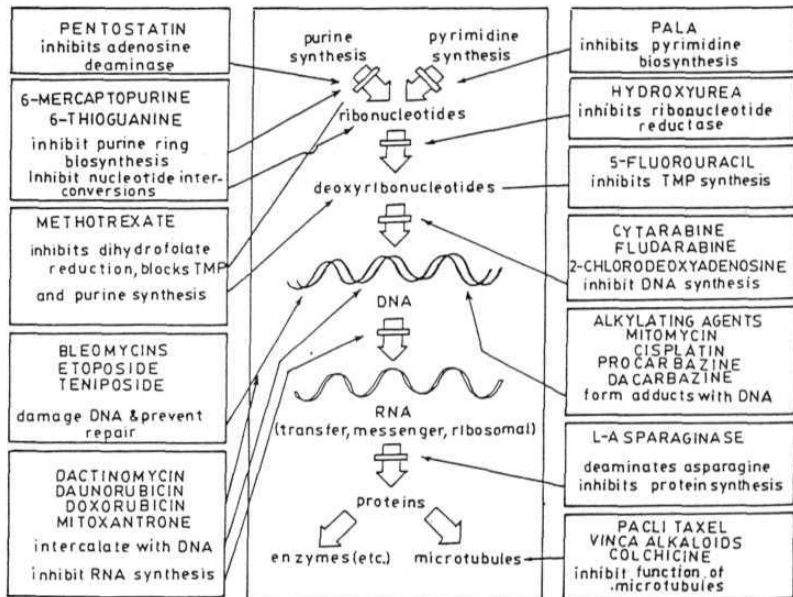
Chemotherapy is the treatment of choice because of its effectiveness on various types of cancers. It is used as a combination regimen of different drugs or as an adjunct to surgery and radiation.

Development of Chemotherapeutics:

Traditionally, cancer chemotherapeutics were discovered through random large-scale screening of synthetic chemicals and natural products against tumor systems, primarily murine leukemias. Advances in molecular cell biology and knowledge of the macromolecules involved in cellular functions has lead to the identification of target sites and mechanisms of action of these drugs. An overview of different chemotherapeutic drugs and their sites of action is presented in **panel 1**. The identification of specific

intracellular targets for various drugs has paved the way for the development of drugs targeted at these sites of action.

PANEL 1



Anticancer targets:

A large number of anticancer drugs target DNA at various stages, causing lethal genetic aberrations, which results in death of the cancer cells. Unfortunately, this generalized action takes a huge toll on normal cells too, which narrows the therapeutic index of these agents. In the light of this drawback, it would be more meaningful to develop drugs which target a specific molecule involved in cancer progression, without whose function, the division of cancer cells, but not normal cells will be grossly affected. Numerous such cellular targets have been identified and have become the basis for the development of cancer therapeutics. Some of these anticancer targets are-

- Adenosine deaminase
- Ribonucleotide reductase
- Dihydrofolate reductase
- Farnesyl transferase
- Topoisomerases

TOPOISOMERASES

DNA is a very dynamic molecule and during the lifetime of a cell, it constantly undergoes various topological changes without affecting its genetic makeup. Numerous topological problems like negative/positive supercoiling and catenation arise in DNA during replication and transcription. This causes intertwining of DNA that has to be resolved in order to maintain normal functioning of the genome. Topoisomerases resolve this intertwining and thus maintain genome integrity (Wang, 1985, 1991, 1996; Prus and Drlica, 1986; Watt and Hickson, 1994). The enzymes are also involved in decatenation of DNA in the G2 phase of cell division for separation of newly replicated chromatids (Downes et. al., 1994). In the M phase, they help in chromosome condensation and segregation (Adachi et. al, 1991).

The catalytic activity of these enzymes typically involves breaking one strand (topoisomerase I) or both strands (topoisomerase II) of a duplex DNA segment and passing the other strand in case of a single strand break or a duplex DNA segment in case of a double strand break through a gate created by the broken DNA strand(s), and then resealing the broken strands. The strand passage reaction is central to the various functions of topoisomerases.

CLASSIFICATION OF TOPOISOMERASES:

Topoisomerases in general, are of two types in both **prokaryotes** and eukaryotes. They are the type I topoisomerases and type II topoisomerases (Reviewed by Roca, 1995; Wang, 1996).

Type I topoisomerases: These are **monomeric** enzymes which do not require ATP for their activity. They change the linking number of DNA in steps of one (*linking number is the number of right handed turns that one DNA strand makes around the other in a DNA duplex*). The type I topoisomerases are of two types.

Topoisomerase I- 5': Molecular weight of this protein is ~97 kDa. This enzyme binds to a single strand of duplex DNA and forms an **enzyme-DNA** intermediate through a **covalent** bond between a tyrosine residue of the enzyme and the 5' -phosphate at the DNA break site.

Functions: Partial relaxation of negatively supercoiled DNA and knotting of single stranded DNA rings into a double stranded ring.

Examples: E. coli DNA topoisomerase I, III and eukaryotic topoisomerase III.

Topoisomerase I- 3': This is a 95-135 kDa protein. It is similar to the 5' enzyme but binds preferentially to double **stranded** DNA and cleaves a single strand of DNA. It forms a phosphotyrosyl linkage between a tyrosine residue of the enzyme and the 3' - phosphate at the break site. The unbroken strand is passed through this break to release the twisting stress on the helix.

Functions: complete relaxation of both positive and negative supercoils in DNA.

Examples: eukaryotic topoisomerase I, vaccinia virus topoisomerase I and topoisomerase V of hyperthermophilic bacteria.

Type II topoisomerases: These are essential enzymes for the life of all organisms. They are dimeric molecules and are ATP dependent. These enzymes change the linking number of DNA in steps of 2. Depending on whether they are prokaryotic or eukaryotic, they are divided into two types.

DNA gyrase : This is the prokaryotic topoisomerase II. Its catalytic activity is the same as that of the eukaryotic enzyme as described below.

Functions: Preferential relaxation of positive supercoils and induction of negative supercoiling in the bacterial chromosome and **extrachromosomal** DNA (plasmids).

Examples: All the prokaryotic type II topoisomerases and topoisomerase IV fall under this category.

Topoisomerase II : This is the eukaryotic equivalent, which is a 160-180 kDa protein and is highly conserved in all organisms. It binds to duplex DNA and breaks both the strands, 4 base pairs apart. The 5' broken ends are covalently bonded to two tyrosine residues (one from each monomer) through **phosphotyrosyl** linkages. Additional interactions restrict free rotation of the free 3' ends at the break site. A second duplex segment is transported through this break.

Functions: If the gated and transported segments reside in the same DNA segment, this enzyme catalyzes relaxation of supercoils or **knotting/unknotting** of DNA. If they are in different DNA segments, the enzyme catalyzes their catenation or decatenation.

Examples: All the eukaryotic **topoisomerase II** enzymes.

Human topoisomerase II: In humans and also most mammals, two genetically distinct isoforms of topoisomerase II have been detected (Drake et. al., 1987). The first type is the topoisomerase **II α** , which is a ~170 kDa protein, similar to the topoisomerase II of all eukaryotes and performs all the functions of the typical type II enzymes (Woessner et. al., 1990). The second is topoisomerase **II β** , which shares a sequence **homology** of 68% with the **α isoform** and has a molecular weight of ~ 180 kDa. The two isoforms appear to have arisen from a recent gene duplication event which included several flanking markers like the retinoic acid receptor **α** and **β** genes (Coutts et. al., 1993). The **α isoform** has been mapped to chromosome 17q21-22 (Tsai-pflugfelder et. al., 1988) while the **β enzyme** is on chromosome 3p24 (Tan et. al., 1992). The two isoforms show distinct patterns of expression during cell cycle and also during oncogenic transformation (Woessner et. al., 1990, 1991). While the **α enzyme** is over-expressed during the G2 and M phases of the cell cycle, the **β enzyme** is constant throughout. The functions of the **β isoform** are not clearly known, but it is believed that it may be required for housekeeping functions during the resting phase of the cell cycle, while the **α enzyme** is required for cell cycle progression and for fast growth and division of cancer cells.

STRUCTURE, CATALYTIC ACTIVITY, FUNCTIONS AND REGULATION OF TOPOISOMERASE II

Among the eukaryotic topoisomerases, topoisomerase II is the major target for some of the most important anticancer drugs. This is comprehensible because this enzyme is absolutely essential for viability of cells; though the function of topoisomerase I can be replaced by topoisomerase II, the latter enzyme's function cannot be replaced in most cases (DiNardo et al., 1984; Uemura and Yanagida, 1986). A closer look at the structure and functions of topoisomerase II will explain its importance in the growth and division of living cells.

Structure of topoisomerase II:

The crystal structure of topoisomerase II was worked out in detail by Berger et al. in 1996. The study shows that topoisomerase II in its active form is a heart shaped homodimer with a large central hole (**panel 2**). The monomer is a flat crescent shaped fragment which can be distinguished into three discrete domains. The first is the ATP binding domain in the N-terminal region (**B'** region). It has a consensus sequence for ATP binding and has the capacity to hydrolyze ATP. This domain **dimerizes** with the other monomer upon binding of ATP, and imposes a conformational change all over the enzyme, required for catalytic activity. The second is the DNA binding domain or the DNA **breakage/reunion** domain, present in the A' region. The active site tyrosines which associate with the broken ends of DNA during the catalytic cycle are present in this domain. The third is the primary **dimer** interface in the **C-terminal** region which forms the

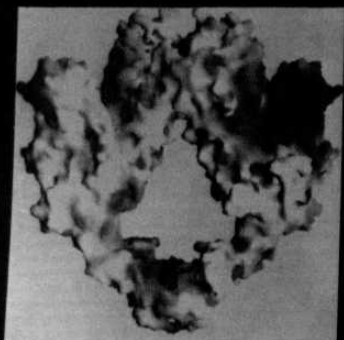
dimer interface of the enzyme by associating with the other monomer. Apart from forming the dimer interface, this region is also implicated in regulation of enzyme activity and nuclear localization.

PANEL 2

CRYSTAL STRUCTURE OF TOPISOMERASE II

(reproduced from Berger et. al., 1996)

SPACE FILL MODEL



RIBBON MODEL



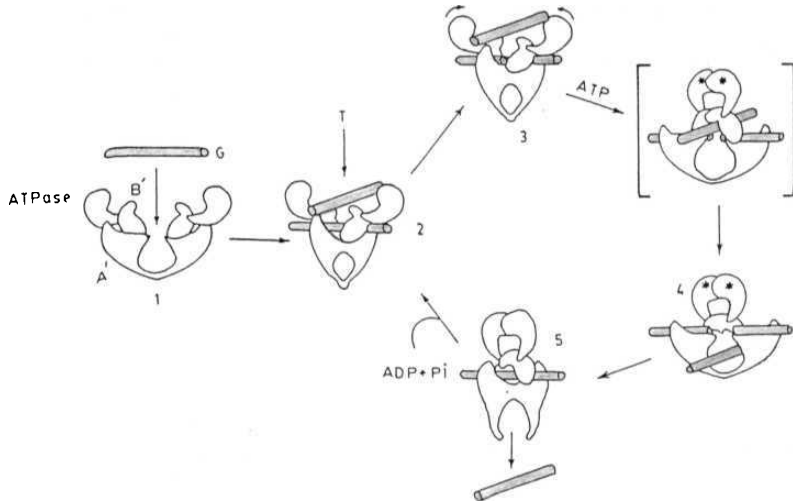
Catalytic Activity:

In its catalytic cycle shown in **panel 3** (described by Berger et al, 1996), the **topoisomerase II dimer** first binds to a duplex DNA segment termed as the '**G**' (gated) segment and undergoes a **conformational** change. It then binds to ATP with the ATP binding domain and also binds to a second DNA segment called the '**T**' (transported) segment. This binding causes a series of conformational changes in the enzyme, which causes the **A'** regions to be pulled apart from each other, leading to cleavage of the **G-segment** in both the strands, four base pairs apart. The active site tyrosines in the DNA binding domains then form covalent bonds with the nicked DNA strands through a trans-esterification reaction between the phenolic hydroxyl groups of the tyrosines and the 5-phosphoryl ends of the nicked DNA. **Concomitantly**, the ATP domains dimerize and the T-segment is transported through the gate formed by the nicked DNA into the central hole. Following this transport, the G-segment is rejoined by a second trans-esterification reaction and the T-segment is transported out of the enzyme through the opening formed in the dimer interface. The monomers immediately dimerize at the interface and the ATP is hydrolyzed and released. This regenerates the starting state and the enzyme is ready to begin a fresh catalytic cycle.

The DNA cleavage/religation reactions do not require energy from a high energy co-factor (like ATP) because the phosphate bond energy is conserved in the two successive trans-esterification reactions (Roca, 1995). The ATP binding and hydrolysis is involved in introducing conformational changes in the enzyme for carrying out its catalytic functions and not for DNA nicking and resealing.

PANEL 3

CATALYTIC CYCLE OF TOPOISOMERASE II



*Topo II binds to the 'G' segment of DNA and undergoes a conformational change. Upon binding of a second segment ('T' segment) and ATP, the enzyme further undergoes conformational changes leading to generation of double strand breaks in the 'G' segment and passage of the 'T' segment through the gate formed by the broken strand into the large central hole in the enzyme. **Following** this transport, the 'G' segment is rejoined and the 'T' segment is released out of the enzyme through an opening of the primary dimer interface. At this stage, ATP is hydrolyzed and the enzyme starts a fresh reaction cycle.*

Functions of topoisomerase II:

Resolving the need for a ‘Molecular Swivel’ : The local unwinding of the DNA helix during DNA replication and transcription leads to positive supercoiling ahead of the advancing fork and negative supercoiling in the region behind the fork (Lockshon and Morris, 1983, Liu and Wang, 1987). This causes torsional stress on the **DNA**, which is removed either by topoisomerase I or II by relaxing the positive and negative superhelices (Kim and Wang, 1989).

Decatenation of replicated chromatids and segregation : DNA replication in the dense **chromatin** results in catenation of the replicated chromatids. The separation of these intertwined daughter strands requires decatenation, which is performed by topoisomerase II in the G2 phase of the cell cycle (Ishida et al., 1994). This helps in segregation of the newly replicated daughter strands at mitosis and **meiosis**. Cells lacking topoisomerase II accumulate multiply-intertwined, catenated **dimers** (DiNardo et al, 1984, Uemura and Yanagida, 1986). The failure to segregate intertwined DNA molecules eventually leads to cell death as the cells attempt to divide (Holm et al., 1985).

Maintaining Genome Stability : . Both the type I and type II **topoisomerases**, through relaxation of supercoils and unlinking of inappropriately paired intertwined DNA strands, greatly reduce recombination frequency, especially in the rDNA clusters and help in maintenance of genome stability (Christman et al., 1988). Topoisomerase II plays an important role in recombination suppression during meiosis (Holm et al., 1989). Absence

of any of these enzymes inadvertently results in a hyper-recombination phenotype, in which the rDNA gene clusters tend to get excised as **extrachromosomal** DNA rings (Kim and Wang, 1989b).

Chromosome Structure : Topoisomerase II is associated with interphase chromatin as well as the cell division stage chromosomes (Swedlow et al., 1993, **Earnshaw** and **Heck**, 1985). In fact, topoisomerase II is the major component of the chromosome scaffold and is concentrated at the base of the chromosomal loops, called the scaffold attachment regions (Gasser and **Laemmli**, 1987). Though the detailed structural interaction of topoisomerase II with chromosomes is yet to be worked out, it is believed that topoisomerase II gives structural alignment to chromosomes prior to mitosis but is not required for maintaining the chromosomal scaffold through mitosis (Hirano and Mitchison, 1993).

Chromosome condensation/decondensation: Topoisomerase II is required for chromosome assembly and condensation **prior** to cell division (Adachi et al., 1991; Wood and **Earnshaw**, 1990). The enzyme is believed to interact with other proteins of the chromosomal scaffold like the SMC proteins (**SCII**, XCAP-C and XCAP-E) during chromosome condensation (Ma et al., 1993; Saitoh et al., 1994). Removal of topoisomerase II activity either through **immuno-depletion** or antibody blocking completely inhibits chromosome assembly and condensation (Hirano and Mitchison, 1993). Similarly, the enzyme is also required for chromosome decondensation after cell division.

Regulation of topoisomerase II activity :

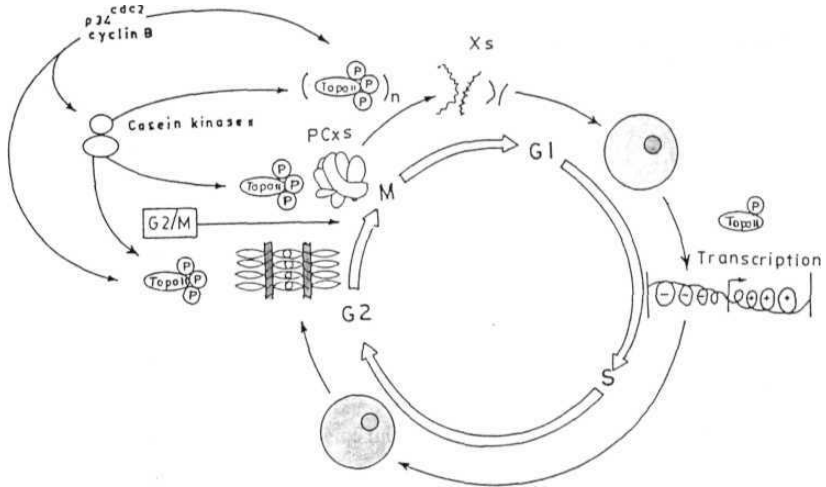
Topoisomerase II expression and activity is tightly regulated in cells. In the G1 and S phases of the cell cycle, topoisomerase II activity is largely confined to the relaxation of supercoils generated during the processes of transcription and replication (Cardenas and Gasser, 1993). This requires low expression levels and the enzyme activity is also very less, which is regulated through phosphorylation. As the cell passes on to the G2 and M phases, the phosphorylation status of enzyme is very high, consistent with its high activity (Cardenas and Gasser, 1993). The **functions** of topoisomerase II and its regulation in the cell cycle are schematically shown in **panel 4**.

Fast growing cancer cells, unlike the normal cells show very high expression of topoisomerase II in all the phases of the cell cycle (Hsiang et al., 1988). The enzyme is also highly phosphorylated in these fast dividing cells, without which the cells cannot accomplish their high turnover.

Depending on the requirement, phosphorylation of the enzyme can lead to increase in its activity by 2 to 15 fold (Corbett et al., 1992, 1993b; **Takano** et al. 1991). Casein Kinase II and protein kinase C are the major enzymes that phosphorylate topoisomerase II (**Ackerman** et al., 1985, 1988; DeVore et al., 1992). In addition, other 'mitotic kinases' like the mitogen-activated protein kinase (MAP kinase) phosphorylate the enzyme during the G2 and M phases (Kuang and Ashorn, 1993). The phosphorylation of topoisomerase II by these kinases may be regulated by the master controller of mitotic events, the p34^{cdc} kinase (Cardenas et al., 1992).

PANEL 4

TOPOISOMERASE II ACTIVITY IN THE CELL CYCLE



In the G1 and S phases of the cell cycle, topo II expression and activity is very less. Phosphorylation of the enzyme is also very minimal (shown as 'P'). In these cell cycle phases, the enzyme is involved mostly in resolving the supercoiling generated during transcription. As the cell cycle passes on to the G2 and M phases, topo II expression and activity through phosphorylation is drastically increased. The enzyme in these phases helps in replication, segregation of daughter chromosomes (shown in red), condensation of chromosomes through precondensation complex (PCx) formation and during decondensation. The enzymes that phosphorylate topo II are Casein Kinase II, Protein Kinase C, etc. Cancer cells generally over-express topo II throughout the cell cycle because of the heavy requirement for this enzyme during the various DNA topological transformation processes.

ANTAGONISM OF TOPOISOMERASE II ACTIVITY

In contrast to the limited number of drug classes that act on topoisomerase I or DNA gyrase, topoisomerase II is a target for a number of structurally disparate compounds (Chen and Liu, 1994). The present topoisomerase II drugs can be classified into four groups (Drlica and Franco, 1988; D'Arpa and Liu, 1989, Liu, 1989). They are -

DNA intercalating topoisomerase II poisons : These molecules possess a domain for intercalation with DNA and a domain for enzyme interaction. Through this bi-directional interaction, they form an Enzyme-Drug-DNA ternary complex called the 'cleavage complex'. The formation and importance of this 'cleavage complex' has been described in the next section. Examples of this class of drugs are **amsacrine (m-AMSA)**, adriamycin, ellipticine.

DNA non-intercalating topoisomerase II poisons :

These molecules also form the ternary cleavage complex, but do not intercalate with DNA. They interact with the enzyme and may or may not interact with DNA, but without intercalation. Examples: Etoposide and Teniposide

Drugs that interfere with the ATP hydrolysis reaction of topoisomerase II:

ATP hydrolysis causes a conformational change in the enzyme which opens a molecular clamp for passing a double stranded DNA segment through the distal (C-terminal) end of the enzyme. Drugs which inhibit ATP hydrolysis by the enzyme do not allow the passage of the DNA segment through this clamp. Examples are Novobiocin, Coumeromycin and Amonafide.

Topoisomerase II inhibitors:

These class of drugs bind to the enzyme and inhibit the catalytic activity of the enzyme without forming the cleavage complex or interfering with the ATP hydrolysis. Example of this class is Fostriecin.

These four classes of topoisomerase II drugs are important antineoplastic agents because topoisomerase II antagonism brings about anticancer action. Among these classes of drugs, the DNA intercalating and non-intercalating poisons are the most effective anticancer agents for the specific reasons which are described in the next heading.

TOPOISOMERASE II IS AN ANTICANCER DRUG TARGET

The strand passage event in the catalytic cycle of topoisomerases comes with a heavy price, which is, generation of double stranded breaks in the DNA. Under normal circumstances, these DNA breaks are fleeting intermediates between the DNA cleavage and religation action of the enzymes (Reece and Maxwell, 1991; Gupta et al., 1995). However, conditions that significantly increase the lifetime and physiological concentrations of these DNA breaks unleash a myriad of deleterious effects on the genetic material (Corbett and Osheroff, 1993; Anderson and Berger, 1994; Ferguson and Baguley, 1994).

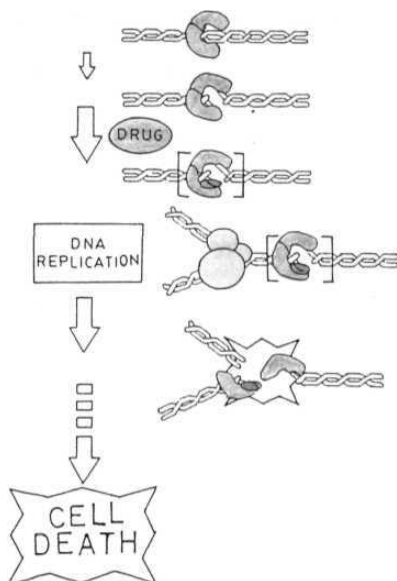
In the early 1980's, researchers had shown that some of the well known anticancer drugs like etoposide and amsacrine (m-AMSA) act on this aspect of the enzyme activity (Nelson et al., 1984, Chen et al., 1984). These drugs, which allow DNA cleavage by the enzyme but block the DNA religation event are known as '**topoisomerase II poisons**', unlike the topoisomerase II inhibitors which basically interfere with enzyme turnover (Smith, 1990). Typically, these poisons interact bi-directionally with the enzyme and DNA or with the enzyme alone (when the enzyme is bound to DNA). The drug bound topoisomerase II, as per its normal catalytic cycle, cleaves the DNA. At this point, the transient intermediate of the covalently linked 'enzyme-cleaved DNA complex' is frozen by the drug. This ternary complex consisting of enzyme-drug-DNA is called the 'cleavage complex' (Liu, 1989, Smith, 1990). Formation of this complex disturbs the DNA cleavage/religation equilibrium, which shifts towards DNA cleavage and the enzyme is no

longer capable of resealing the breaks (Maxwell, 1992; Pommier, 1993). This results in permanent double strand breaks in DNA which are protected by the covalently linked topoisomerase II (**Froelich-Ammon** and Osheroff, 1995).

Cancer cells generally over-express topoisomerase II (Hsiang et al., 1988; Tricoli et al., 1985; Bodley et al., 1987), and these cells when treated with topoisomerase II poisons, tend to harbor numerous topoisomerase II induced DNA cleavage complexes (**Potmesil** and **Kohn**, 1991; **Slischenmyer** et al., 1993; **Sinha**, 1995). Traversal by replication or transcription complexes in the region of the breaks will apparently split up these cleavage complexes, which will expose the DNA breaks. Once exposed, these breaks will become targets for repair and recombination pathways. This in turn stimulates sister chromatid exchange, large **insertions/deletions**, translocations and large chromosomal aberrations (Corbett and Osheroff, 1993, Chen and Liu, 1994, Anderson and Berger, 1994; Ferguson and Baguley, 1994). When these genetic aberrations accumulate at high concentrations, they trigger a **series** of events which will ultimately lead to cell death through apoptosis or necrosis (Liu, 1994; Pommier et al., 1994; Beck et al., 1994). The impact of topoisomerase II poisons on enzyme activity and the subsequent effects are depicted schematically in **panel 5**.

PANEL 5

HOW TOPOISOMERASE II POISONS KILL CANCER CELLS



*In its normal catalytic cycle, topo II (shown in red) binds to DNA and generates double strand breaks. Binding of a topo II poison (green) freezes topo II and DNA in a 'cleavage complex', in which the enzyme cannot rejoin the broken DNA. When such a cleavage complex encounters unwinding stress due to an advancing DNA replication machinery or a transcription complex (shown in yellow), the cleavage complex dissociates, exposing the DNA double strand breaks. Accumulation of numerous such DNA breaks due to cleavage complex formation, eventually leads to **cell death** (described in the **text**).*

METAL COMPLEXES AS CANCER THERAPEUTICS

The therapeutic use of metal containing compounds can be traced back to the ancient Chinese (between 2000 and 2500 B.C.), who used gold in **metallotherapy** for various diseases including cancer. Paracelsus (1493-1541), who is regarded as the father of metallothrapy, used alchemical mixtures of various heavy metals such as **iron**, **cadmium**, mercury, arsenic and antimony to treat patients with diseases like cancer. **Ehrlich** had used the arsenic compound, Salvarsan® to treat syphilis, until the discovery of penicillin (**Ehrlich**, 1910). In 1929, Bell had demonstrated the use of Lead phosphate and colloidal Lead for curing neoplastic diseases. The ancient Indian system of therapy called 'Siddha' also uses mixtures of metallic compounds with plant juices for treating numerous diseases.

The modern era of cancer chemotherapy started with the accidental discovery of the cytostatic properties of a platinum coordination complex, cis-diamine dichloro platinum (II) (cisplatin) (Rosenberg et al., 1969).

Cisplatin therapy produced such dramatic results on testicular, ovarian, head and neck carcinomas that it spurred an extensive search for other platinum containing complexes. Subsequently, the derivatives of cisplatin- carboplatin, iproplatin and spiroplatin were synthesized, which showed increased efficacy (DeVita et al., 1985; Nicolini, 1988). But surprisingly, compounds like transplatin (trans **isomer** of cisplatin, whose ligands are in the trans-conformation) did not show any anticancer action. Detailed analysis revealed that cisplatin and its analogues interact with DNA by predominantly (>90%) forming the 1,2-intrastrand cross-links with adjacent purine bases (especially guanine) (Lippard, 1993).

Transplatin shows very less cross-linking with adjacent bases. This explains the difference in the anticancer action between cisplatin and transplatin. But most importantly, this suggests that the ligand orientation and possibly the type of ligand attached to the metal atom may influence the anticancer activity of such metal complexes.

Cisplatin discovery also sparked off an extensive search for anticancer metal complexes which contain a metal atom other than platinum. A very few among these complexes actually matched the cytostatic efficacy of cisplatin, but more importantly, some of these non-platinum metal complexes were active against tumor types which were unresponsive to cisplatin and other existing anticancer drugs, eg., gastrointestinal carcinomas insensitive to cisplatin and other chemotherapeutic treatment are very responsive to treatment with **antitumor** titanium compounds (Kopf-Maier, 1989). This is a promising aspect for development of non-platinum anticancer metal complexes. The noteworthy point here is that, apart from the type and orientation of the ligands, the central metal atom may also be an important determinant for anticancer action.

To date, the most effective non-platinum cytostatic agents are **spirogermanium**, a germanium complex (Rice et al., 1977), gallium nitrate (Adamson et al., 1975), titanocene dichloride and budotitane, which are titanium complexes (Kopf-Maier, 1989, Keppler et al., 1991) and **trans-indazolium** (bis indazole) tetrachloro ruthenate, a ruthenium complex (Keppler et al., 1989). The purported mechanism of cytostatic action by these complexes is through inhibition of **DNA**, RNA and protein synthesis (Waalkes et al., 1974; Hill et al., 1982, Kopf-Maier and Kopf, 1988; Fruhauf and Zeller, 1991). But, as mentioned earlier, this generalized action also causes enormous toxicity on the body.

A more viable approach for the development of anticancer metal complexes would be through a rational drug design. This concept stresses on the need to recognize specific targets of **action**, and then design antagonistic molecules that bind to the targets with a very high affinity to bring about specificity of action. This would not only increase the potency of anticancer **action**, but also decrease toxic side effects to a great extent. The work presented in this thesis is an attempt to develop anticancer organometallic complexes of iron and ruthenium which target topoisomerase II, and which can be safely delivered to cancer cells by using a natural delivery approach.

OBJECTIVES OF THE WORK

For developing potent anticancer metal complexes with minimal associated toxicity, a three pronged approach was adopted.

- 1 Metal induced toxicity of anticancer metal complexes can be reduced if the metal atom is strongly bonded with one or more ligands. The strongly bonded metal atom would, at least in part be inert towards biological molecules, which may otherwise easily interact with a metal which has lost its ligands. **Organometallic** compounds are excellent candidates for this purpose because they possess a strong bond (organometallic bond) between the metal atom and the π -electron cloud of an aromatic ring of the ligand. This linkage would prevent non-specific association of the metal atom with biological molecules.
2. Toxicity can be further reduced if the compounds are designed to specifically interact with a single molecular target in cancer cells, in the present case, topoisomerase II.
3. Targeted delivery of the drugs in a bound or encapsulated form to achieve selective localization in cancer cells will further reduce non-specific toxicity.

In the present study, organometallic compounds of iron and ruthenium have been designed to specifically poison the activity of topoisomerase II. Detailed analysis on their molecular interaction with topoisomerase II and DNA have been carried out to determine their mechanism of action. Anticancer activity of these compounds was tested using ^3H -

thymidine incorporation assays. Lastly, a delivery approach was attempted for the ruthenium compounds to improve their potency of anticancer activity.

Chapter 2

EXPERIMENTAL PROCEDURES

MATERIALS

- RPMI-1640** and **DMEM** cell culture media, **Amsacrine (m-AMSA)**, **PMSF**, **DTT**, **Polymin-P**, **Calf thymus DNA** and human **Apotransferrin** (Mr 80,000) were from **Sigma Chemical Co.**, U.S.A.
- Anti-topoisomerase II** antibody was from **Topogen Inc.**, U.S.A.
- Protein A-agarose**, **fetal calf serum**, **trypsin** and **antibiotics** were from **Gibco-BRL**, U.S.A.
- Biogel-HTP** (hydroxyapatite) was from **Bio-rad**.
- PEI** (polyethyleneimine) **Cellulose-F** TLC sheets were from **Merck**.
- Proteinase K** and **ATP** were from **Boehringer-Mannheim**, Germany.
- The radioactive chemicals- γ ^{32}P - **ATP** and ^3H labeled **thymidine** were supplied by the **Board of Radiation and Isotope Technology**, India.
- Chemicals** used for synthesis of the **iron** and **ruthenium** metal complexes were from **Aldrich**, **Fluka** and **Lancaster**.
- Other chemicals** and **biochemicals** were of **analytical grade**.

SYNTHESIS OF THE ORGANOMETALLIC COMPLEXES

SYNTHESIS OF THE IRON (FERROCENE) COMPLEXES:

Ferrocene: Di- π -cyclopentadiene iron (II)

This was synthesized according to the procedure of Wilkinson et. al. (1956). Di-cyclopentadiene was monomerized by cracking the dimer in liquid paraffin at 240 °C. In these conditions, the monomeric cyclopentadiene (b.p. 42 °C) vaporises which was distilled out and collected in an air-tight flask and was immediately mixed with dry tetrahydrofuran. This solution was slowly added to sodium metal in tetrahydrofuran and stirred for 3 h to form sodium cyclopentadienide solution.

Anhydrous FeCl_3 and Fe powder in dry tetrahydrofuran were refluxed for 5 h. to give a gray powder of FeCl_2 . The FeCl_2 powder was added to the sodium cyclopentadienide solution and refluxed for 2 h to form iron cyclopentadiene (ferrocene). Ferrocene was extracted from the remaining residue with large portions of petroleum ether and purified by elution with hexane from an alumina column. All the reactions were carried out in dry nitrogen atmosphere.

Proton NMR spectra: Singlet peak at 4.18 PPM, corresponding to the cyclopentadiene ring hydrogens (spectra I).

Note: Spectral data for all the synthesized compounds are given at the end of the thesis, under the heading "Spectral data of the synthesized complexes"

The following derivatives of ferrocene were synthesized according to the procedure of Broadhead **et.al.** (1955).

Acetyl Ferrocene: 1-acetyl di- π -cyclopentadiene iron (II)

Acetyl chloride in chloroform was added to dry aluminum chloride and allowed to stand for 2 h to form a binary complex of the two constituents. This was added to ferrocene in chloroform and stirred for 90 min to form red solution. To this solution, ice was added and stirred for 2 h. The organic layer was separated from the aqueous layer and dried. This was chromatographed on alumina with hexane to purify red colored acetyl ferrocene.

Proton NMR spectra: 4.2 PPM corresponding to the un-substituted lower ring hydrogens, 2.42 PPM corresponding to methyl group hydrogens, 4.5 and 4.8 PPM corresponding to the shifted hydrogens in the acetyl substituted ring (spectra 2).

Diacetyl ferrocene: 1,1'-diacetyl di- π -cyclopentadiene iron (II)

Acetyl chloride in chloroform was added to aluminum chloride and allowed to stand for 2 h to form the binary complex. This was added to acetyl ferrocene in chloroform and stirred for 90 min to form a red solution.

To this, ice was added and stirred for 2 h. The organic layer was separated, dried and chromatographed on alumina with hexane to yield diacetyl ferrocene.

Proton NMR spectra: 2.3 PPM corresponding to the methyl group hydrogens. 4.48 and 4.7 PPM corresponding to the hydrogens on the acetyl substituted ring (spectra 3).

Ferrocene Carboxaldoxime: 1-carboxaldoxime di- π -cyclopentadiene iron (II)

N-methyl formanilide (4 ml) was added to 5 ml of phosphorous oxychloride and mixed for 1 h at room temperature. To this, 2.9 gm ferrocene was added while shaking. The solution was then allowed to stand for 72 h. To this resulting solution, ice was added and the organic phase was extracted. The organic phase was dried and chromatographed in hexane to purify ferrocene carboxy aldehyde.

To 1.5 gm of this aldehyde, 0.7 gm of hydroxylamine hydrochloride in 10 ml of dry ethanol was added and refluxed for 2 h.

After cooling, the black oxime was filtered and suspended in ether to liberate free ferrocene carboxaldehyde. This was crystallized in benzene.

FT-IR spectra: IR band at 3412 cm⁻¹ confirms the presence of carboxaldoxime group in ferrocene (spectra 4)

Ferrocene dicarboxaldoxime: 1,1'-di-carboxaldoxime di- π -cyclopentadiene iron (II)

4 ml of N-methyl formanilide was added to 5 ml of phosphorous oxychloride and mixed for 1 h at room temperature. To this, 2.9 gm of ferrocene carboxyaldehyde was added while shaking. The solution was then allowed to stand for 72 h. To the resulting solution, ice was added and the organic phase was extracted. This was chromatographed to purify a dark brown compound of ferrocene dicarboxaldehyde.

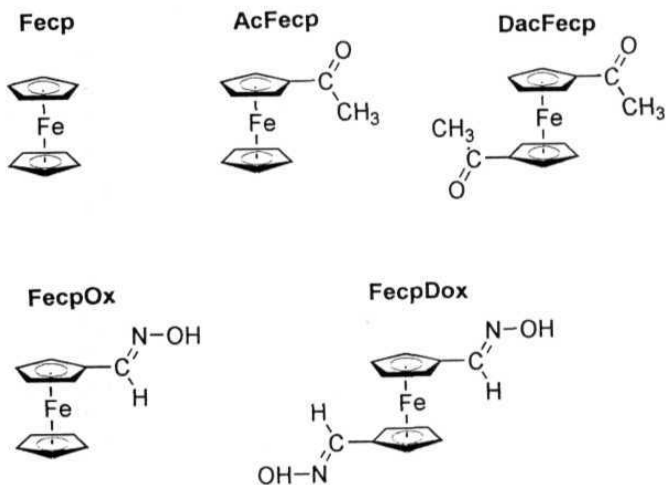
To 1.5 gm of this di-aldehyde, 0.7 gm hydroxylamine hydrochloride in 10 ml of dry ethanol was added and refluxed for 2 h. After cooling, the di-oxime was filtered and suspended in ether to liberate the dicarboxaldehyde. This was crystallized in benzene and

separated from the monoxime on an alumina column using hexane. The **di-oxime** was crystallized in benzene.

FT-IR spectra: Hi band at 3557 cm^{-1} confirms the formation of the dicarboxaldoxime (spectra 5).

PANEL 6

CHEMICAL STRUCTURES OF THE FERROCENE COMPLEXES



SYNTHESIS OF THE RUTHENIUM COMPLEXES:

Ruthenium Coordination Complexes:

RuSAL: Trans bis salicylaldoximate ruthenium (II)

This was synthesized following a slightly modified procedure of Lumme et al. (1984) for the synthesis of copper salicylaldoxime. Dry salicylaldoxime (10 millimole) was dissolved in dry methanol and anhydrous ruthenium trichloride (5 millimole) was added in the presence of dry nitrogen gas. The constituents were refluxed at 70 °C for about 1 hour until a green solution formed. This was vacuum dried and crystallized to form dark green complex of ruthenium (II) salicylaldoxime.

IR spectra: Band at 1608 cm^{-1} confirms the formation of a coordination bond between imine nitrogen and metal atom; band at 1493 cm^{-1} confirms the metal- oxygen bond (spectra 6).

RuInd: trans-indazolium (bis indazole) tetrachloro ruthenate (III):

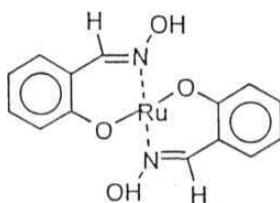
RuIm: trans-imidazolium (bis imidazole) tetrachloro ruthenate (III):

These two metal complexes were generous gifts from Prof. B.K. Keppler, Department of Inorganic Chemistry, University of Heidelberg, Heidelberg, Germany. The synthetic procedures of these complexes are described by Keppler et. al. (1989).

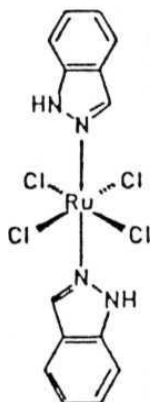
PANEL 7

CHEMICAL STRUCTURES OF THE RUTHENIUM
COORDINATION COMPLEXES

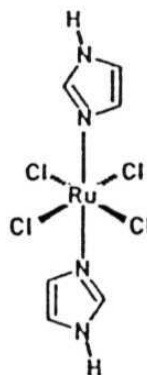
RuSAL



Rulm



Rulnd



Ruthenium Organometallic Complexes:

Synthesis of the dimeric starting compound:

This complex was synthesized as previously described by Zelonka et. al. (1972). Briefly, freshly synthesized 1,3-cyclohexadiene (6 ml) was added to $\text{RuCl}_3 \cdot 3\text{H}_2\text{O}$ (1.7 gm) in 100 ml of aqueous ethanol. The solution was maintained at 45 °C for 3 h to form a red precipitate which was washed in ethanol and dried in vacuo to give the dimeric complex of $[\text{RuCl}_2(\text{C}_6\text{H}_6)_2]$. This **dimer** was the starting compound for the synthesis of all the complexes of the 'RuBen' type.

RuBen(dmsO): f (η^6 -benzene)dichloro sulfinyl bis(methane)-O-ruthenium (II) /

To the dimer, DMSO was added to form the monomeric DMSO complex $[\text{RuCl}_2(\text{C}_6\text{H}_6)\text{dmsO}]$, referred as RuBen(dmsO) throughout this thesis. This was vacuum dried to give a bright red precipitate.

Proton NMR spectra in d6- DMSO (the 'dmsO' ligand is also d6-DMSO): δ 4.07 PPM corresponding to the organometallic bonded benzene ring hydrogens (spectra 7).

RuBenPy: f (η^6 -benzene) (pyridine)-N-ruthenium (II) /

100 mg of the above dimer was stirred in 10 ml of pyridine for 48 h. at room temperature to give an orange-red solid. This was filtered and washed in methanol followed by diethyl ether.

*Proton NMR spectra in **d6-DMSO**: 8.6 and 7.4 PPM corresponding to the shifted pyridine hydrogens, δ 3.4 PPM corresponding to the benzene ring hydrogens (spectra 8).*

RuBenAPv: $f(\eta^6\text{-benzene})(3\text{-amino pyridine})\text{-N1-ruthenium (II) I}$

5 mmole of the dimer was suspended in absolute ethanol and 10 mmole of 3-amino pyridine was added. The mixture was refluxed for 12 h. in dry nitrogen atmosphere. A dark green product formed which was filtered and washed in ethyl alcohol: diethyl ether (70:30) mixture.

*Proton NMR spectra in **d6-DMSO**: 8.71, 7.65 and 8.7 PPM corresponding to the shifted pyridine ring hydrogens, 8.3.9 PPM corresponding to the benzene ring hydrogens (spectra 9).*

RuBenABa: ($\eta^6\text{-benzene})(p\text{-amino benzoic})\text{-O-ruthenium (II) I}$

To 5 mmole of the dimer in dry ethanol, p-amino benzoic acid was added. This was refluxed for 6 h. in dry nitrogen atmosphere to give a dark purplish-pink precipitate. This precipitate was dried in diethyl ether.

FT-IR Spectra: Bands at 3462 cm^{-1} and 3364 cm^{-1} correspond to the anti-bonding stretching by the hydroxyl oxygen upon coordination with the ruthenium atom (spectra 10).

RuBenAGu: [$\eta^6\text{-benzene}(\text{amino guanidine})\text{-N1-ruthenium (II) I}$

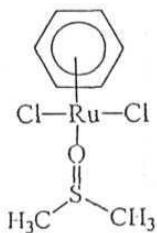
10 **mmole** of amino guanidine was added to 5 **mmole** of the **dimer** in dry alcohol and refluxed for 6 h. The solution was cooled and allowed to stand at room temperature for 24 h. A dark blue precipitate formed, which was washed and dried in diethyl ether.

Proton NMR spectra in *d*6-DMSO: 8 5.9 and 7.3 PPM corresponding to the amino hydrogens *of* the amino guanidine group, δ 3.3 PPM (spectra 11).

PANEL 8

CHEMICAL STRUCTURES OF THE ORGANOMETALLIC COMPLEXES

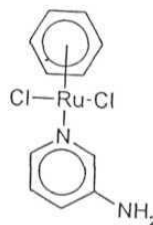
RuBen(dmso)



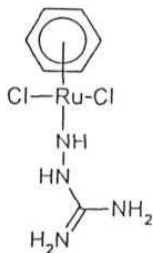
RuBenPy



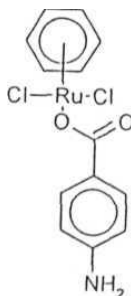
RuBenAPy



RuBenAGu



RuBenABa



MOLECULAR MODELING OF THE SYNTHESIZED COMPLEXES:

Structural conformations of the synthesized metal complexes were determined by computer-aided molecular modeling analysis. Molecular models were generated on a **IBMRS/6000**, model 530 Unix based silicon graphics workstation, using the SPARTAN molecular modeling package (Wave Functions Inc.).

The following tasks were performed to obtain minimum energy standard conformations of the metal complexes.

1. The SPARTAN graphic interface was used for generating 3-dimensional models of the molecules, which were subjected to energy minimization using the **AM1 semi empirical** calculation.
2. Frequency vibration calculations were carried out to bring the optimized conformations to a stable minima.

This produced minimal energy conformational structures of the molecules which should correspond with the actual conformations of these molecules.

BIOCHEMICAL PROTOCOLS

GENERAL PROTOCOLS:

- Protein estimation was done according to the colorimetric method described by Bradford (1976).

SDS-PAGE electrophoresis was carried out according to the procedure of **Laemmli** (1970).

Silver Staining of the SDS-PAGE protein gels was carried out according to the method of Blum et. al. (1987).

- Western Blotting was done following the procedure of Towbin et. al. (1979).

PURIFICATION OF pBR 322 NEGATIVELY SUPERCOILED PLASMID DNA:

The negatively supercoiled pBR322 **plasmid** DNA was purified from the E.coli **HB101** strain containing the plasmid, using the alkaline lysis procedure of Wang and **Rossman** (1994). The procedure described is for a 1 litre culture, which can be scaled up to 4 liters. An overnight culture of the plasmid containing bacteria (grown in the presence of 70 $\mu\text{g/ml}$ ampicillin and 20 $\mu\text{g/ml}$ tetracycline) was used for purification of the plasmid.

Buffers used in the purification:

Lysis buffer: 50 mM glucose, 25 mM **tris-HCl**, pH 8.0, 10 mM EDTA and 5 mg/ml lysozyme.

Alkaline solution: 0.2 N NaOH and 1% SDS.

Acid extraction solution: 0.75 M NaCl, 10 mM EDTA, 0.3 M sodium acetate (pH 4.2).

Reverse extraction buffer: 1.5 M tris and 5 mM EDTA.

Tris-EDTA buffer: 10 mM tris-HCl, pH 7.5 and 1 mM EDTA.

Procedure:

Bacterial cell growth and harvesting:

25 ml of LB broth was inoculated with a single bacterial colony containing the plasmid. The culture was grown in a shaking incubator for 8 h at 36 °C. This culture was used for inoculating 1 litre of LB broth. The 1 liter culture was grown overnight (12 -14 h) at 37 °C in a shaker incubator. The purification procedures were carried out 4 °C.

Cells were harvested by **centrifugation** at 5000 rpm for 10 min. The cells were **lysed** with 40 ml of lysis buffer by constant **stirring** over a period of 15 min.

Alkaline lysis:

80 ml of freshly prepared alkaline solution was added and the constituents were mixed by swirling in a bottle. The mixture was placed on ice for 10 min. 50 ml of freshly prepared saturated ammonium acetate solution was added gently against the walls of the bottle. The bottle was placed on ice for 10 min. The precipitated proteins were removed by centrifugation at 12,000 rpm. The supernatant was clarified by filtering it through glass wool. Ice cold isopropanol (0.7 volume) was added to the supernatant and placed on ice for 20 min.

Acidic phenol extraction of RNA:

The precipitated DNA was pelleted at 12,000 rpm. The supernatant was removed and the pellet allowed to dry. This pellet was dissolved in 25 ml of ice-cold acid extraction solution. After 5 min on ice, an equal volume of water saturated phenol was added and vortex mixed for 2 min in 50 ml tubes. The tubes were centrifuged at 12,000 rpm for 10 min. The aqueous phase (containing RNA) was removed and the phenol phase was again washed with an equal volume of the acid extraction solution.

Extraction of DNA from phenol:

To the phenol phase, 15 ml of reverse extraction buffer and 15 ml of chloroform were added and vortex mixed for 2 min. The tubes were centrifuged again at the same speed. The aqueous phase containing the pure **plasmid** DNA was taken and the phenol phase containing proteins was discarded.

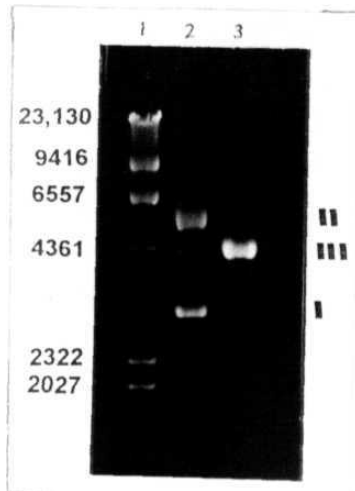
Precipitation and dissolution of DNA:

The aqueous phase containing the DNA was treated with 0.7 volume of ice cold isopropanol and 0.1 volume of 3 M sodium acetate (pH 4.2) and placed on ice for 20 min. The DNA was pelleted and washed twice with ice-cold ethanol (70%). The pellet was dissolved in a proper volume of **Tris-EDTA** buffer.

Panel 9 shows the characterization of pBR322 DNA by *Eco RI* digestion.

PANEL 9

CHARACTERIZATION OF pBR 322 PLASMID DNA



Lane 1: DNA molecular weight marker (bp)

Lane 2: Purified pBR 322 DNA;
lower band- supercoiled DNA (indicated by I)
Upper band- nicked circular DNA (indicated by II)
(also referred as relaxed DNA)

Lane 3: Eco *R1* digestion of the pBR 322 DNA linearizes the closed circular plasmid DNA to show the actual molecular weight of the the plasmid (4.36 kb). The linear DNA is indicated by III

PURIFICATION OF TOPOISOMERASE II FROM RAT LIVER:

Topoisomerase II was purified from rat liver tissue following the procedure of Galande and Muniyappa (1996). In principle, the procedure involves the isolation of enriched nuclei for minimization of protease action. From the nuclei, topoisomerase II is isolated by polyanion P precipitation of **chromatin**, followed by salt extraction of proteins, ammonium sulfate precipitation and finally two rounds of gradient elution in a hydroxyapatite column. All the steps were carried out in a cold room at 4 °C.

Buffers used in the purification:

Buffer A: 10 mM Tris-HCl (pH 7.5), 5 mM MgCl₂, 25 mM KCl, 0.34 M sucrose and 0.1 mM PMSF.

Lysis Buffer: 5 mM potassium phosphate (pH 7.5), 100 mM NaCl, 10 mM 2-mercaptoethanol and 0.5 mM PMSF.

PR buffer: 20 mM potassium phosphate (pH 7.5), 10 mM NaHSO₃, 10% glycerol, 10 mM 2-mercaptoethanol and 0.5 mM PMSF.

Storage buffer: 30 mM potassium phosphate (pH 7.5), 50% glycerol, 0.1 mM EDTA and 0.5 mM DTT.

Procedure:

Isolation of enriched nuclei:

400 **gm** liver from 2 month old rats (wistar strain) was washed twice in ice cold saline, minced thoroughly and homogenized in 2.5 litres of buffer A. The cell-free **homogenate** was centrifuged at 5000 rpm for 10 min. The pellet suspended in 700 ml of buffer A containing 2.2 M sucrose and the supernatant was discarded. Enriched nuclei were obtained by ultracentrifugation of the reconstituted pellet at 28,000 rpm for 1 h in a Beckman Ti-70 rotor. The nuclear pellet was washed once at 15,000 rpm with 200 ml of buffer A containing 1 M sucrose followed by 200 ml of buffer A with 0.1% triton **X-100**.

Lysis of Nuclei:

The nuclear pellet was resuspended in lysis buffer and subjected to lysis in an MSE sonicator with a macroprobe for 4 times, 30 s each, with two min intervals.

Polymin P precipitation:

10% Polymin P (pH 7.8) was added slowly to the lysate, while stirring to a final concentration of 0.35% during a period of 15 min. The precipitate was pelleted at 6000 rpm for 10 min. The Pellet was resuspended in 200 ml of PR buffer. Proteins were extracted from the **chromatin-polymin P** complex with 0.55 M NaCl, while stirring for 30 min. Nucleic acids were reprecipitated by adding extra polymin P up to concentration of 0.7% while stirring for **15** min. The nucleic acid precipitate was removed by centrifugation and the supernatant was filtered through glass wool.

Ammonium sulfate precipitation and dialysis:

The clarified supernatant was subjected to ammonium sulfate (60%) precipitation with continuous stirring for 1 h. The precipitate was collected by centrifugation at 12,000 rpm for 20 min. The pellet was resuspended in 100 ml of PR buffer and dialyzed against 3 X 1 liters of the same buffer over a period of 15 h. A precipitate formed during the dialysis, which was removed by centrifugation at 26,000 rpm for 20 min.

Chromatography on hydroxyapatite:

The clarified supernatant was loaded on a biogel-hydroxyapatite column equilibrated with PR buffer containing 200 mM potassium phosphate. The Proteins were eluted with a linear gradient of potassium phosphate from 200 mM to 700 mM. In these conditions, topo II elutes between 400 and 500 mM. The chromatography was repeated on a second biogel-hydroxyapatite column in the same conditions. The topo II containing fractions were pooled and concentrated in **centricon-10** concentrators. The final enzyme preparation was dialyzed in 2 X 1 liters of storage buffer.

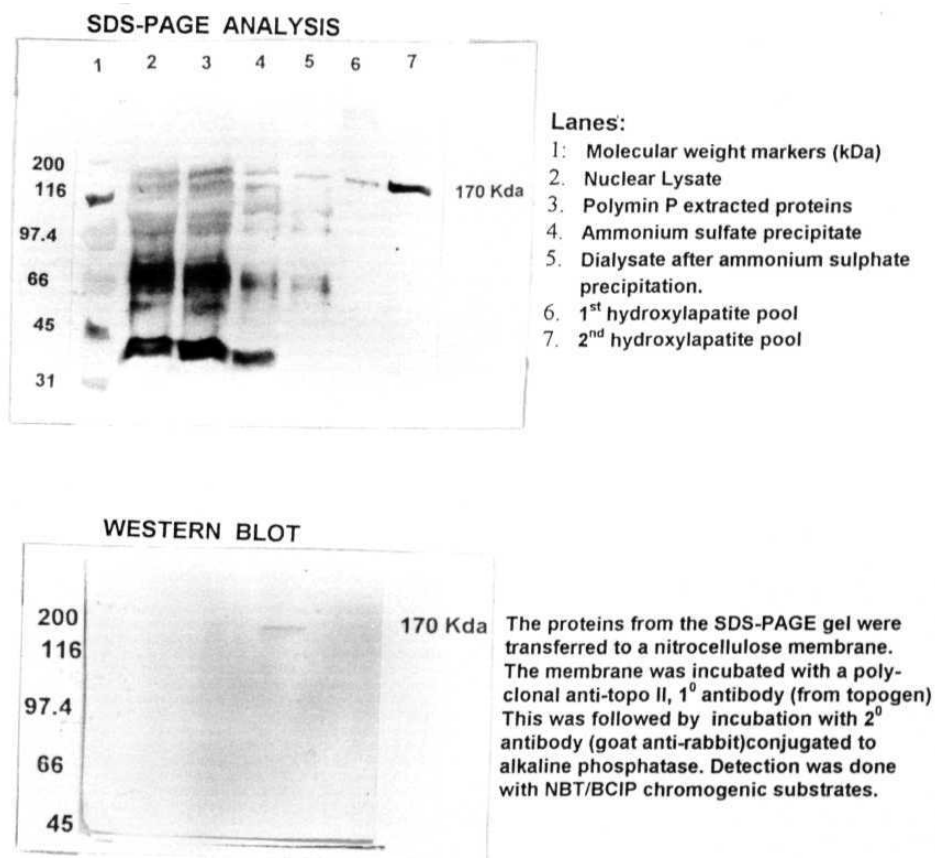
Characterization of topoisomerase **II**:

The purification profile of topo II is shown in a silver stained **SDS-PAGE** gel (10%) in Panel 10. The protein was confirmed by western blotting, with a polyclonal antibody against topo II. Protein concentration was determined by the Bradford method (1976). Enzyme activity was determined using the relaxation assay described in the 'Topoisomerase II Activity Assays' section.

Definition of enzyme activity: One unit of topo II activity is defined as the minimal amount of the enzyme required to completely relax 0.3 μg (0.5 nM base pairs) of negatively supercoiled pBR322 plasmid DNA in the presence of Mg^{2+} ions, in a specified period of time at 30 °C.

PANEL 10

CHARACTERIZATION OF RAT LIVER TOPOISOMERASE II



DNA BINDING STUDIES:

Thermal denaturation studies on calf thymus DNA to determine binding of the metal complexes to DNA:

Calf thymus DNA (sodium salt) was dissolved in 1 mM sodium phosphate buffer containing 1 mM sodium chloride. DNA concentration was adjusted to give an absorbance of 1.0 in 1 ml at 260 nm. The metal complexes were added to DNA at concentrations which gave drug to nucleotide ratios of 1:40, 1:20, 1:10, 1:5 and 1:1 respectively. The samples were incubated in 1 ml quartz cuvettes for 2 minutes to allow drug-DNA interaction. A Hitachi 150-20 spectrophotometer was set to give a 1 °C rise in temperature per minute with a KPC-6 thermo-programmer and SPR-7 temperature controller. Increase in absorbance at 260 nm was recorded from 40 to 90 °C. T_m was determined from the denaturation curves and the data was plotted.

Curve Width Analysis of the melting temperature curves:

Curve width is the temperature range between which 10% to 90% of the absorbance increase occurs during the temperature induced melting of DNA. Curve width of the individual melting curves was calculated by the procedure of Kelly et al. (1985). The data was plotted as drug/nucleotide (D/N) versus curve width and analyzed.

Circular Dichroism Studies to Determine Conformational Changes induced in DNA upon Interaction with the Drugs:

The RuBen drugs and pBR322 DNA proportionately corresponding to that required for inhibition of topo II relaxation activity and 0.6 μg DNA (the maximum concentration of drug and DNA used in the relaxation assay) were incubated in the relaxation buffer for 5 min to allow drug-DNA interaction. The DNA intercalator, **m-AMSA**, corresponding to 100 μM in the topo II assay was included as a control. CD. spectra of the samples was measured between 240 and 300 nm wavelength in a Jasco J-715 spectropolarimeter. Molar ellipticity [9] was calculated from the CD. spectra using the formula- $[\theta] = \frac{M_r}{c \cdot l} \cdot [\psi]$ where [9] is molar ellipticity, M_r is mean residual weight, ψ is CD. value in milli degrees, l is path length of the cuvette in cm and c is the concentration of the sample (DNA) in gm nucleotide phosphate per ml.

TOPOISOMERASE II ACTIVITY ASSAYS TO DETERMINE MOLECULAR MECHANISM OF ACTION OF THE METAL COMPLEXES:

DNA relaxation assay:

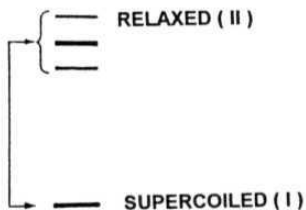
Relaxation of the supercoiled DNA occurs in a stepwise manner. Each DNA relaxation step of topo II involves a change in the linking number of DNA by 2. Thus, in an incomplete reaction, the supercoiled DNA band (form I DNA) disappears and a ladder of bands (each band differing in linking number by 2 from its successive band) in different

stages of relaxation appear. Complete relaxation of the plasmid DNA can be visualized as a single band (form II) of DNA. This is because, all the bands in the ladder are completely relaxed into form II DNA. In the present study, an incomplete relaxation reaction has been employed for the drug assays.

This assay was performed following the procedure of Osheroffet al. (1983). The reaction mixture (20 μL) contained relaxation buffer (50 mM Tris-HCl, pH 8.0), 120 mM KCl, 0.5 mM EDTA, 0.5 mM DTT, 10 mM MgCl_2 , 30 $\mu\text{g/mL}$ BSA, 1 mM ATP), 0.6 μg of negatively supercoiled pBR322 plasmid DNA and increasing concentrations of the RuBen drugs. The reaction was initiated by adding 2 units (~8 nmole) of topo II and incubated at 30 $^{\circ}\text{C}$ for 15 min. The reaction was stopped by adding 2 μL of 10% SDS. To this, 3 μL of loading dye (0.5% bromo-phenol blue, 0.5% xylene cyanol, 60% sucrose, 10 mM tris-HCl, pH 8.0) was added, and the products were separated on a 1% agarose gel in 0.5x TAE buffer (20 mM tris-acetate, 0.5 mM EDTA) at 50 V for 8 h. The gel was stained with ethidium bromide, visualised using a Photodyne UV transilluminator and photographed.

PANEL II

PATTERN OF RELAXATION BANDS IN AN AGAROSE GEL



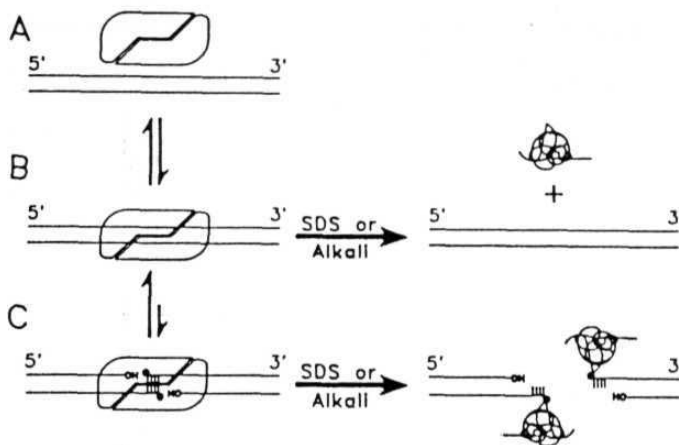
DNA Cleavage Assay:

In presence of a topo II poison, a ternary 'cleavage complex' consisting of 'cleaved DNA-drug-topo II' is formed. The formation of this complex is confirmed by treating the reaction products of the cleavage assay with SDS. This detergent treatment denatures the enzyme, thus liberating the cleaved DNA. Proteinase K treatment completely disrupts the association of enzyme with DNA. This cleaved DNA is visualized as a form III (linear plasmid DNA) in an agarose gel.

The formation of cleavage complex was assayed following the procedure of Zechiedrich et al (1989). The 20 μL reaction mixture contained relaxation buffer (minus ATP), 0.6 μg of pBR322 supercoiled DNA and increasing concentrations of drugs. The reaction was initiated by adding 10 units (40 nmol) of topo II and incubated at 30 °C for 15 min. The reaction was stopped with 2 μL of 0.5 M EDTA and 2 μL of 10% SDS. The DNA bound protein was degraded by incubating the reaction mixture with 2 μL of 1 mg/mL Proteinase K at 45 °C for 1 h. The products were separated on 1% agarose gel for 8 h at 50 V in 1x TAE buffer (40 mM tris-acetate, 1 mM EDTA), stained and photographed. The linear DNA band was quantified in terms of percentage of total DNA in a UVP gel documentation system.

PANEL 12

DNA CLEAVAGE ASSAY OF TOPOISOMERASE II



DNA stimulated ATPase activity of topoisomerase II:

Binding of DNA and ATP to topo II induces **conformational** changes in the enzyme, which stimulates ATP hydrolysis by the enzyme. Drugs that inhibit the relaxation activity of topo II also interfere with the ATPase activity of topo II. The products of the ATPase reaction were subjected to thin layer chromatography. The resolved components (ATP, ADP and P_i) were cut out of the TLC sheet and quantified as described below.

This assay is a modified procedure of Osheroff et al (1983). The 20 μL reaction mixture contained relaxation buffer (the 1 mM ATP component contained 0.025 μCi $\gamma\text{P}^{32}\text{-ATP}$), 0.6 μg of pBR322 DNA and increasing concentrations of drugs. The reaction was initiated with 2 units of topo II and incubated at 30 $^{\circ}\text{C}$ for 15 min. The reaction was stopped with 2 μL of 0.5 M EDTA. The reaction mixture was spotted on PEI cellulose-F TLC sheets and the sheets were subjected to thin layer chromatography in 1 M lithium chloride solution. In these conditions, $\gamma\text{P}^{32}\text{i}$ migrates first followed by ADP and $\gamma\text{P}^{32}\text{-ATP}$. After resolution, the bands were monitored under reflected UV light at 366 nm in a Photodyne transilluminator. The illuminated bands of $\gamma\text{P}^{32}\text{ATP}$, ADP and ^{32}Pi were cut out of the sheet and counted for ^{32}P in a liquid scintillation counter.

Immuno-precipitation assay to determine presence of drug in the Cleavage complex:

Cleavage assay was performed in the presence of 500 μM of the drugs. After the reaction, topo II in the cleavage complex and in free form was immuno-precipitated with 0.04 units of anti-topo II antibody. The antibody-antigen complex was trapped in 20 μL of protein A agarose. This was washed twice with 1x relaxation buffer at 1000 rpm to remove unbound reactants. Topo II in the immuno-precipitate was released by adding 20 μL of 1% trichloro acetic acid (TCA). To this, 10 μL of 1 N HCl was added and the samples were boiled in steam to dryness. Samples were then analyzed for parts per million of iron or ruthenium metal by Atomic Absorption Spectroscopy in an ECIL-AAS4129 atomic absorption spectrometer. For the RuBen(dmso) and RuSAL, the same assay was also performed with

³H-thymidine labeled DNA. After TCA treatment, the samples were spotted on filter paper strips and the radioactivity was measured.

APOTRANSFERRIN BINDING BY THE RUTHENIUM (RuBen) DRUGS:

uv-visible spectroscopic studies to determine apotransferrin binding:

This assay was carried out by the procedure described by Kratz et al. (1994). Briefly, ATr was dissolved in a physiological buffer containing 4 mM NaH₂PO₄, 100 mM NaCl, 25 mM NaHCO₃ (pH 7.4) and the uv-visible spectra of the RuBen drugs (50 μM) in absence and presence of 50 μM ATr was monitored after incubating the samples in the above buffer for 4 and 8 h at 37 °C. The data was plotted as absorbance versus wavelength in nm.

Circular Dichroism studies to determine apotransferrin binding:

The circular dichroism studies were carried out in the same manner as the uv-visible spectroscopic studies by following the method of Kratz et. al. (1994). In these studies, 100 μM ATr was incubated with 100, 200 and 300 μM of the drugs (drug to ATr ratios of 1:1, 2:1 and 3:1) for a fixed time period of 8 h. The increasing drug concentrations were used for determining the concentration of drug required for saturated binding with ATr, after 8 h. incubation. The C.D. spectral data was converted to molar ellipticity [8] using the formula described in the DNA binding studies. The molar ellipticity data of ATr alone was subtracted from that of drug-bound ATr to give the change in ellipticity (Δθ). Δθ was plotted against wavelength in nm and the data was analyzed.

Release of the RuBen drugs from ATr:

To analyze if Tr binding by the RuBen drugs was reversible, pH of the drugs in solution was lowered to 4.5 with citric acid to simulate the low pH of the endosomes (in **endosomes**, the natural release of iron from Tr occurs at this pH). Release of the RuBen drugs from Tr was monitored through **uv-visible** spectroscopy. To analyze if Tr binding and release affected the topo II poisoning ability of RuBen drugs, the **Tr-released** drugs were first subjected to **TCA** precipitation (**final** concentration of 10%) for 1 h on ice and the samples were **centrifuged** at 12,000 **rpm** to sediment the protein. The supernatants containing the drugs were taken, the concentration of drugs adjusted to that required for cleavage complex formation, and the cleavage assay was carried out in presence of these Tr-released drugs.

ANTICANCER ACTIVITY ASSAY:

[³H]-Thymidine incorporation by proliferating cells was the assay used for determining the *in vitro* anticancer activity of the Ferrocene and RuBen drugs. Five different human cancer cell lines were used for performing this assay. The cell lines are HL-60 (promyelocytic leukemia), HUT-78 (T-cell lymphoma), Colo-205 (colon **adeno-carcinoma**), A-431 (skin carcinoma) and **ZR-75-1** (breast carcinoma). The cells were procured from the National Centre for Cell Science, Pune.

The cells were grown in **RPMI-1640** medium supplemented with 10% fetal calf serum (A-431 cells were grown in **DMEM** with 10% serum). 0.2×10^6 **cells/200 μ l** were distributed in triplicates in 96 well microtitre tissue culture plates. The cultures were incubated for 16

hours at 37 °C in a CO₂ incubator (Forma Scientific) maintaining 5% CO₂ atmosphere. Increasing concentrations of the drugs were added to the cells in culture. The DNA intercalating topo II poison, **m-AMSA**, was used as a positive drug control (positive and negative controls always contained an equal amount of DMSO present in the drug treated samples). The drug treatment was stopped after 6 h by **centrifugation** and change of media. After this, the cultures were further incubated for 48 h. The cultures were then pulsed with 0.5 μ Ci of ³H-thymidine and incubation was continued for 4 h to allow thymidine incorporation by the proliferating cells. In case of non adhering cells (HL-60 and **HUT-78**), the cultures were directly harvested on glass microfibre strips using a **Skatron** automated cell harvester. In the adhering cell cultures (**A-431**, Colo-205 and ZR-75-1), the medium was removed and the adhering cells were treated with 10 μ L of trypsin-EDTA (0.25% trypsin, 1mM EDTA) for 5 min at 37 °C to release the cells from the adhering surface. Trypsinization was stopped by adding 10 μ L of serum to the cells. The original cultures were then added back to the wells and the cells were harvested as described above. Radioactivity was measured in a Wallac liquid scintillation counter. The mean result of three independent experiments conducted in triplicates was plotted as drug concentration versus percentage of proliferation.

ANTICANCER ASSAY USING THE Tr-BOUND RuBen DRUGS:

The same procedure described above was used for estimating the anticancer activity of the Tr-bound RuBen drugs. The colon carcinoma (colo-205) and breast carcinoma (ZR-75-1)

cells were used in this study. Increasing concentrations of the Tr-bound RuBen drugs (at saturated binding) were added to the cells. **m-AMSA**, in presence and absence of ATr was included as a control. The incubation and harvesting was carried out as described above. The data was plotted as a comparison between the Tr-bound and unbound drugs.

Chapter 3

TOPOISOMERASE II POISONING AND ANTICANCER ACTIVITY BY DNA NON-BINDING DERIVATIVES OF FERROCENE.

INTRODUCTION

Numerous inorganic and organic iron compounds and ionic ferricinium salts of the type $[(C_5H_5)_2 Fe^+ X^-]$ have earlier been shown to possess anticancer activity, but they also cause typical iron toxicity (Collier and **Krauss**, 1981; Kopf-Maier and Kopf, 1988). The toxicity arises due to release of inorganic iron from the compounds, and its association with several biological molecules in various tissues. The toxic effects arise because of two reasons. The first is, since iron is an oxidant, It produces hydroxyl radicals which attack all classes of biological molecules and produce effects like depolymerization of polysaccharides, inactivation of enzymes and initiation of lipid peroxidation (McCord, 1996). The second reason is that iron is a **nutrient** for invading **microbial** and neoplastic cells, and these cells possess exceptionally powerful mechanisms for obtaining host iron (Weinberg, 1995).

Neutral ferrocene compounds which are less toxic compared to the above mentioned derivatives have been used in the present study. The **organometallic** bonds between the metal atom and the cyclopentadiene rings as well as the uncharged iron atom account for the low toxicity. Mono- and di- substituted acetyl and **carboxaldoxime** derivatives were synthesized for this study (described in the Experimental Procedures section). Acetyl substitutions were used because the acetyl groups are strongly interacting ligands. The carboxaldoxime substitutions were designed because an earlier study with a cobalt salicylaldoxime complex showed that the **oxime** group plays a critical role in topo II poisoning (Jayaraju et. al., 1999).

In the present study, mechanism of topo II interaction and the resulting antagonism of the enzyme's activity was investigated. Anticancer activity of the ferrocene derivatives has also been carried out using **five** different human cancer cell lines.

Anticancer activity of the ferrocene drugs:

The^[3H] thymidine incorporation assays were carried out on five different cancer cell lines. The results (**Figure 1**) suggest that Fecp does not appreciably inhibit proliferation of any of the five cancer cell lines tested. The mono substituted acetyl and **carboxaldoxime** derivatives (AcFecp and FecpOx) showed a markedly higher inhibition than the parent molecule, Fecp. The di-substitued derivatives, DacFecp and FecpDox were more effective than the mono-substituted derivatives. FecpDox showed the highest potency of proliferation inhibition, almost comparable to that of the DNA intercalating drug, **m-AMSA**. These drugs were most effective on the Colo-205 cell line followed by HL-60, Hut-78, **ZR-75-1** and least on **A-431** cell line.

Topoisomerase II activity assays:

Inhibition of relaxation activity of topo II.

The relaxation assay using ferrocene derivatives (Figure 2) shows that Fecp had no inhibitory effect on the relaxation activity of topo II. AcFecp and FecpOx could completely inhibit the enzyme activity at 500 μM concentration. DacFecp could inhibit the enzyme activity at 400 μM and FecpDox at 300 μM concentrations respectively. The

DNA intercalating topo II poison, **m-AMSA** showed complete inhibition of relaxation activity at 75 μM concentration (**Figure 2, lane 3**).

Formation of Cleavage complex.

The formation of **enzyme-drug-DNA** cleavage complex could be evidenced by the appearance of linear DNA (form III plasmid DNA) in an agarose gel after SDS treatment of the cleavage products. The linearized DNA results from dissociation of the topo II homodimer from cleaved DNA by SDS. Neither Fecp nor AcFecp and FecpOx could induce cleavage complex formation, but the di-substituted compounds do so. DacFecp induces formation of linear DNA at a concentration of 400 μM and FecpDox shows a higher potency of cleavage complex formation at 200 μM concentration (**Figure 3**). **m-AMSA** induces cleavage complex at 150 μM concentration and also causes a small shift in DNA migration through agarose gel due to DNA intercalation. No such shift was observed for the ferrocene drugs.

Inhibition of ATPase activity of topo II.

This assay was performed to examine the effect of the drugs on the DNA stimulated ATPase activity of topo II. Relaxation assay was performed with increasing concentrations of the drugs in presence of $\gamma^{32}\text{P}$ ATP and the products were resolved on PEI Cellulose-F TLC sheets. Radioactivity of the resolved components was measured and data was plotted (Figure 4). The results show that Fecp could inhibit only 5.2% of the

DNA stimulated ATPase activity at 250 μM concentration while AcFecp, FecpOx and DacFecp could inhibit 37%, 40% and 46% of this activity. FecpDox was most effective in inhibiting the ATPase activity of topo II (52%). These results correlate well with the DNA relaxation assay.

Immuno-precipitation of the topoisomerase II cleavage products to determine the presence of ferrocene drugs in the cleavage complex:

Cleavage assay was conducted in the presence of 500 μM concentration of the ferrocene drugs. After incubation, the enzyme in the cleavage complex as well as the free enzyme was immuno-precipitated with anti-topo II antibody. The antigen-antibody complex was then trapped in protein A-agarose matrix. Samples were washed to remove unbound components and the bound enzyme was released from protein A agarose by 1% TCA and analyzed for presence of iron by atomic absorption spectroscopy. The results presented as percentage of drug bound (Figure 5, table) show that AcFecp and FecpOx associate with topo II alone and with topo II-DNA complex with the same affinity (~ 6%). DacFecp and FecpDox show a small increase in binding to topo II alone (9% and 12%) compared to the mono substituted compounds. In case of all the drugs, some amount of drug may be released from topo II in absence of DNA during the wash and TCA treatments. In presence of DNA however, DacFecp and FecpDox seem to be more strongly associated with topo II compared to AcFecp and FecpOx (15% DacFecp and 19% FecpDox is present in the topo II-DNA complex) due to which, there is a marked reduction in the release of the drug from the enzyme-DNA complex.

Melting temperature studies to determine Drug-DNA interaction:

Melting of calf thymus DNA was monitored in presence of increasing concentrations of drugs and T_m was determined from the melting curves. In the absence of drugs, DNA showed a T_m of 59 °C. The melting temperature curves for the highest concentration of drug used (1:1 drug to nucleotide ratio) are represented in **Figure 6A**, which show no change in the T_m of calf thymus DNA in presence of Fecp and a very minor increase in T_m in presence of FecpOx and FecpDox (~61 °C for both drugs). AcFecp and noticeably DacFecp slightly increased the T_m (64 ° and 68 °C at the highest concentration). On the other hand, **m-AMSA** induced a very steep increase in T_m (74 °C) at a drug to nucleotide ratio of only 1:10. The curve width analysis to determine the mode of DNA interaction revealed that though the acetyl groups increased the T_m of calf thymus DNA, they are essentially **DNA** non-binders as they show no change in curve width of the melting curves plotted against **drug/nucleotide (D/N)** (**Figure 6B**). m-AMSA however showed a steep increase in the curve width, a typical feature of DNA intercalators.

Molecular Modeling Analysis:

Molecular models of the ferrocene derivatives were generated as described in the experimental section. The models are shown in **Figure 7**. The lateral and longitudinal views of Fecp show an iron atom in the centre bonded to two cyclopentadiene rings through **organometallic** bonds between the iron atom and the π -orbitals of the ring hydrogens. In AcFecp and DacFecp, the acetyl groups orient towards the ferrocene backbone, along the longitudinal axis. This ‘closed-in’ conformation of the acetyl

derivatives may confer a weak DNA binding ability to them, but it may not provide the orientation for a strong topo II interaction. The carboxaldoxime groups in FecpOx and FecpDox, unlike the acetyl groups, extend out further from the backbone. This extended molecular conformation may allow the two oxime derivatives to interact strongly with topo II, but not with DNA, which explains their stronger topo II antagonism but not DNA binding. The double substitution in DacFecp and FecoDox may help these molecules to get a stronger hold on the enzyme. The extended conformation plus two electronegative atoms (nitrogen and oxygen) may confer on FecpDox, a stronger topo II poisoning ability. But the 'closed in' conformation and a single electronegative oxygen atom may limit a strong topo II interaction by DacFecp.

DISCUSSION

In the present study, two active chemical moieties, acetyl and **carboxaldoxime**, were substituted on ferrocene and tested whether the resulting compounds show anticancer action by interfering with the activity of **topoisomerase II**, an important molecular anticancer target.

The *in vitro* anticancer assay shows that while Fecp could not inhibit the proliferation of any of the cancer cell lines tested, the acetyl and carboxaldoxime substitutions on ferrocene (AcFecp and FecpOx) conferred potency to the compounds in this action. In the next step, by making a second substitution of the same groups to the singly substituted compounds, **anti-proliferative** action was substantially increased. The di-substituted derivatives (DacFecp and FecpDox) were clearly more effective than the mono-substituted compounds in proliferation inhibition. In both mono and di derivatives, it was observed that the carboxaldoxime group conferred a higher potency of proliferation inhibition compared to the acetyl group. Tests with more than two substitutions were not attempted as such compounds were inherently unstable.

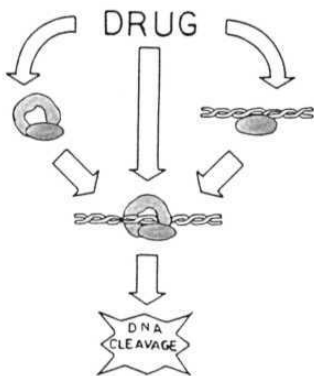
Topo II relaxation assay with the substituted ferrocenes showed that firstly the carboxaldoxime substitution on ferrocene was more potent than the acetyl substitution in inhibiting topo II activity and secondly the di-substituted derivatives were more effective than the mono-substituted derivatives. These compounds also inhibited the ATPase activity of the enzyme which was concomitant with inhibition of DNA relaxation. These

results argue that interfering with topo II activity may be a major mechanism for anticancer action of these compounds. But a stronger correlation between anticancer action and topo II inhibition would be established if the molecular mechanism of topo II inhibition by these compounds is known, i.e., whether they inhibit the enzyme activity by interfering with the ATPase activity alone (which only inhibits catalytic activity of topo II) or by forming an enzyme-DNA cleavage complex. The cleavage assay showed that only the di-substituted derivatives were able to form the cleavage complex. FecpDox was most potent in this action.

To determine if DacFecp and FecpDox were actually present in the cleavage complex which they induce and to partly understand the mode of cleavage complex formation, an **immuno-precipitation** assay with anti-topo II antibody was performed. In this assay, presence of drug in the cleavage complex was verified by atomic absorption spectroscopy of the **immuno-precipitated** cleavage products. The results show that AcFecp and FecpOx bind to topo II alone and were also present in the topo II-DNA complex at similar levels. But since they could not form the cleavage complex (as shown by the cleavage assay), the drugs may associate weakly with the enzyme and also the enzyme-DNA complex, thus interfering with the relaxation activity and ATPase activity of the enzyme to a certain extent but without forming the cleavage complex. As expected, DacFecp and FecpDox bound more strongly to topo II, showing a definite increase of the drug in the topo II-DNA complex compared to only topo II, especially in the case of FecpDox. This shows that the di-substituted compounds interact more strongly with the enzyme-DNA complex than only with the enzyme.

Several lines of evidence suggest that there are generally three routes of ternary complex formation by topo II poisons (Hertzberg et. al., 1989; Nabiev et. al., 1994; Corbett et. al., 1993). The first route is that the drugs predominantly interact with DNA (by intercalation or otherwise) and poison topo II when the enzyme binds to DNA. The DNA thermal denaturation studies in presence of the ferrocene compounds suggested that none of them interact with DNA. Though DacFecp slightly increases the T_m of calf thymus DNA, the curve width analysis suggests that it is essentially a DNA non-binder but the slight increase in T_m may be due to non specific electrostatic interaction with the phosphate backbone.

THREE MODES OF CLEAVAGE COMPLEX FORMATION



The second route is that, the drugs may not actually interact with the enzyme or DNA individually, but may bind specifically and exclusively to the binary complex of topo II and DNA. The third route is, the drugs may first bind to the enzyme in absence of DNA and then enter the ternary complex when the drug bound topo II interacts with DNA. The immuno-precipitation assay was helpful in interpreting which of the latter two mechanisms

are followed by the two di-substituted drugs. This assay showed that the enzyme alone does not show as much drug bound to it compared to the **enzyme-DNA** complex. Also, since the drugs do not bind to DNA, the conformational change induced in the enzyme after interaction with DNA may stabilize the drug association with the enzyme, which results in a stable topo **II-drug-DNA** ternary complex. In such an association, the drug promotes the cleavage of DNA but prevents DNA religation. These results suggest that DacFecp and FecpDox may follow the third mechanism of cleavage complex formation i.e., the drug **first** interacts with topo II in absence of DNA, the drug bound enzyme then interacts with DNA and cleaves it, leading to the formation of cleavage complex.

The carboxaldoxime group on ferrocene consistently conferred a higher potency compared to the acetyl group. The nitrogen and oxygen atoms of the carboxaldoxime group can form N-donor and O-donor interactions with topo II, whereas in the acetyl group, the single electronegative atom (carbonyl oxygen) may show a relatively weak enzyme interaction. The higher potency of DacFecp and FecpDox compared to AcFecp and FecpOx could be because the double substituted drugs could interact with two different regions on the enzyme, which may result in an overall stronger enzyme interaction compared to the mono-substituted drugs. Such an interaction may be responsible for the formation of the cleavage complex by these di-substituted drugs. Also, as suggested by the molecular modeling analysis, the extended orientation of the carboxaldoxime groups in FecpOx and FecpDox may also be an important determinant for a stronger interaction with topo II, leading to a stronger **antagonism**, compared to the acetyl derivatives.

DNA intercalating topo II poisons intercalate freely with the DNA of normal cells too and interfere with various genetic processes, posing a potential threat to the genetic material. It would be desirable to develop DNA non-intercalating topo II poisons, which should be relatively non-toxic to the genetic machinery, but specific for topo II poisoning. Though DacFecp and FecpDox are not as potent as m-AMSA in topo II poisoning and anticancer action, they are nevertheless promising candidates in their class of topo II poisons. **It** would be worthwhile to explore new substitutions on the ferrocene backbone to **specifically** poison the action of topo II and increase anticancer activity.

Figure 1: *In vitro* anti-proliferation activity of Ferrocenes was tested on five different cancer cell lines- Colo-205 (A), ZR-75-1 (B), A-431 (C), HL-60 (D) and HUT-78 (E). The cells were incubated with increasing concentrations of the ferrocene drugs for 6 h., after which the drug treatment was stopped. Following a further incubation for 48 h, ³H thymidine incorporation was performed for 4 h. as described in methods. The cells were harvested and radioactivity was measured. Values are presented as mean of three independent experiments. Data is graphically expressed as percentage of cell proliferation versus concentration of drug in μM . The drugs are most potent on the colon carcinoma (colo-205) followed by HUT-78, HL-60, ZR-75-1 and A-431. m-AMSA also showed a similar profile of anticancer activity in all the cell lines except in the case of ZR-75-1, on which it was more potent than on HL-60.

FIGURE 1

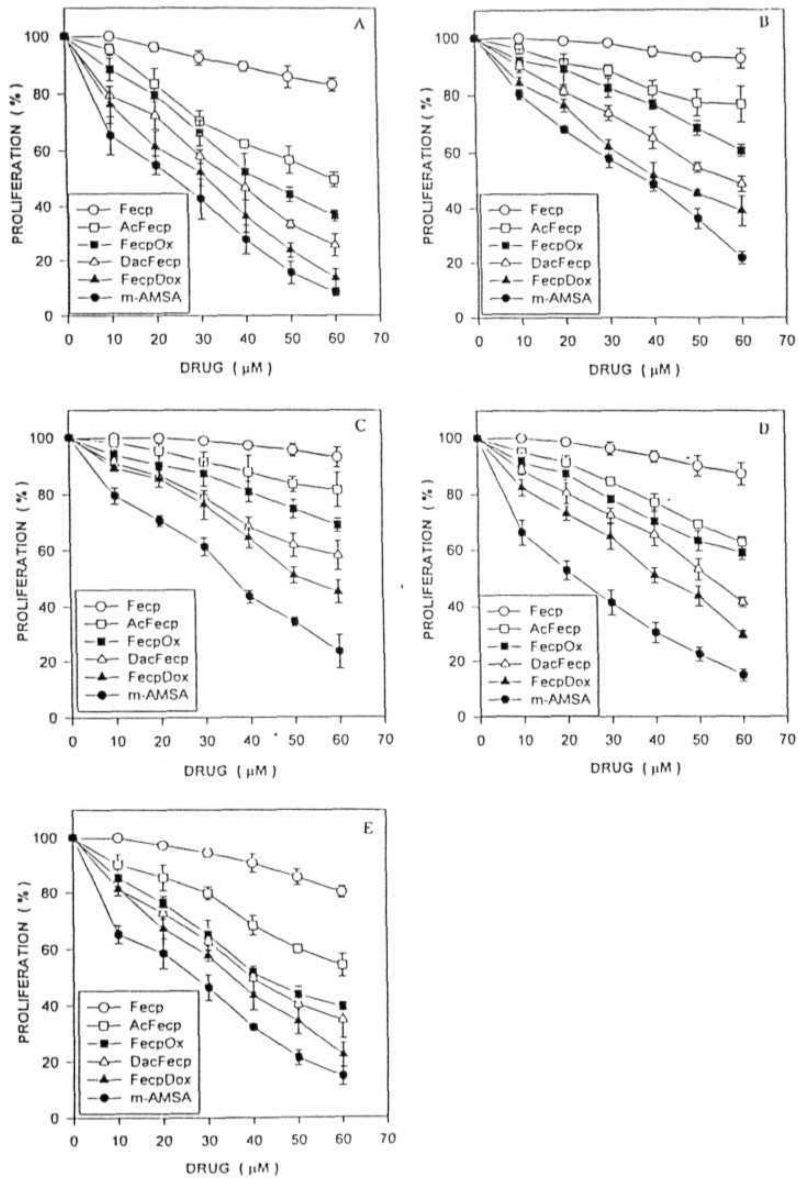


Figure 2: Effect of Fecp, AcFecp, FecpOx, DacFecp and FecpDox on topo II catalyzed DNA relaxation activity. Supercoiled pBR322 DNA(lane 1) was incubated with topo II in the absence(lane 2) or presence of 75 μM m-AMSA(lane 3) and 100, 200, 300, 400 & 500 μM Fecp (lanes 4-8), 100, 200, 300, 400 & 500 μM AcFecp (lanes 9-13), 100, 200, 300, 400 & 500 μM FecpOx (lanes 14-18), 100, 200, 300 & 400 μM DacFecp (lanes 19-22) and 100, 200 & 300 μM FecpDox (lanes 23-25). The positions of supercoiled (form 1) and nicked circular (form 2) DNA are indicated by I and II.

FIGURE 2

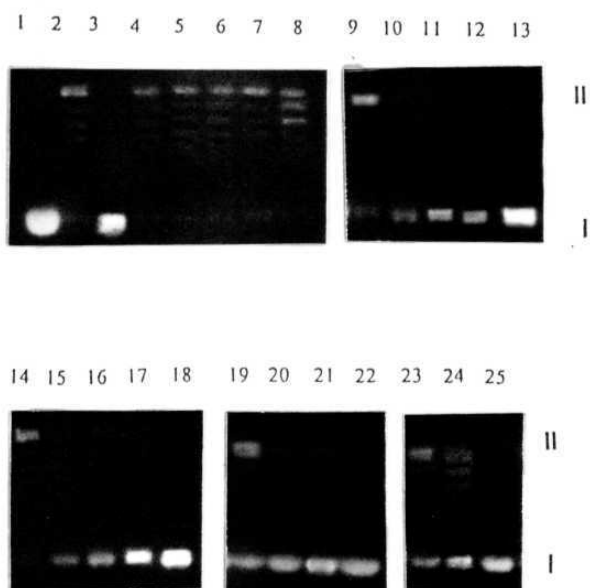
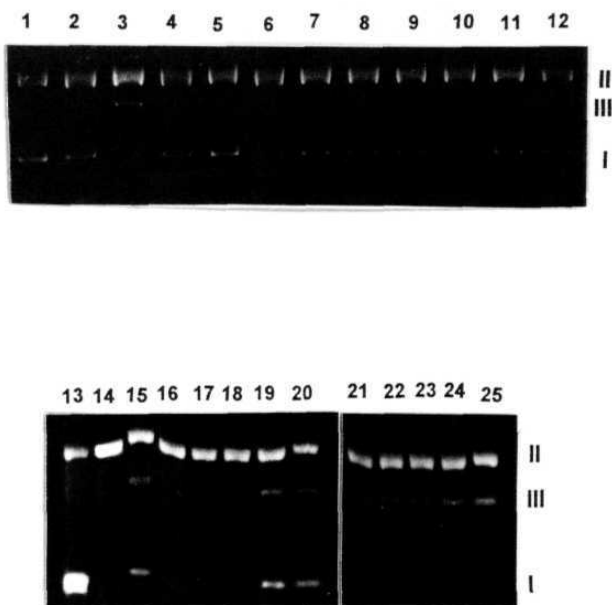


Figure 3: (A) Cleavage reaction was performed by incubating **supercoiled** pBR322 DNA (lane 1) with topo II (lane 2) in presence of 100 μM m-AMSA (lane 3), 300, 400 and 500 μM of Fecp (lanes 4 to 6), the same concentrations of AcFecp (lanes 7 to 9) and FecpOx (lanes 10 to 12); Lane 13 is DNA alone, lane 14 is DNA+topo, lane 15 is DNA+topo II+ 150 μM m-AMSA; DNA+topo II+ 100, 200, 300, 400 & 500 μM of DacFecp (lanes 16 to 20) and 100, 200, 300, 400 & 500 μM of FecpDox (lanes 21 to 25). The positions of supercoiled, nicked circular and linear (form 3) DNA are indicated by **I**, **II** and **III**. (B) Percentage of linear DNA formed with increasing concentration of DacFecp and FecpDox.

FIGURE 3

A



B

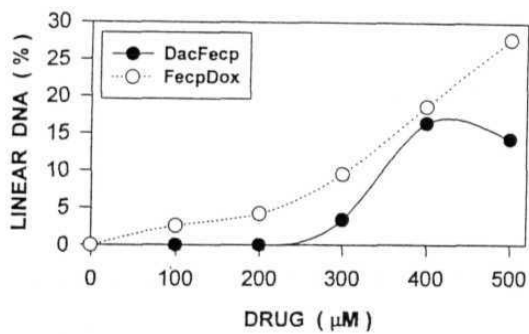


Figure 4: Inhibition of ATPase activity of topo II by Fecp, AcFecp, FecpOx, DacFecp and FecpDox. ATP hydrolysis in presence of increasing concentrations of the drugs are presented as mean of 3 experiments. Data is plotted as percentage inhibition of ATP hydrolysis versus concentration of drug in μM .

FIGURE 4

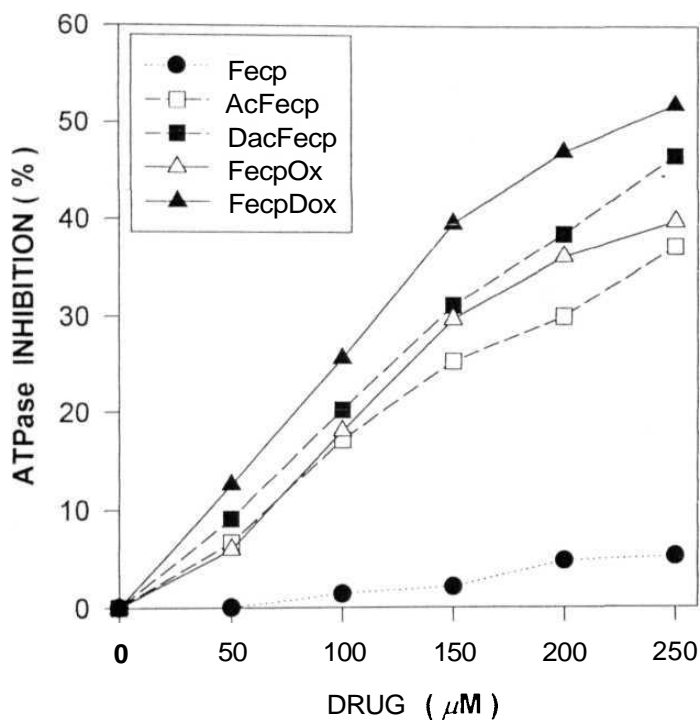


FIGURE 5

Table: Cleavage assay was conducted with drug + topo II and drug + topo II + DNA. The cleavage products were immunoprecipitated with topo II antibody. A drug control and drug + DNA control were included in the cleavage assay to check for non specific interaction of the drugs with DNA, antibody and Protein A agarose matrix. These controls did not show any significant non specific interaction. The concentration of the bound drugs is expressed as percentage of total drug bound.

	Fecp	AcFecp	FecpOx	DacFecp	FecpDox
Drug	0	0.8	09	1 +0.3	1
Drug + DNA	0	1+0.4	1 +0.3	1 +0.8	1 +0.3
Drug + Topo II	0.3	6 + 0.3	6 + 0.5	9 + 0.6	12+ 1.3
Drug + Topo II + DNA	0.5	5 + 0.7	6 + 0.2	15+ 13	19+ 1.8

^a Data are presented as a mean of three independent experiments conducted in triplicates, with standard deviations given against each value

Figure 6: (A) In the thermal denaturation assay, calf thymus DNA showed a T_m of 59 °C (—) in the absence of drugs. At a drug to DNA nucleotide ratio 1:1, Fecp (—) does not change the T_m , whereas FecpOx (--) and FecpDox (••••) induce a very small increase of ~2°, showing a T_m of 61 °C. AcFecp (—) and DacFecp (—) increase the T_m slightly at 64 ° and 68 °C. The DNA intercalator, m-AMSA induces a strong increase in T_m (74 °C) at a drug to nucleotide ratio only 1:10 (—). The melting curves of the other drug to DNA ratios which have been tested, are not shown. (B) D/N plotted against curve width shows a characteristic increase in curve width by m-AMSA (•). The ferrocenes do not change the curve width of the melting temperature curves suggesting that these compounds are essentially DNA non binders

FIGURE 6

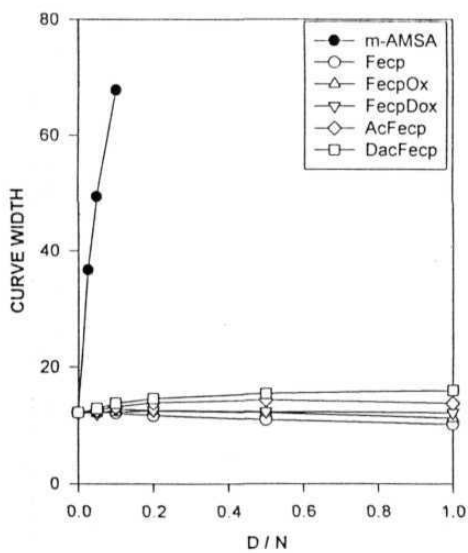
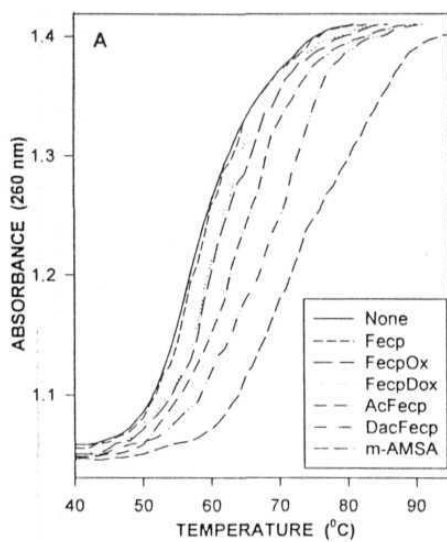
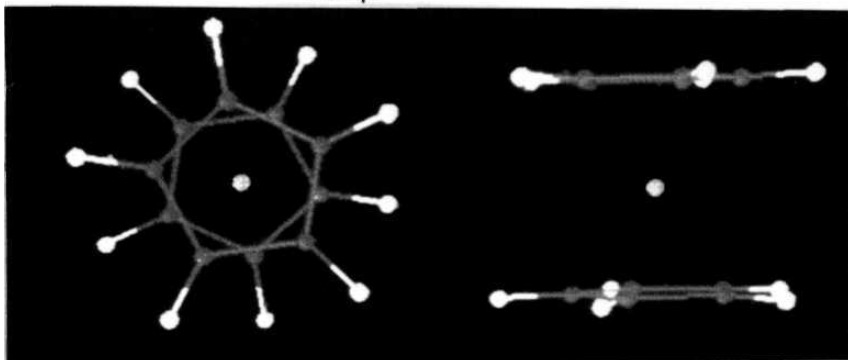


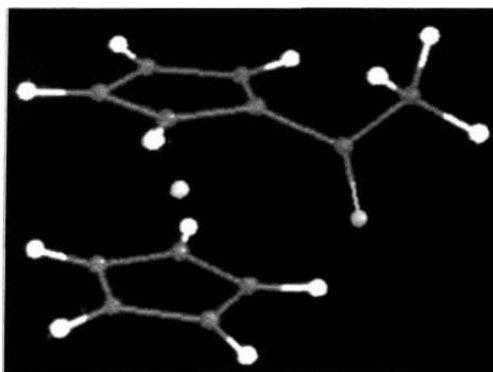
Figure 7: The lateral (left) and longitudinal (right) views of the molecular model of Fecp show an iron atom in the center (shown in light yellow) bonded to two cyclopentadiene rings through organometallic bonds between the iron atom and the π -orbitals of the ring hydrogens. The organometallic bond between the aromatic ring and the iron atom is not shown (the Spartan molecular modeling software does not show the organometallic linkages in energy minimized structures of organometallic molecules). In AcFecp and DacFecp, the acetyl groups orient towards the ferrocene backbone, along the longitudinal axis. The enzyme interacting oxygen atoms are shown in green. The carboxaldoxime groups in FecpOx and FecpDox, unlike the acetyl groups, extend out away from the backbone. The nitrogen atom of the 'N-OH' (oxime) group is shown in white and the oxygen in green.

FIGURE 7

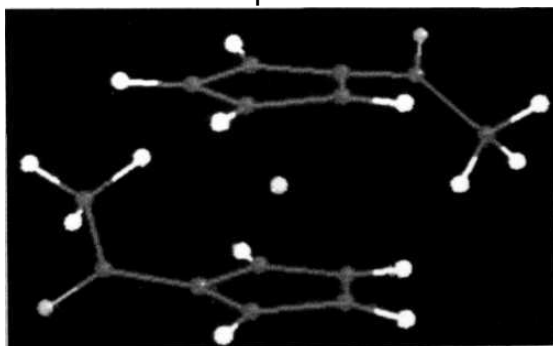
Fecp



ACFecp

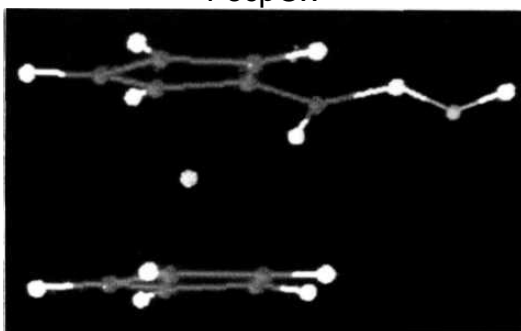


DacFecp

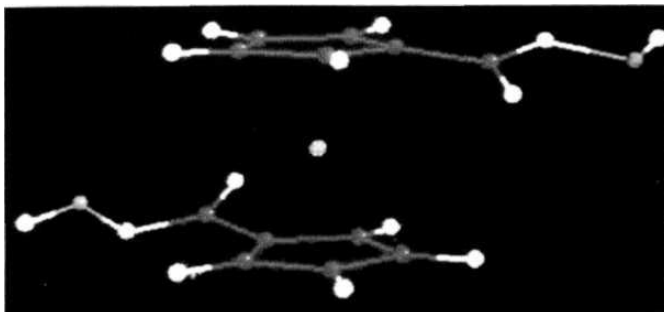


CONT'D.. FIGURE 7

FecpOx



FecpDox



Chapter 4

TOPOISOMERASE II ANTAGONISM BY TWO STRUCTURALLY DISTINCT RUTHENIUM COMPOUNDS: ELUCIDATION OF A LIGAND DEPENDENT MODE OF ACTION

INTRODUCTION

Among the metal atoms used in anticancer metal complexes, ruthenium is most unique. It is a rare noble metal unknown to living systems and has a strong complex forming ability with numerous ligands. Numerous *in vitro* and *in vivo* studies reveal that ruthenium complexes bind covalently to DNA via N-7 atom of purines and cause cytotoxicity by possibly inhibiting cellular DNA synthesis (Kopf-Maier, 1994; Haiduc and Silvestru, 1994). Ruthenium complexes have a particularly strong affinity for cancer tissues than normal tissues. This is because ruthenium binds readily to transferrin molecules in plasma and is transported to the tumor tissues. Here, the ruthenium-transferrin complex is internalized into tumor cells through transferrin receptors which are abundantly expressed on the surface of tumor cells (Sava et. al. 1991). Hence, ruthenium compounds are not only promising cytostatic drugs, but can also serve as diagnostic tumor imaging agents, using the nuclides- ^{97}Ru or ^{103}Ru (Srivastava et. al., 1989). Ruthenium(III) complexes have been hypothesized to function as pro-drugs which are reduced to the more reactive ruthenium(II). In the 2+ oxidation state, they coordinate with biological macromolecules and induce cytotoxicity (Sava et. al. 1991). Numerous ruthenium complexes have earlier been reported to possess anticancer activity, some of these being more potent than cisplatin (Giraldi et. al., 1977, Clarke, 1989; Sava et. al., 1984, 1989, Mestroni et. al., 1989; Pacor et. al., 1991, Keppler et. al., 1990). A few of these compounds possessing exceptionally high anticancer activity are trans-[indazolium bis (indazole) tetrachlororuthenate(III), cis-[$\text{Ru}^{\text{II}}\text{Cl}_2$ (dimethylsulphoxide) $_4$] and trans-[$\text{Ru}^{\text{III}}\text{Cl}_4$ (dimethylsulphoxide) Imidazole] Na^+ . Though potent in anticancer action, these

compounds induce major liver and kidney damage which has hindered their clinical use until now. With an aim to develop novel anticancer ruthenium compounds which act on a single anticancer target, an organometallic ruthenium compound, RuBen(dmso) and a coordination complex of ruthenium, RuSAL, have been tested for topo II antagonism. Anticancer activity studies of these two ruthenium compounds have been carried out through [³H] thymidine incorporation on two human cancer cell lines.

RESULTS

Topoisomerase II activity assays:

Relaxation Assay:

DNA relaxation activity of topo II in the presence of increasing concentrations of RuBen(dmso) was significantly inhibited, and at 500 μ M, the drug could completely inhibit topo II catalysed relaxation of supercoiled pBR322 DNA (**Figure 8/1**). RuSal partially inhibits the relaxation activity at 300 μ M, with no significant increase in inhibition up to 500 μ M (**Figure 8/2**).

Cleavage assay:

The ability of the two drugs to induce stabilization of 'topo II-cleaved DNA' complex was studied through this assay. The formation of 'enzyme-drug-DNA' cleavage complex can be evidenced by the appearance of linear DNA which results from DNA strand breaks caused by dissociation of the topo II homodimer in presence of SDS. RuBen(dmso)

stabilizes the enzyme-DNA cleavage complex at 200 μ M in a very low level, as analyzed by quantification of the form III DNA (linear) which was found to be equivalent to 17% of total DNA. At 300 μ M, the linear DNA increases to 40.5% and slightly decreases to ~37% for the higher drug concentrations (Figure 9). RuSal does not form the cleavage complex even at a concentration of 500 μ M or higher.

Presence of ruthenium and DNA in Cleavage complex:

The immuno-precipitation assay was performed to get a direct evidence for the involvement of RuBen(dmsO) in the drug induced cleavage complex. Cleavage assay was carried out in the presence of 500 μ M concentrations of the ruthenium drugs. The immuno-precipitation was carried out and after the TCA precipitation step, the samples were analyzed for presence of ruthenium by atomic absorption spectroscopy. The results presented in Figure 10, table A, show that 46% of 500 μ M RuBen(dmsO) is present in the cleavage complex, but only 9% of RuSal is found in the cleavage complex. Concentrations less than 2% (20 ng) could not be determined accurately by the instrument used (ECIL-AAS4129) and they were expressed as such

Presence of DNA in the cleavage complex was confirmed by repeating the same assay in the presence of ^3H labeled DNA. After TCA treatment, the products were spotted on filter paper strips and radioactivity was measured. The results presented in Figure 10, table B, show that 21% of the 0.6 μ g DNA is present in the RuBen(dmsO) induced cleavage complex, as compared to 3% in the RuSal induced complex. All the controls correlate well

with the atomic absorption spectral data. These results confirm the bi-directional interaction of RuBen(dmsO) with DNA and topo II while RuSal does not exhibit a similar effect.

Effect of the ruthenium compounds on ATPase activity of topoisomerase II:

This assay was performed to examine the effect of ruthenium drugs on the DNA stimulated ATPase activity of topo II. Relaxation assay was performed with increasing concentrations of the drugs in presence of $\gamma^{32}\text{P}$ ATP and products were resolved on PEI Cellulose-F TLC sheets. The bands corresponding to the individual components were cut out and were counted for $\gamma^{32}\text{P}$ in a liquid scintillation counter. The results show that RuBen(dmsO) inhibits ATP hydrolysis in a dose-dependent manner. At 500 μM concentration, it inhibits 50% of the total ATPase activity while RuSal does so at a concentration of 13.5% (Figure 11).

Drug-DNA binding studies:

*Thermal **denaturation** studies to determine Drug-DNA interactions.*

Melting of calf thymus DNA was studied in the presence of increasing concentrations of the drugs. The melting temperature curves show a gradual increase in T_m with increasing concentrations of RuBen(dmsO) and RuSal (Figure 12, **A,B**). Curve width analysis of the melting curves shows that RuBen(dmsO) and RuSal exert a minor increase, while the DNA intercalator, m-AMSA, induces a sharp increase in the curve width of the melting curves

Figure 13 A shows the curve width analysis. In the next figure (**Figure 13 B**), D/N was plotted against T_m , and the slopes of the curves were calculated to determine the stoichiometric binding of drug to DNA. RuBen(dmsO) showed a DNA binding stoichiometry of 4 nucleotides and a weak binding stoichiometry of 7 nucleotides per drug molecule, while RuSal showed a stoichiometry of 4 nucleotides per molecule.

Circular dichroic spectra of pBR322 DNA shows that RuBen(dmsO) and RuSal marginally affect DNA conformation at the concentration which shows maximum inhibition of topo II relaxation activity. In comparison, m-AMSA induces a significant change in DNA conformation (**Figure 14**).

Anticancer activity assay:

The anticancer activity studies on the ferrocene drugs revealed that the colo-205 and ZR-75-1 cells were most stable in terms of proliferation and reproducibility of drug assays. Consequently, these two cell lines were used in all the anticancer assays with the ruthenium compounds. The results of the thymidine incorporation assay on the two human cancer cell lines (colo-205 and ZR-75-1) suggest that both RuBen(dmsO) and RuSal possess significant anticancer activity, that of RuBen(dmsO) being superior to RuSal (**Figure 15**). As was the case with the ferrocene drugs, the two ruthenium drugs were also most effective on the colo-205 cells and less effective on the ZR-75-1 cells. The DNA intercalating drug, m-AMSA, was however the most potent and completely inhibited the proliferation of colo-205 cells at 80 μM concentration, while the ZR-75-1 cells showed a minimal proliferation of 10% in the presence of this drug.

Molecular modeling analysis:

The molecular models of RuBen(dmsO) and RuSal reveal that the two ruthenium complexes are structurally disparate (**Figure 16**). In RuSal, the ruthenium atom is in a bidentate coordination with two salicylaldoxime ligands. The salicylaldoxime ligands are spatially oriented in two different planes at an angle of $\sim 40^\circ$ to each other along the horizontal axis. RuBen(dmsO) with its octahedral geometry is a more complex molecule. The ruthenium atom has an organometallic bond with the benzene ring and ionic bonds with two chloride atoms. A 'dmsO' group is in a coordination bond with the ruthenium atom. The chlorides and the dmsO group are oriented in one direction, and these may constitute the topo II interaction domain on the drug molecule. The ruthenium atom, oriented in the opposite direction, may constitute the DNA binding domain (details in discussion).

DISCUSSION

Inhibition of DNA replication and the associated effects has been implicated as the major reason for anticancer activity of ruthenium compounds (Clarke, 1989). The data presented in this work suggests that apart from DNA, topo II poisoning may also be an effective mode of anti-neoplastic activity for some of the anticancer ruthenium compounds. The relaxation, cleavage and immuno-precipitation assays clearly show that RuBen(dmsO) can poison topo II through the formation of a drug-induced cleavage complex, while RuSal shows partial inhibition of relaxation activity and does not poison the enzyme through cleavage complex formation.

Analysis of the curve width of DNA melting curves is a useful way to distinguish between intercalative and external binding (Kelly et. al., 1985). DNA intercalators substantially increase the width of melting curves, while external binders have lesser effect on this parameter. m-AMSA shows a curve width typical of a DNA intercalator while RuBen(dmsO) and RuSal exhibit curve widths similar to DNA external binders, like the 2,2'-bipyridyl and terpyridyl complexes of ruthenium (Kelly et. al., 1985). RuBen(dmsO) and RuSal show similar DNA binding ability, suggesting that the ruthenium atom (similar in both) may directly interact with DNA. The ruthenium atom may interact with DNA through ionic or covalent bonding with the nucleotide bases, without disturbing the helix. In RuBen(dmsO), an intercalative mode of DNA binding is not possible because the benzene ring forms an organometallic bond with the ruthenium atom, which prevents π -orbital stacking interaction of the aromatic ring with DNA bases. In RuSal, since there are

no organometallic bonds, the π -stacking orbitals in the salicylaldoxime ligand are not affected. But the compound does not intercalate to DNA. Whether the orientation of the salicylaldoxime ligands or the presence of the metal atom absolve an intercalative mode of binding, it cannot be explained at present. Interestingly, RuBen(dmsO) and RuSal bind similarly to DNA but show different sensitivity for topo II poisoning. This points towards ligand involvement for topo II poisoning.

The strong DNA binding ability of the ruthenium drugs prompted us to examine if these compounds produce conformational changes in DNA which could simply block the enzyme activity without actually interacting with the enzyme. Circular Dichroism analysis of DNA in the presence of RuBen(dmsO) and RuSal showed an inconsequential change in DNA conformation. Further, the ATPase assay shows that RuBen(dmsO) inhibits the DNA-stimulated ATPase activity of topo II. This is possible only if the drug induces formation of an enzyme-drug-DNA cleavage complex, or the drug directly interacts with the enzyme at the ATPase domain. The first possibility appears true, which is supported by the cleavage reaction

Based on molecular modeling analysis and superimposition of drug structures, a putative structure was proposed for topo II cleavage complex forming drugs, which shows that these drugs have three distinct domains in them; the first is a planar ring system, the second is a pendant ring and the third is a pendant moiety of heterogeneous structure (MacDonald et. al., 1991). Though studies have shown that this structure is not an absolute requirement for topo II poisoning (Capranico et. al., 1994), most poisons do have large planar aromatic domains for DNA binding and substituents for enzyme interaction. It

is interesting that a small molecule like RuBen(dmsO), with only one aromatic ring could poison topo II by cleavage complex formation. RuBen(dmsO) has an octahedral geometry (Bennet and Smith, 1974) which may facilitate the spatial orientation of its ligands to form interactions with enzyme. Thus, interaction by the benzene, chlorides and the dmsO ligand of RuBen(dmsO) may play an important role in poisoning of the enzyme.

Prior to enzyme action, RuBen(dmsO) bound to DNA may interact with a catalytic domain of topo II through any of its ligands. The benzene ring may fit into some pocket in the enzyme and sterically hinder the conformational changes in the enzyme required for DNA religation. Whatever is the mode of action, RuBen(dmsO) traps the cleaved DNA and topo II in the cleavage complex and prevents DNA religation activity of the enzyme. The cleavage assay confirms that RuBen(dmsO) indeed shifts the enzyme's cleavage/religation equilibrium towards DNA cleavage.

In RuSal, the planar salicylaldoxime ligands are attached to the metal atom and oriented with an angle of $\sim 40^\circ$ to each other along the planar axis. This orientation may block enzyme action to a certain extent when the DNA bound drug approaches the catalytic domain of topo II, but may not allow a strong interaction with the enzyme. Even if an interaction does take place, the coordinated metal-ligand bonds may not provide a strong interface for cleavage complex formation. This could explain why RuSal partially inhibits the relaxation activity of topo II, but does not induce cleavage complex formation.

DNA intercalating topo II poisons intercalate to DNA through π -stacking interactions of their planar rings with DNA bases. The side chains of these drugs are involved in enzyme interaction. Such an interaction is important in facilitating the formation of drug-enzyme-

DNA ternary complex. Though **RuBen(dmso)** binds externally to DNA nucleotides, it may still form a similar ternary complex in which the metal atom binds to DNA and ligands on the metal atom interact with topo II.

These findings allow us to propose a probable mode of topo II poisoning by **RuBen(dmso)**. The metal atom interacts covalently or non-covalently with DNA nucleotides and the ligands form cross-links with the enzyme and prevent DNA religation step, leading to the formation of a stable drug induced cleavage complex, which is the hallmark of most topo II poisons. Such topo II poisons increase the steady state concentration of cleavage complexes which harbor topo II associated double strand breaks. The accumulation of such DNA breaks in cells ultimately results in cell death by apoptosis or necrosis as described earlier. **RuBen(dmso)** could be categorized as a topo II poison which is a cleavable complex forming, DNA binding but non intercalating agent.

The anticancer activity assay shows that though **RuBen(dmso)** exhibited a higher potency of proliferation inhibition, **RuSal** also showed a very good proliferation inhibition of the cancer cells. This is interesting because **RuSal** does not interfere with the activity of topo II. This result and the similar DNA interaction of **RuBen(dmso)** and **RuSal** indicate that inhibition of cancer cell proliferation by both drugs may in part be due to a topo II independent mechanism, probably at the DNA level. In **RuSal**, the salicylaldoxime ligand may also cause significant anti-proliferative action. As an analogue of pyridoxal, salicylaldoxime is known to inhibit pyridoxal kinase activity and hinder transamination and decarboxylation processes leading to inhibition of protein synthesis, causing appreciable

cytotoxicity (**Lumme** and **Elo**, 1984). The higher anti-proliferation activity of **RuBen**(dmsO) in comparison with **RuSal** may possibly be due to topo II poisoning.

Studies indicate that antitumor activity of DNA binding drugs in most cases depends on their capacity to interfere with catalytic activity of topo II (Osheroff et. al., 1983; Zechiedrich et. al., 1989). We have limited the scope of this work to topo II targeting, though ruthenium drugs being DNA binding agents, may interact with other DNA binding proteins (eg. DNA polymerases) and other biomolecules in the cell leading to toxicity generally associated with chemotherapy.

A better understanding of the molecular action of **RuBen**(dmsO) and the inherent advantage of ruthenium compounds (in lieu of their selectivity for entering tumor tissues) can aid in designing novel ruthenium compounds which poison topo II with higher potency and show substantial anti-cancer action, while mitigating the toxic side effects to a certain degree.

Figure 8: **Effect of RuBen(dmso) (A) and RuSal (B) on topo II catalyzed DNA relaxation activity** Supercoiled pBR322 DNA (lane 1) was incubated with topo II in the absence (lane 2) or presence of 100 μ M-AMSA (lane 3) and 100, 200, 300, 400 & 500 μ M ruthenium drugs (lanes 4-8). The positions of supercoiled (form 1) and nicked circular (form 2) DNA are indicated by I and II. RuBen(dmso) completely inhibits the relaxation of DNA at 500 μ M while RuSal does not.

FIGURE 8

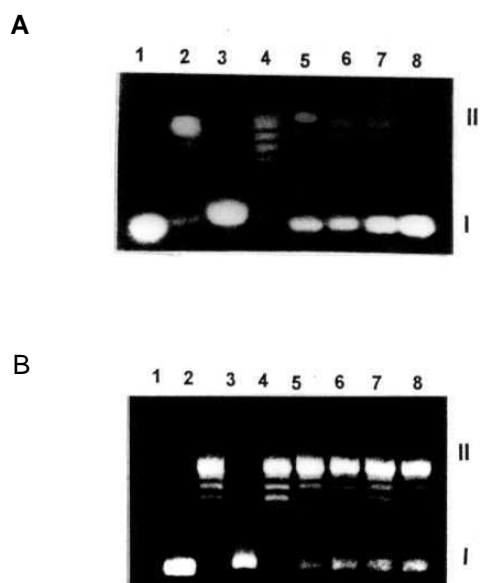
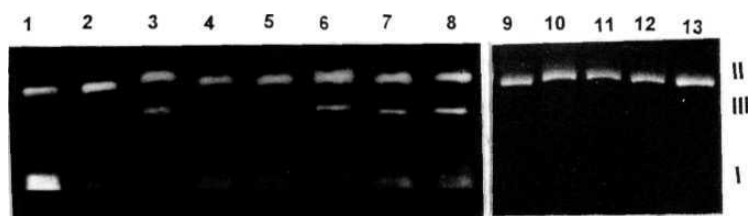


Figure 9: (A) Cleavage reaction was conducted by incubating pBR322 DNA (lane 1) with topo II (lane 2) in presence of 100 μ M-AMSA (lane 3) and 100, 200, 300, 400 & 500 μ M of RuBen(dmso) (lanes 4-8) and the same concentration range of RuSal (lanes 9-13). The positions of supercoiled, nicked circular and linear (form 3) DNA are indicated by **I**, **II** and **III**. (B) The plot shows the percentage of linear DNA formed with increasing concentration of RuBen(dmso). RuSal does not show any linear DNA formation.

FIGURE 9

A



B

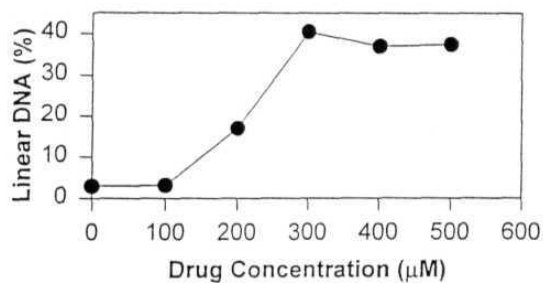


FIGURE 10

TABLE: (A) Immuno-precipitation of the *cleavage assay* products was carried out followed by atomic absorption spectroscopy to determine the presence of ruthenium in the cleavage complex. (B) The same assay was carried out in presence of [^3H] labeled DNA, followed by scintillation counting of the cleavage products to determine presence of DNA in the cleavage complex. The controls included in the experiments are shown in the tables.

(A)	RuBen (%)	RuSal (%)
DNA + Topo II	0	0
Drug	< 2	< 2
DNA + Drug	< 2	< 2
Topo II + Drug	8 \pm 0.82	<2
DNA+ Topo II + Drug	46 \pm 3.05	9 \pm 1.63

(B)	RuBen (%)	RuSal (%)
DNA + Topo II	3.0 \pm 0.5	3.0 \pm 0.5
DNA	0.5	0.5
DNA + Drug	1.0 \pm 0.5	1 \pm 0.7
Topo II + Drug	0	0
DNA+ Topo II + Drug	21 \pm 1.63	3 \pm 0.82

^a Data is presented as a percentage mean of three independent experiments conducted in triplicates, and standard deviations are given against each value

Figure 11: Inhibition of ATPase activity of topo II by RuBen(dmso) (•) and RuSal (O). ATP hydrolysis in the control sample was taken as 100% and values in presence of increasing concentrations of the drugs are presented as mean of three experiments; data is plotted as the percentage of ATP hydrolyzed versus concentration of drug in μM .

FIGURE 11

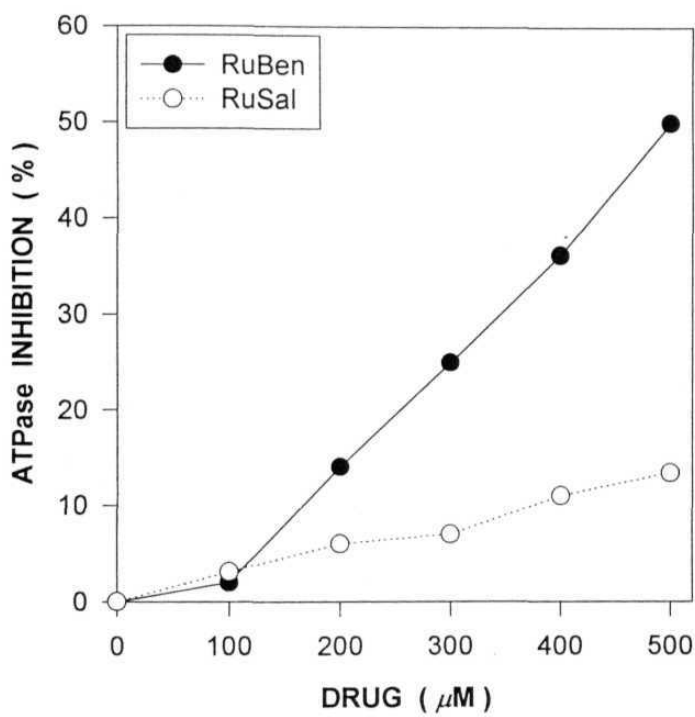


Figure 12: (A) RuBen(dmsO) increases the T_m of calf thymus DNA from 57 °C for DNA control(—) to 66, 73, 76, 78 and 80 °C for DNA nucleotide to drug ratios of 20:1(--), 10:1(—), 5:1(---), 2:1(—) and 1:1(....) respectively. (B) RuSal shows a T_m of 65, 70, 79, 81 and 81 °C for the same drug to DNA ratios

FIGURE 12

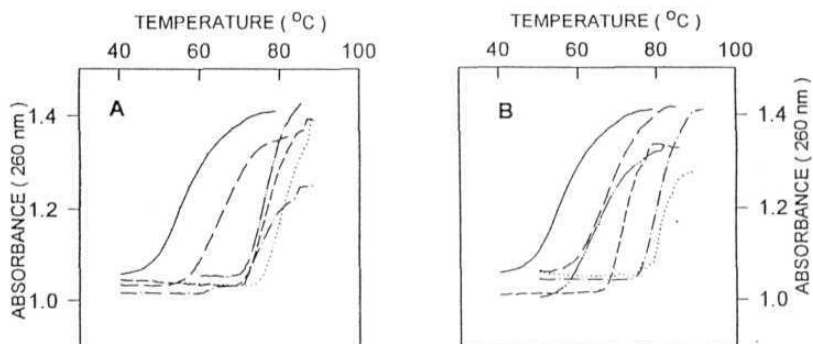


Figure 13: (A) D/N plotted against curve width of the melting curves shows a characteristic increase in curve width by m-AMSA (\bullet), which is typical of DNA intercalators, and a very small increase by RuBen(dmsO) (A) and RuSal (O). (B) D/N (drug/nucleotide) plotted against increase in T_m by RuBen(dmsO) (\bullet) and RuSal (O) to determine specific drug binding to DNA nucleotides. The stoichiometry of binding was determined from the slopes of the curves which indicated that RuBen(dmsO) bound to DNA with a stoichiometric ratio of one drug molecule per 4 nucleotides and a weak binding stoichiometry of 7 nucleotides, while RuSal bound to 4 nucleotides.

FIGURE 13

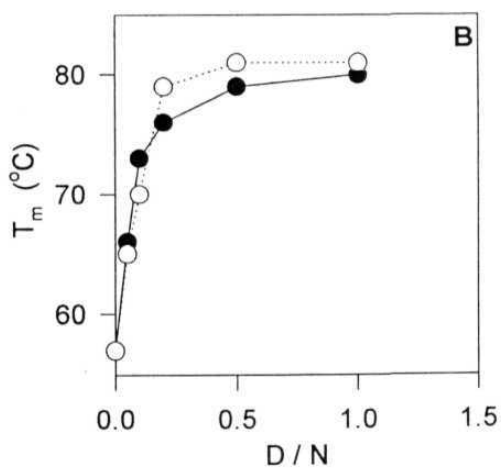
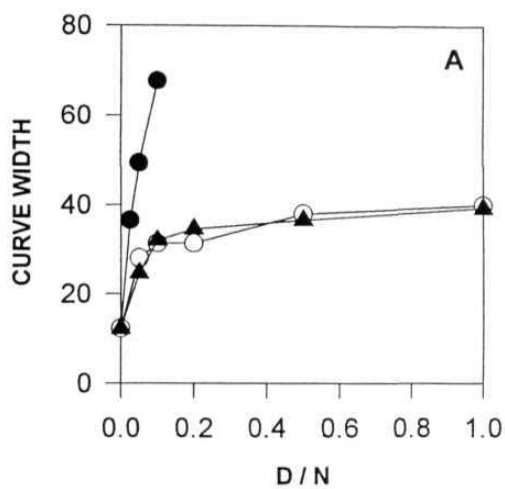


Figure 14: The Circular Dichroism spectra of pBR322 DNA (—) in the presence of 500 μM RuBen(dmsO) (••••) and RuSal (—) shows a small change in the molar ellipticity of DNA while m-AMSA(---) shows a very prominent increase in the positive and negative regions of the spectra at a concentration 5 times less than (100 μM) the ruthenium drugs

FIGURE 14

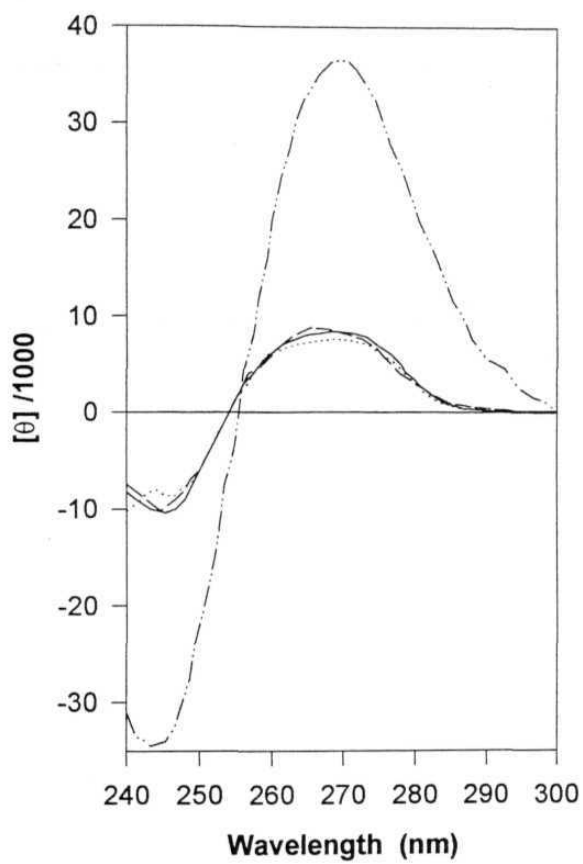


Figure 15: The anticancer activity of RuBen(dmsO) and RuSal was examined using [³H] thymidine incorporation on the two cancer cell lines, colo-205 and ZR-75-1. The results of the study indicate that RuBen(dmsO) shows a higher potency of cell proliferation inhibition compared to RuSal. The ruthenium drugs were more effective on the colo-205 cells (A) compared to the ZR-75-1 cells (B) The highest potency of inhibition was shown by m-AMSA

FIGURE 15

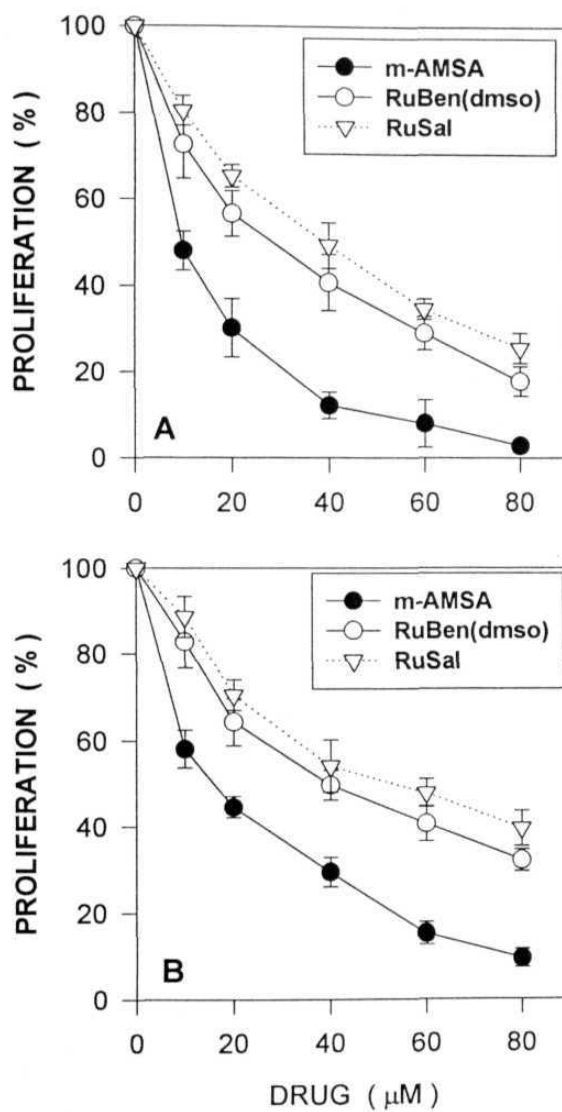
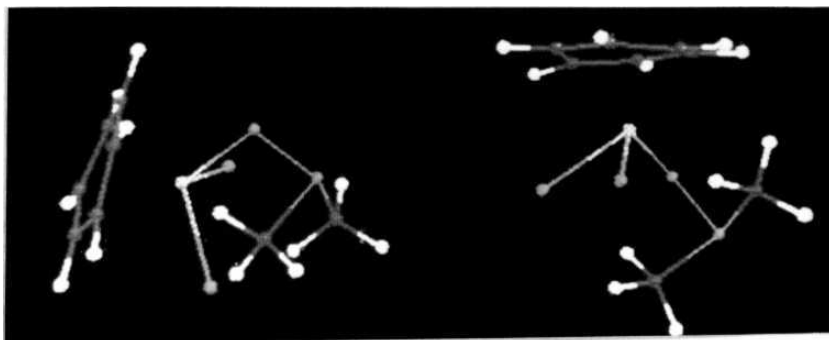


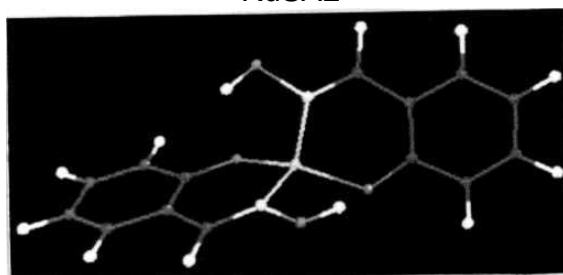
Figure 16: In RuSal, the ruthenium atom (shown in yellow) is in a bi-dentate coordination with two salicylaldoxime ligands. The salicylaldoxime ligands are spatially oriented in two different planes at an angle of $\sim 40^\circ$ to each other along the horizontal axis of the molecule. RuBen(dmsO) has an octahedral geometry. The ruthenium atom (shown in yellow) has an organometallic bond with the benzene ring (the organometallic bond is not shown) and also has ionic linkages with two chloride atoms (dark yellow). A 'dmsO' group is coordinated to the ruthenium atom in this molecule. The oxygen and sulphur atoms are shown in green. The left part of the figure is a 3-D view of the model which shows that the chlorides and the 'dmsO' group are oriented in a single direction and have the shape of a clamp. This may constitute a domain for topo II interaction, which could hook on to an active site of the enzyme. The right part of the figure shows a 3-D view of the model, with the probable topo II interacting domain at a right angle to the plane of the paper. The ruthenium atom, at the opposite region of this domain could interact with DNA.

FIGURE 16

RuBen(dmso)



RuSAL



Chapter 5

DEVELOPMENT OF NOVEL RuBen DERIVATIVES TO ENHANCE POTENCY OF TOPOISOMERASE II POISONING

INTRODUCTION

RuBen(dmso) was a promising starting compound for the development of novel derivatives with potential enzyme interacting groups because it possess significant topo II poisoning and anticancer activity. In addition, association of the ruthenium atom with the benzene ring through an organometallic linkage may partly minimize its random interaction with biological molecules, thus reducing toxic side effects. Molecular modeling analysis on RuBen(dmso) suggested the involvement of 'dmso' in topo II interaction. Consequently, the 'dmso' group was replaced by other active ligands on the 'RuBen' backbone (the RuBen backbone is the ruthenium atom bonded to the benzene ring and the chloride atoms). Numerous compounds were generated and tested for topo II antagonism. Out of these, only three compounds showed efficient topo II poisoning and anticancer activity. These compounds are RuBenApy, RuBenABa and RuBenAGu, in which the 'dmso' group was replaced with 3-amino pyridine, p-amino benzoic acid and amino guanidine (synthesis described in the Experimental Procedures section). Mechanism of action of these compounds on the catalytic activity of topo II and their anticancer activity has been carried out in detail in the present study.

RESULTS

Topoisomerase II activity assays:

Topoisomerase II poisoning by the RuBen drugs:

Inhibition of topo II mediated relaxation of supercoiled DNA was investigated through the relaxation assay. RuBenPy does not affect the DNA relaxation activity of topo II over the concentration range employed while RuBenAPy completely inhibits topo II activity at a concentration of 200 μM . RuBenABa and RuBenAGu show complete inhibition at 350 and 250 μM . All the three complexes exhibit a dose-dependent inhibition of DNA relaxation (Figure 17).

Inhibition of ATPase activity by the RuBen drugs:

Drugs that inhibit the relaxation activity of topo II also interfere with the DNA-stimulated ATPase activity of the enzyme. The results of the ATPase assay indicate that RuBenAPy, RuBenAGu and RuBenABa inhibit the DNA dependent ATPase activity of topo II, with a potency of inhibition in the same order, while RuBenPy does not produce appreciable inhibition (Figure 18). The inhibition of ATPase activity by the three drugs is dose dependent and is concomitant with their action on the relaxation activity of topo II.

Drug induced, topoisomerase II-mediated cleavage of DNA:

The topo II mediated cleavage of DNA in presence of the RuBen drugs was monitored through the cleavage assay. Linearization of supercoiled circular DNA occurs when the

cleavage assay is carried out in the presence of increasing concentrations of RuBenAPy, RuBenABa and RuBenAGu (**Figure 19A**) but not RuBenPy. The linear DNA results from SDS and proteinase K treatment of the ternary cleavage complex containing topo II, drug and *cleaved* DNA. Hence, these RuBen drugs effectively shift the DNA cleavage/religation equilibrium of topo II towards DNA cleavage. Quantification of linear DNA shows that RuBenAPy is the most potent drug, forming the cleavage complex at a concentration 150 μM . RuBenABa and RuBenAGu form the cleavage complex at 250 and 200 μM (**Figure 19B**). These results correlate well with the relaxation and ATPase inhibition activities of the three RuBen drugs.

DNA interaction by the RuBen drugs:

DNA thermal denaturation studies:

The DNA thermal denaturation studies show that the four RuBen drugs bind to DNA with almost similar affinity (**Figure 20**). Curve width analysis of the denaturation curves was carried out to determine the mode of DNA interaction by the RuBen drugs. The study shows that these drugs are essentially DNA external binders which interact with the nucleotides without disturbing the DNA helix (**Figure 21**). CD. spectral analysis of DNA in presence of the drugs reveals that they do not induce any conformational change in DNA, which confirms the result of curve width analysis. Where as, m-AMSA causes a very high change in curve width of the denaturation curves and also induces a steep increase in the CD. signal of DNA, which is characteristic of a DNA intercalating molecule (**Figure 22**).

Anticancer action of the RuBen drugs:

The [^3H] thymidine incorporation assays on the two cancer cell lines (**colo-205** and ZR-75-1) show that the anti-proliferation activity of the RuBen drugs is concomitant with their topo II poisoning ability. RuBenAPy shows the highest **anti-proliferative** action followed by RuBenAGu and RuBenABa. RuBenPy also has a significant action on the proliferative **response** of the cancer cells (**Figure 23**). The DNA intercalating drug, **m-AMSA** shows the highest anti-proliferative action. All the drugs including m-AMSA are very active against the colo-205 cell line, while the ZR-75-1 cells are less sensitive to the anti-proliferative action of these drugs (**Figure 24**).

Molecular modeling analysis:

The molecular modeling analysis of the four RuBen drugs (RuBenPy, RuBenAPy, RuBenAGu and RuBenABa) suggest that these molecules have distinct spatial orientations of the ligands around the ruthenium atom, which are completely different from that of RuBen(dmsO) (**Figure 25**). The coordinated ligands in these molecules (Py, APy, AGu and ABa) are oriented away from the chloride atoms, unlike in RuBen(dmsO). The orientation of the coordinated ligands is such that they may easily be able to align into an active site of topo II and possibly interact with the electropositive sites on the protein through their free electronegative nitrogen atoms. This interpretation is supported by the observation that RuBenPy, which does not have any free nitrogen atoms on its ligand, does not poison topo II activity and also does not show very good anticancer action.

DISCUSSION

The DNA nicking **function** of topo II has widespread implications and has given the cancer pharmacologist, a worthy reason to develop drugs targeted at this action of topo II. These topo II drugs are popularly known as topo II poisons because, rather than inhibiting the catalytic activity of the enzyme, they promote one part of the reaction mechanism, namely, DNA cleavage and block the second part, which is **religation** of the cleaved DNA (Robinson and Osheroff, 1990). Our earlier study with RuBen(dmsO) introduced this molecule as a potential anticancer drug whose molecular target is topo II. Though a rather high concentration of this drug is required for topo II poisoning and anticancer activity, it nevertheless served as a good lead molecule for the development of potent derivatives, in which the topo II interacting 'dmsO' group was replaced with pyridine, 3-amino pyridine, p-amino benzoic acid or amino guanidine. All the four molecules bind to DNA with a similar affinity indicating that a common entity in these molecules, the ruthenium atom, may be the exclusive DNA binding group. The chlorides on the ruthenium atom may also serve this function, but such an interaction, similar to that of cisplatin with DNA, would lead to drug-DNA adduct formation. That seems improbable because the DNA binding studies do not suggest such a drug-DNA adduct formation by any of these RuBen drugs. The results of the relaxation assay, ATPase assay and the cleavage assay indicate that RuBenAPy, RuBenAGu and RuBenABa poison topo II by cleavage complex formation. RuBenAPy is the most potent followed by RuBenAGu and RuBenABa. Surprisingly, RuBenPy, which has a structure and DNA binding affinity similar to RuBenAPy, does not

poison topo II. This profound difference between the two similar molecules may be due to the **amino** group on the pyridine ring of RuBenAPy, which may solely interact with topo II. Similarly, in RuBenAGu and RuBenABa, the amino groups may be responsible for topo II interaction leading to effective poisoning of the enzyme. Though the higher potency of RuBenAGu could be due to multiple interactions by the three amino groups of the AGu ligand with topo II, as compared to that of a single amino group in RuBenABa, the drug conformation during topo II interaction may also be an important determinant for topo II poisoning. This is because RuBenApy has a single amino group, but is the most potent topo II poison among the RuBen drugs. The conformation and spatial orientation of the ligands on the drugs may be appropriate for effectively freezing topo II in the cleavage complex. The molecular modeling analysis of the RuBen drugs argues in this direction. The spatial orientation of the amino pyridine ligand may help the drug to secure a strong hold on the enzyme, which could explain the highest potency of topo II poisoning by this drug.

Our studies reveal that the three RuBen drugs interact bi-directionally with DNA and topo II, similar to RuBen(dmso). The ruthenium atom binds to DNA and the ligand (APy, ABa or AGu) interacts with topo II. It is not clear if the chloride atoms and the **organometallic** bonded benzene ring involve in topo II interaction, because these groups are oriented away from the coordinated ligand. Even if they do, they may interact with a region on the enzyme which is away from the ligand interaction site, unlike in the case of **RuBen(dmso)**, where all the groups may interact with one region of the enzyme.

The thymidine incorporation assay on the two human cancer cell lines shows that the RuBen drugs are effective anticancer agents and merit a detailed analysis. RuBenPy does not poison topo II but still shows significant anti-proliferation activity, indicating that this drug as well as the other RuBen drugs may act on other cellular constituents as well. Though m-AMSA is more effective than the RuBen drugs in topo II poisoning and anticancer activity, it is a DNA damaging agent and a possible mutagen, which limits its therapeutic potential, while the RuBen drugs interact externally with DNA without destabilizing the DNA helix. This is an important factor to be considered for the development of anticancer drugs because most of the DNA destabilizing anticancer drugs like cisplatin, m-AMSA and adriamycin cause permanent genetic damage to the host, often resulting in the development of neoplasticity as a long term effect.

Figure 17: Supercoiled pBR322 DNA (lane 1) was incubated with topo II in the absence (lane 2) or presence of 75 μ M m-AMSA (lane 3), 100, 150, 200, 250, 300 and 350 μ M of RuBenAPy (lanes 4 to 9), RuBenAGu (lanes 10 to 15), RuBenABa (lanes 16 to 21) and 100, 200, 300, 400 and 500 μ M of RuBenPy (lanes 22 to 26) The positions of supercoiled (form 1) DNA and relaxed (nicked circular or form 2) DNA arc indicated by I and II.

FIGURE 17

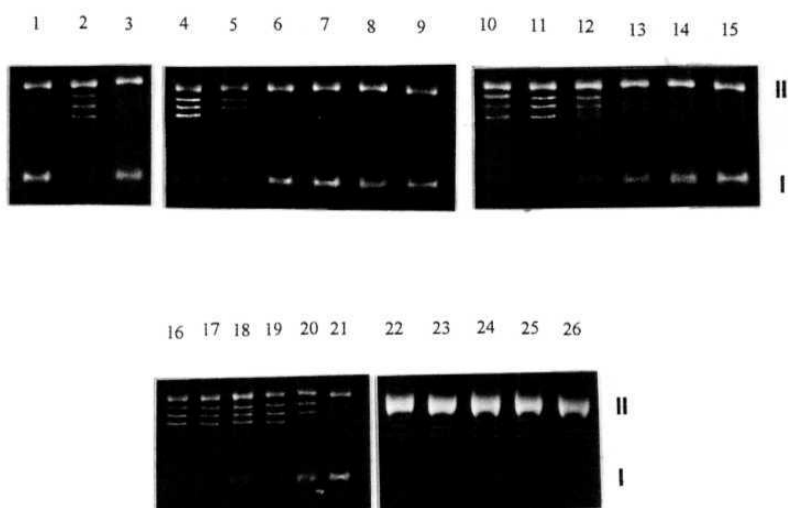


Figure 18: Inhibition of the ATPase activity of topo II by RuBenPy, RuBenAPy, RuBcnAGu and RuBenABa. ATP hydrolysis in the presence of increasing concentrations of the drugs are presented as mean of 3 experiments. Data is plotted as percent inhibition of ATP hydrolysis versus concentration of drug in μM . RuBenAPy showed the highest inhibition of ATP hydrolysis (~80%) followed by RuBcnAGu and RuBenABa. RuBenPy does not show significant inhibition of ATP hydrolysis.

FIGURE 18

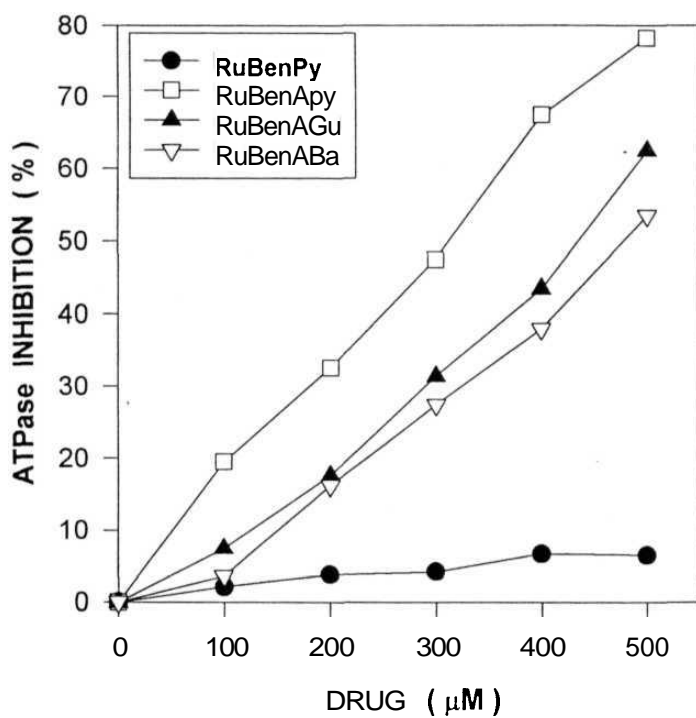
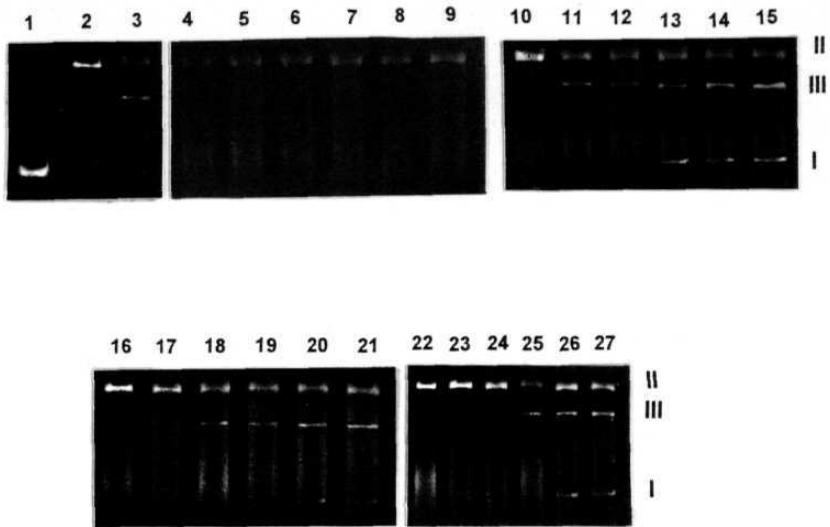


Figure 19: (A) Cleavage assay was performed by incubating supercoiled pBR322 DNA (lane 1) with topo II (lane 2) in presence of 100 μM m-AMSA (lane 3), 100, 150, 200, 250, 300 and 350 μM RuBenPy (lanes 4 to 9), the same concentrations of RuBenAPy (lanes 10 to 15), RuBenAGu (16 to 21) and RuBenABa (22 to 27). The positions of supercoiled, nicked circular and linear (form 3) DNA are indicated by **I**, **II** and **III**. The formation of the cleavage complex is evidenced by the appearance of the linear DNA (**III**).

(B) Quantification of the linear DNA shows that RuBenAPy is the most potent in cleavage complex formation followed by RuBenAGu and RuBenABa. RuBenPy does not show any visible linear DNA formation even at the highest concentration of 350 μM . The lower concentration of 50 μM is not shown in the gel photographs.

FIGURE 19

A



B

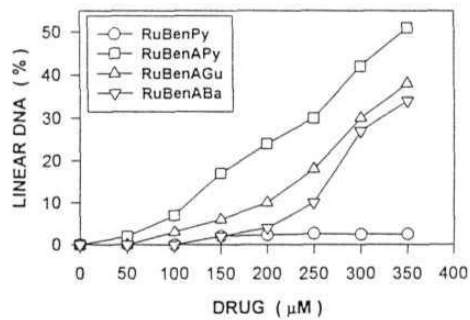


Figure 20: In the absence of any drug, the melting temperature curve of calf thymus DNA shows a T_m of 57 °C (—). At a drug to DNA nucleotide ratio 1:5, RuBenAGu (—) increases the T_m , to 68 °C, whereas RuBenPy (--) and RuBenAPy (—) and RuBenABa (—) increase T_m to 69.5, 70 and 70.5 °C. The DNA intercalator, m-AMSA induces a strong increase in T_m (74 °C) at a drug to nucleotide ratio only 1:10 (••••). The T_m curves for the ratios lower than 1:5 (1:10, 1:20, 1:40) are not shown. Drug to DNA ratios of more than 1:5 were not attempted because these complexes show intense visible spectra which interferes with the uv spectroscopic studies.

FIGURE 20

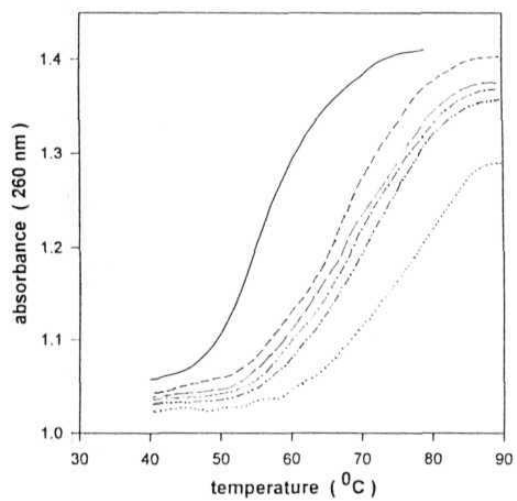


Figure 21: D/N (drug/nucleotide) ratio plotted against curve width of the T_m curves (4 curves for drug to DNA nucleotide ratios of 1:40, 1:20, 1:10 and 1:5 for all the RuBen drugs and 3 for m-AMSA) shows a characteristic increase in curve width by m-AMSA (•). The RuBen drugs however do not greatly affect the curve width of the melting temperature curves suggesting that they are essentially DNA non binders

FIGURE 21

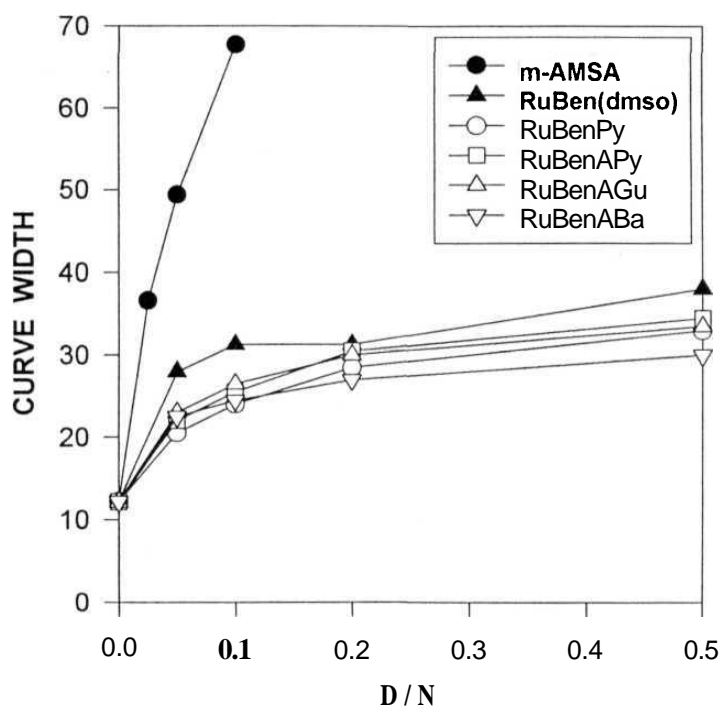


Figure 22: The Circular Dichroism spectra of pBR322 DNA (—) in the presence of RuBenAGu (—), RuBenPy (—), RuBenAPy (•—) and RuBenABa (-•-) shows that these drugs induce very minute changes in the molar ellipticity of DNA, while m-AMSA(-••-) shows a very prominent change at a concentration of ~3.5 times less than that of the RuBen drugs. This large increase in the C.D. signal indicates a **conformational** change induced in the DNA due to intercalation by m-AMSA.

FIGURE 22

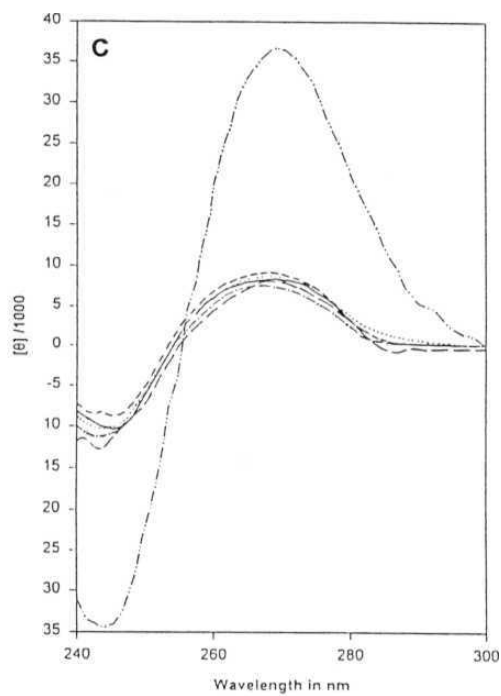


Figure 23: *in vitro* anti-proliferation activity of the RuBen drugs was tested on two fast growing cancer cells- colo-205 (top panel graph) and ZR-75-1 (lower panel graph). The cells were incubated with increasing concentrations of the RuBen drugs and proliferation was quantified by [³H] thymidine incorporation, as described in the experimental section. Cell proliferation at a drug concentration of 80 μ M is shown in the figure m-AMSA is the most effective in anti-proliferative action, followed by RuBenAPy, RuBenAGu, RuBenABa and RuBenPy. The data presented is a mean of three independent experiments conducted in triplicates.

FIGURE 23

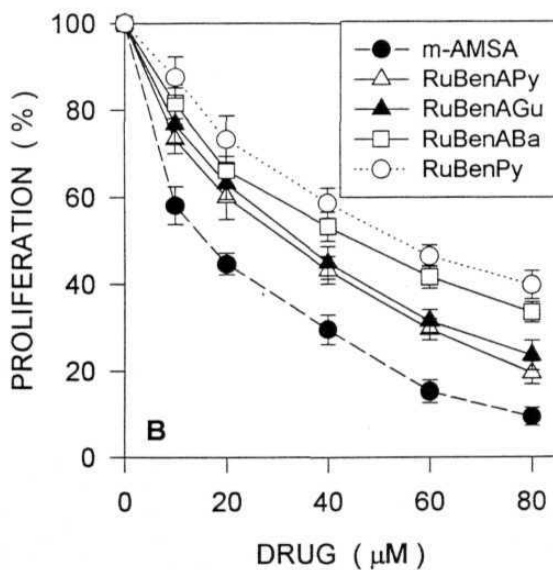
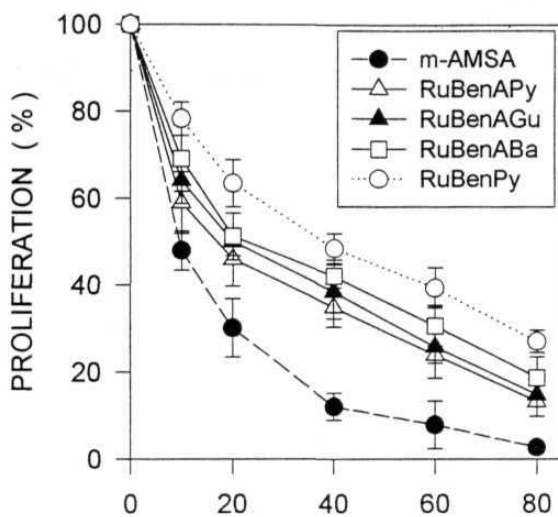


Figure 24: The colon carcinoma cells (black bars) are more sensitive to the action of the RuBen drugs compared to the ZR-75-1 cells. The control, m-AMSA also shows a similar effect. This indicates that the ZR-75-1 cells may have an inherent resistance mechanism which makes them less susceptible to the action of topo II poisons compared to the colo-205 cells.

FIGURE 24

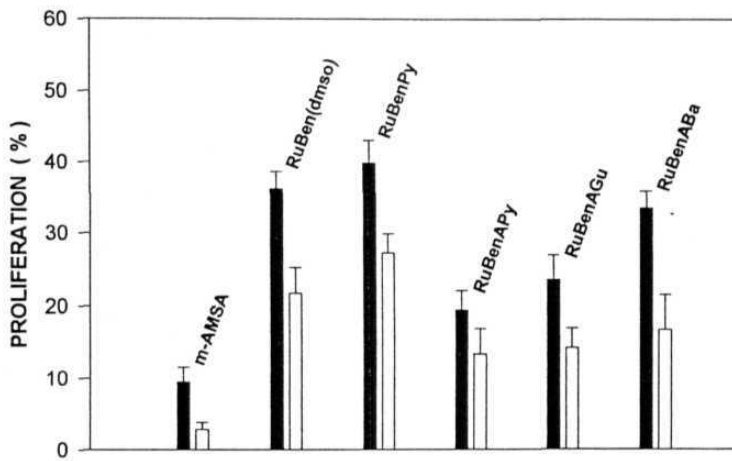
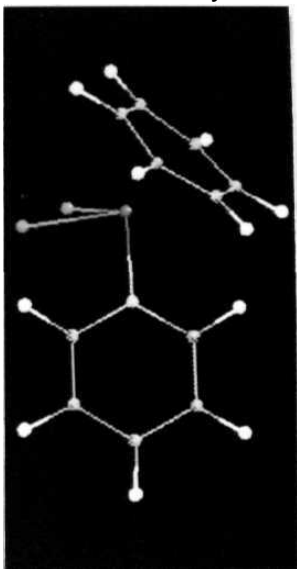


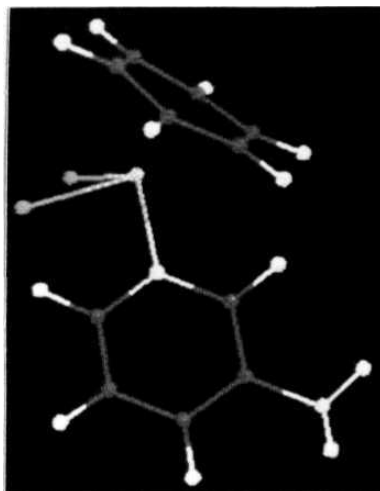
Figure 25: The molecular models of RuBcnPy, RuBcnAPy, RuBcnAGu and RuBcnABa reveal that these molecules do not possess the typical 'chloride' and 'coordinated ligand' interacting domain of RuBcn(dmsO). The coordinated ligands in these molecules are oriented away from the chloride groups. The angular orientation of the ligands may allow them to interact with the enzyme by aligning themselves into an active site in the enzyme. In RuBcnPy, the ruthenium atom is shown in green, chlorides in yellow and the nitrogen atom in the pyridine ring, which interacts with ruthenium, is in white. In RuBcnAPy, ruthenium is shown in light yellow, chlorides in dark yellow, the pyridine ring nitrogen (which interacts with ruthenium) as well as the free NH₂ nitrogen are shown in white. In RuBcnABa, the oxygen atoms are shown in green and NH₂ nitrogen in white. In RuBcnAGu, all the nitrogen atoms are shown in white. The ruthenium-benzene organometallic bonds are not shown in all the molecules.

FIGURE 25

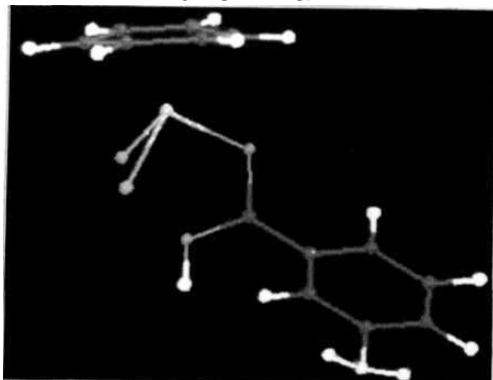
RuBenPy



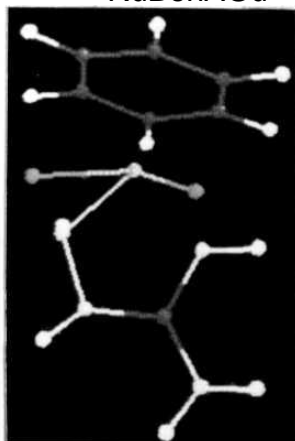
RuBenAPy



RuBenABa



RuBenAGu



Chapter 6

DEVELOPMENT OF A TRANSFERRIN MEDIATED DELIVERY SYSTEM FOR THE ANTICANCER RuBen DRUGS

INTRODUCTION

Though the RuBen drugs may not induce very adverse effects on the human body because of an **organometallic** linkage with a ligand and also due to their mode of DNA interaction, they would still be expected to cause significant toxicity to the body due to the inherent presence of the ruthenium metal atom, which is foreign to the human body. In the light of this situation, it would be desirable to develop a delivery system for these drugs, which would carry the drug molecules to the cancer tissues without allowing them to cause any major organ and tissue damage.

Drug delivery systems have been developed to achieve a high titer of drug in the region of their intended action, which will result in higher specificity of action and reduction of toxic side-effects. Some of the delivery systems in use are **liposome** encapsulation, antisense tagging and antibody tagging (Mayer, 1998; Lu et al., 1999; Juliano et al., 1999). A more recent approach is transferrin mediated delivery (Singh et. al., 1998, 1999; Sava et al., 1991). A schematic diagram of iron delivery by transferrin is shown in Figure 26.

The transferrin mediated delivery has been chosen for anticancer targeting by the RuBen drugs because of the following reasons:

- Transferrin is a natural delivery system for the transport of iron and iron-containing compounds from the plasma in circulation to living cells and this delivery is increased many fold in cancer cells due to over-expression of the transferrin receptors on the plasma membrane. Also, due to the heavy requirement of iron for the rapid growth and

proliferation of neoplastic cells, this transport mechanism cycles continuously to provide the extra iron to these cells.

- Iron and ruthenium possess similar chemical properties and ruthenium compounds have been shown to bind apotransferrin in a similar way as iron (Sava et al., 1991). This drug-transferrin conjugate will be effectively transported into cancer cells where the ruthenium drug is released into the cytosol and the apotransferrin is cycled back into the circulating plasma.

In the present study, binding of the RuBen drugs to apotransferrin was monitored through uv-visible and circular dichroism spectroscopy. In physiological buffer conditions, the binding of these drugs to apotransferrin was complete in a time period of 8 h.

The transferrin-bound RuBen drugs were used for *in vitro* anticancer studies. The transferrin bound drugs showed a higher anticancer action (an average increase of ~5%) compared to that of the unbound drugs.

RESULTS

Binding of the RuBen drugs to apotransferrin.

uv-visible spectroscopic analysis:

The five RuBen drugs show characteristic uv-visible spectra, with two distinct bands, one between 300 and 400 nm and the other between 400 and 600 nm which change typically

upon binding to ATr. The spectra of the drugs remains unchanged at 1 h incubation with ATr. But at 4 h, lowering of the band intensities is observed, which continues up to 8 h, beyond which no further changes occur. This suggests that the drugs interact slowly with ATr over a period of 8 h, at which time, complete binding occurs. The change in spectral band intensities could be due to d- d transitions in the metal atom or possibly due to oxidation of Ru^{2+} to Ru^{3+} upon ligation with ATr. This is because Tr has a higher binding affinity towards iron or ruthenium in the 3+ oxidation state. It has also been suggested that Tr can bind to a metal atom in 2+ state and oxidize it to 3+ in the presence of carbonate or bicarbonate (Bates et. al., 1973). The spectra of the RuBen drugs alone and with ATr after 8 h incubation are shown in **Figure 27**

Circular dichroism analysis:

Circular dichroism is particularly suited for the determination of conformational changes induced in chiral macromolecules upon binding of small chromophores. Incubating ATr with the RuBen drugs in 1:1 ratio for the specified time period induces a sharp positive signal in the CD. spectra of the protein (in the region between 300 and 600 nm). This is due to a conformational change in the **macromolecule** induced by binding of the RuBen drug to the iron binding site of the apo-protein. At this stage, ATr becomes the co-factor loaded Tr. The increase in intensity of the CD. signal is plotted as change in molar ellipticity ($\Delta \theta$) versus wavelength in nm, calculated by subtracting the molar ellipticity of ATr alone from that of ATr in presence of drug (**figure 28**). Increasing the drug to ATr ratio to 2:1 also increases the intensity of the signal. At this point, the protein is saturated

with the drug because, further increase of this ratio does not lead to further increase in the intensity of the signal.

Interaction of ATr with **RuBen(dmsO)** shows a characteristic increase in the CD. signal at 450 nm. RuBenPy, RuBenAPy and RuBenABa register an increase in the signal at 405 nm. Interestingly, binding of RuBenAGu to ATr causes a very sharp increase at a lower wavelength of 330 nm. This band shift may be due to additional interactions of the nitrogen atoms on the drug with ATr, apart from the ruthenium atom.

Release of the RuBen drug from transferrin:

In its natural iron transport cycle, ATr binds to iron and becomes the active iron transport protein, Tr. When this iron loaded Tr comes across a transferrin receptor (TrR) on the plasma membrane of cells, it binds to the receptor and the ligand-receptor (Tr-TrR) complex is internalized through an endosome. The low pH in the endosome promotes release of iron from this complex. The iron is taken up by the cell for its cellular functions while the Tr-TrR complex is transported back to the plasma membrane from where the iron-free ATr is released into the general circulation.

For Tr to function as an efficient delivery vehicle, it should be able to release the RuBen drug in a low pH environment. By lowering the pH to 4.5, all the RuBen drugs were effectively released from the Tr-TrR complex which was followed through uv-visible spectroscopy (**Figure 29**). Release of the drugs is associated with slight changes in the color of these drugs, which attain a light bluish tinge. This change in color may be caused due to a d-d transition or a change in oxidation state of ruthenium atom upon Tr binding.

DNA cleavage assay was carried out with the **Tr-released** drugs, which shows that the topo II poisoning ability of the RuBen drugs is retained at the same concentrations as in the original cleavage assay of *Chapter 5* (**Figure 30**). This shows that though the drugs may undergo chemical changes upon ATr binding and also subsequent to their release, this does not affect their action on topo II.

Anticancer action of the transferrin bound RuBen drugs:

The [^3H] thymidine incorporation assays on the two cancer cell lines show that the anti-proliferation activity of the Tr-bound RuBen drugs is clearly superior to that **of the** unbound drugs. In general, a 5% increase of anti-proliferative action is induced by the Tr-bound drugs compared to the unbound drugs (**Figure 31**). Similar to the effect of the unbound drugs, Tr-bound RuBenAPy shows the highest anti-proliferative action followed by the Tr-bound RuBenAGu, RuBenABa, RuBen(dmsO) and RuBenPy, in the same order. As seen earlier, m-AMSA shows the highest anti-proliferative action, which does not increase in presence of ATr. Also similar to the anticancer action of the unbound drugs, all the drugs including m-AMSA are very active against the colo-205 cells, while not being so effective on the ZR-75-1 cells

DISCUSSION

Fast dividing cancer cells demand a lot of iron for their growth and division and therefore over-express the **transferrin** receptor while most normal resting cells do not (Galbraith et. al., 1980). It follows that, iron bound transferrin is preferentially transported into these cells through receptor-mediated endocytosis. This property has earlier been exploited for anticancer drug delivery by conjugating adriamycin to transferrin by Barabas et. al. (1992) and Singh et. al. (1998). Though this conjugation improved the anticancer action of the drug, full advantage of this delivery mechanism may not have been realized because the approaches that had been used for conjugation do not allow the release of drug from transferrin inside the cell. It would be advantageous to exploit the natural transferrin cycle of binding and release for a more effective drug delivery. By following the elegant experiments of Kratz et. al. (1994), we have analyzed the binding and release of the RuBen drugs from transferrin, which occurs in a manner similar to the natural iron binding and release mechanism of the protein. Most importantly, the drugs released from transferrin were in a topo II active form.

In the *in vitro* anticancer assay, the transferrin bound RuBen drugs were found to be slightly more effective than the unbound drugs. Since the RuBen drugs by themselves have easy access to the cancer cells in liquid culture and can enter the cells either directly through diffusion or any other mechanism, the difference between the transferrin bound and unbound drugs is marginal. But the effect may be more pronounced *in vivo*, where the

transferrin bound drugs selectively localize in cancer cells while the unbound drugs can enter normal cells too. The effect of the transferrin-bound RuBen drugs *in vivo* is yet to be studied. Nevertheless, the *in vitro* study with the transferrin-bound drugs shows that this delivery mechanism holds promise for the delivery of those drugs which are very effective anticancer agents but are limited in use because their toxic effects on the human body.

Figure 26: In its normal iron transport cycle, aTr binds to iron and becomes the active iron transport protein, Tr. When this iron loaded Tr comes across a **transferrin receptor** (TrR) on the plasma membrane of cells, it binds to the receptor and the ligand-receptor (Tr-TrR) complex is internalized to the cell through an endosome. The low pH in the endosome promotes release of iron from this complex. The iron is taken up by the cell for its cellular requirement and the Tr-TrR complex is transported back to the plasma membrane from where the iron-free aTr is released into the general circulation.

FIGURE 26

THE TRANSFERRIN CYCLE

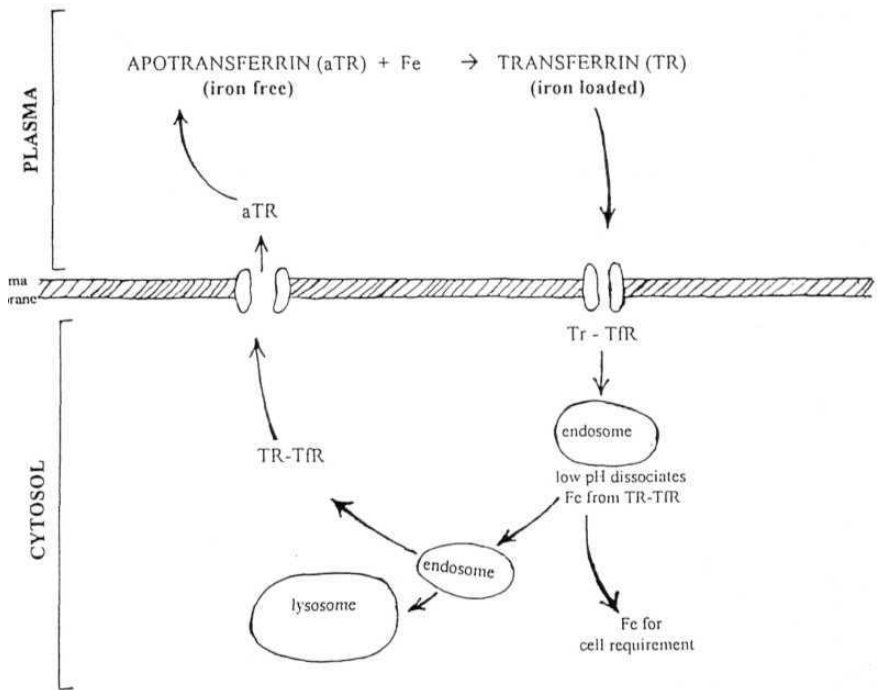


Figure 27: uv-visible spectra of the RuBen drugs incubated with ATr. Drug alone is shown in a continuous line (—), while the drug incubated with ATr for 4 h and 8 h is shown by dotted line (....) and broken line (— · —). m-AMSA (A) shows a band at 425 nm in its uv-visible spectra, which does not change upon incubation with ATr up to a period of 8 h. RuBen(dmso) (B) shows characteristic absorption bands at 420 and 340 nm. After 4 h incubation with ATr, the band at 340 nm disappears and the one at 420 nm broadens, which disappears after 8h. RuBenPy (C) exhibits a band between 600 and 390 nm which disappears after 8 h incubation with ATr. Similarly in RuBenAPy (D), the bands at 600 to 390 nm disappear. The spectra of RuBenAGu (E) exhibits characteristic bands at 340 and 540 nm, which disappear after 8 h, upon binding with ATr. In the case of RuBenABa (F), the band at 530 nm is reduced and the one at 390 nm disappears.

FIGURE 27

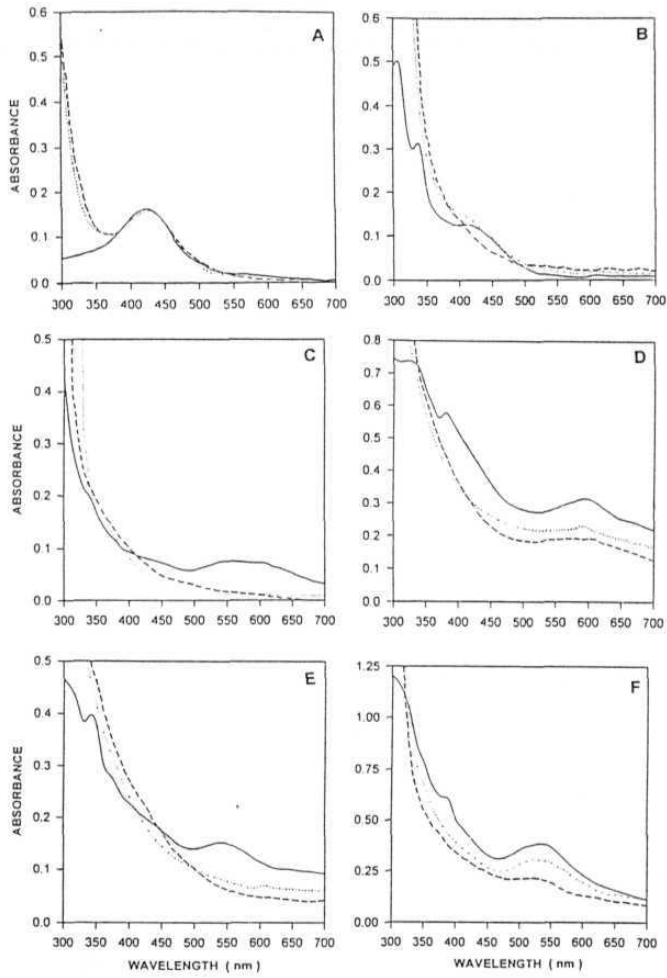


Figure 28: Circular Dichroism spectra of ATr incubated with the RuBen drugs for a period of 8 h. The 1:1 and 2:1 drug to ATr ratios are shown by a broken line (---) and continuous line (—) respectively. The control, m-AMSA (A) does not induce any conformational change in ATr, suggesting that it does not interact with the protein. RuBen(dmso) (B) induces a peak at 450 nm in the C.D spectra of ATr at a drug to ATr ratio of 1:1. This is subtracted from the original CD. spectra and plotted as change in molar ellipticity ($\Delta\theta$) versus wavelength in nm. An increase of the drug per Atr ratio to 2:1 records a further increase in this peak. Similarly, RuBenPy (C), RuBenAPy (D) and RuBenABa (F) induce peaks at 405 nm. RuBenAGu (E) induces an increase at 330 nm. In all the cases, increasing the ratio to 2:1 also increases the peak intensity.

FIGURE 28

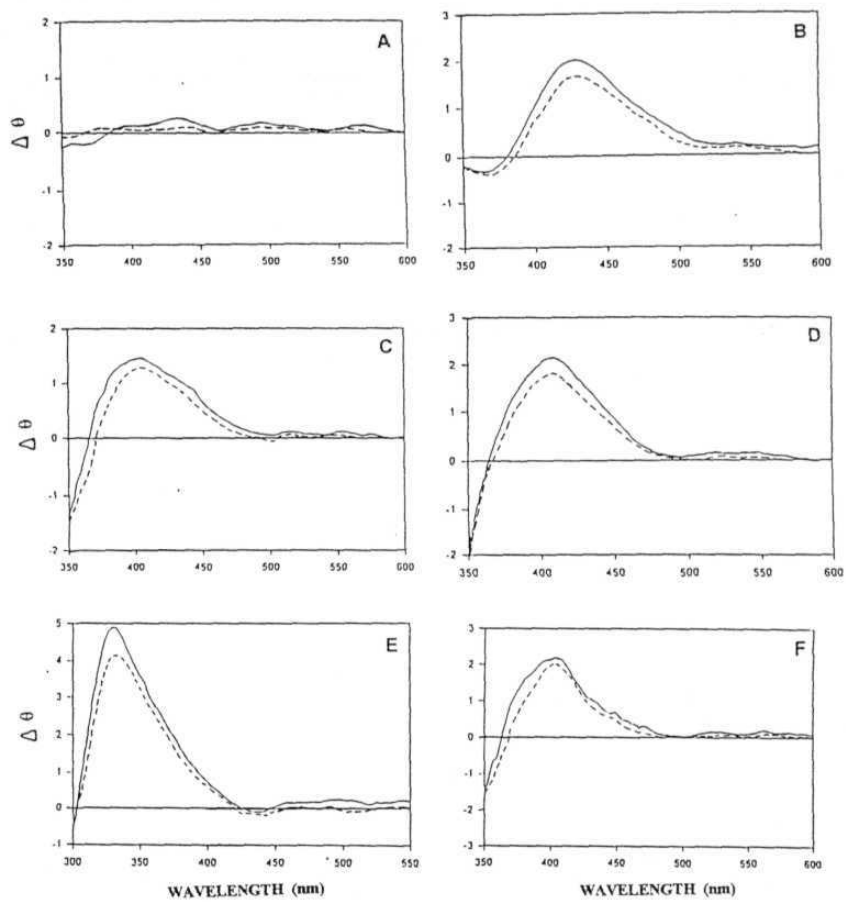


Figure 29: pH of the Tr bound drug samples was lowered to 4.5 with HCl and the samples were incubated for 2 h. at 37 °C. uv-visible spectra of the samples were recorded. The spectra of the Tr-bound drugs is shown by a continuous line (—) and that of the HCl treated samples is shown by a broken line (---). The control, m-AMSA (A) shows no change in the two spectra since no binding and unbinding of the drug to Tr occurs. In the spectra of RuBen(dmso) (B), a band at 430 nm appears, indicating the release of the drug from Tr. Similarly, bands at 540, 550, 570 and 500 nm appear in the spectra of RuBenPy (C), RuBenAPy (D), RuBenAGu (E) and RuBenABa (F) respectively, suggesting the release of the drugs from Tr in the acidic environment

FIGURE 29

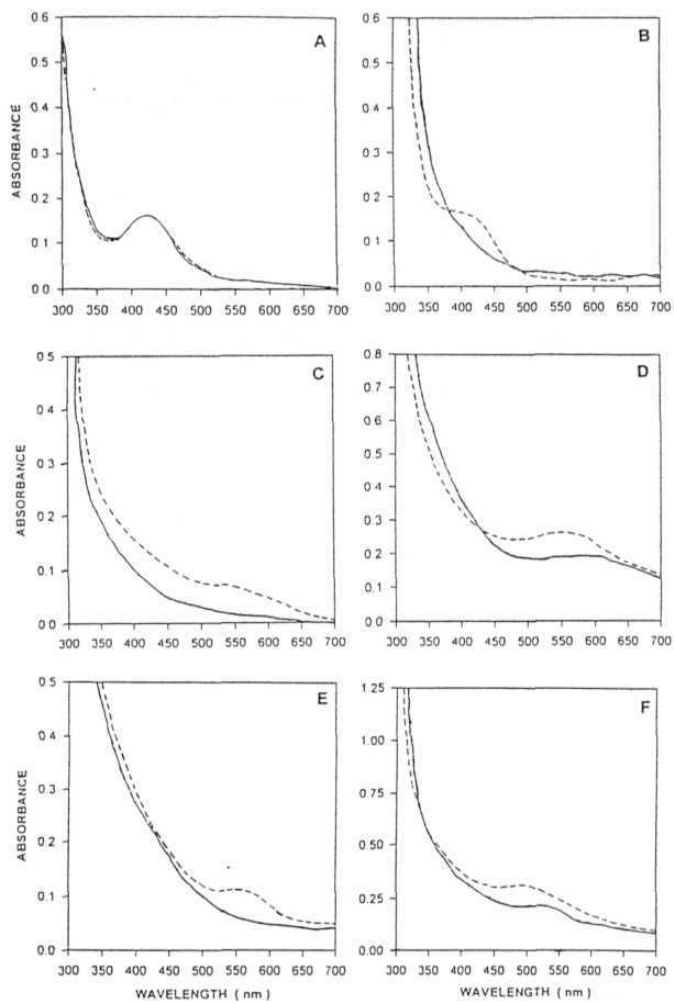


Figure 30: Cleavage complex formation by the Tr-released RuBen drugs. Supercoiled pBR322 DNA is shown in lane 1. The successive lanes from 2 to 10 show the results of the topo II induced DNA cleavage assay, carried out in the presence of the Tr-released RuBen drugs. Lane 2, 500 μ M of RuBenPy, lanes 3 and 4, 200 and 300 μ M of RuBen(dmso); lanes 5 and 6, 150 and 200 μ M of RuBenAPy; lanes 7 and 8, 200 and 250 μ M of RuBenAGu; lanes 9 and 10, 300 and 350 μ M of RuBenABa. For all the drugs from RuBen(dmso), two concentrations of the drugs were used, one below and the other equal to the threshold concentration for linear DNA formation (as gathered from the original cleavage assay). The results show that the cleavage complex forming ability of the RuBen drugs is retained at the same concentration levels. The positions of the three conformational forms of pBR322 DNA are indicated by I, II and **III**.

FIGURE 30

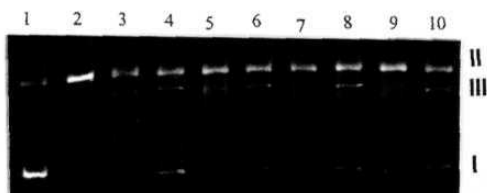
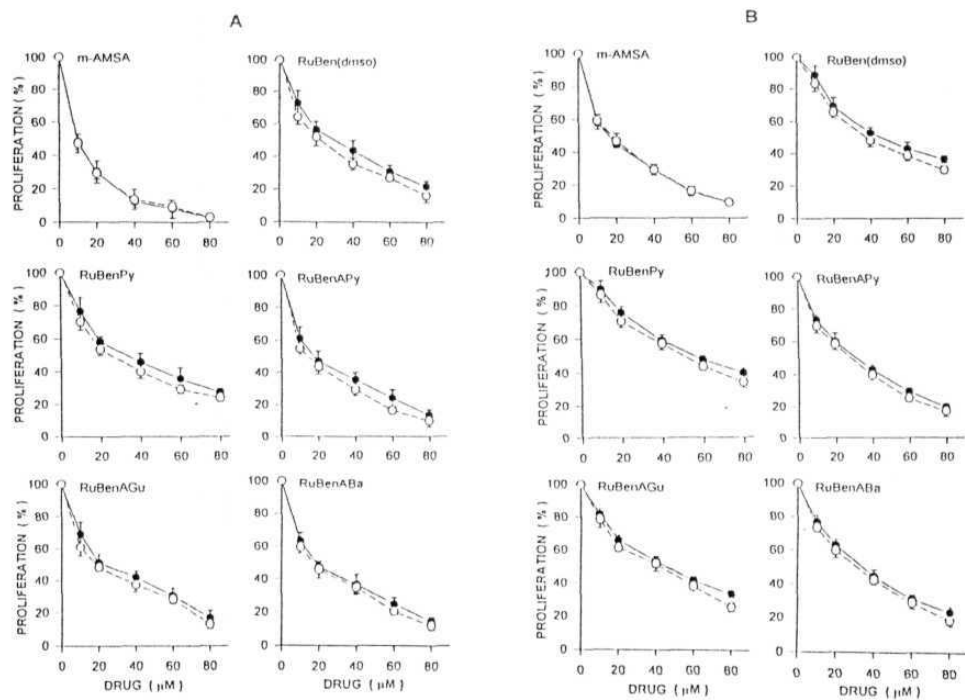


Figure 31: Action of the Tr-bound drugs on colo-205 cells (group A to the left) and ZR-75-1 cells (group B the right). Data presented is a mean of three independent experiments carried out in triplicates. Comparison of the anti-proliferative action of Tr-bound drugs (-o-) with the unbound drugs (-•-) shows that Tr does not cause an increase in the anti-proliferation activity of m-AMSA, while all the RuBen drugs exhibited an increase at varied degrees. An average increase of 3 to 5% was induced by the Tr-Bound RuBen drugs.

FIGURE 31



Chapter 7

TOPOISOMERASE II POISONING BY RUTHENIUM
COORDINATION COMPLEXES: A STUDY OF
STRUCTURE-ACTIVITY RELATIONSHIP.

INTRODUCTION

An earlier study by Jayaraju et. al. (1999) showed that a salicylaldoxime complex of cobalt (cobalt salicylaldoxime) poisons the activity of topo II. Molecular analysis implicated the oxime groups of the salicylaldoxime ligands as the topo II interacting moieties in the molecule. In the present study, we found that replacement of the cobalt atom with a ruthenium atom (RuSal), removed the topo II poisoning ability. This was surprising because, replacement of the central metal atom (which does not interact with topo II) completely abolished the biological activity of the molecule, while there was no alteration in the metal-ligand interaction or the chemical structure. To understand this effect, structural and conformational differences between the two molecules had to be analyzed, for which, minimal energy structural conformations of the molecules were generated through molecular modeling. Also, to examine whether other anticancer coordination complexes of ruthenium behave similarly with topo II, two coordination complexes of ruthenium have been tested for topo II antagonism. The first is RuIm, which has a metal atom flanked by two imidazole ligands. The ruthenium atom is also bonded to 4 chloride atoms. The second is RuInd, an indazole complex of ruthenium, which is similar to the imidazole complex, but with indazole ligands in place of imidazole. The synthesis and anticancer activity was first described by Keppler et. al. (1989). RuInd was found to be a more potent anticancer agent compared to RuIm. Both RuIm and RuInd possess significant antineoplastic activity against the Walker 256 **carcinosarcoma**, MAC 15A colon tumor, B16 melanoma and solid sarcoma 180 (Keppler et. al., 1990). These compounds

were more superior in their action against an autochthonous chemically-induced colorectal adenocarcinoma in rats compared to even 5-fluorouracil, which is an established cytostatic drug against human gastrointestinal carcinomas. Fruhauf and Zeller (1991) observed that RuInd brings about anti-tumor activity by interacting with DNA and inhibiting DNA synthesis. Though very effective, their clinical development was hindered due to extreme toxic effects on the body. Histological and blood-chemical investigations show major liver and kidney damage, hyperplasia and hyperkeratosis of gastric mucosa and anemia (Keppler et. al. 1990).

RESULTS

Topoisomerase II antagonism by RuIm and RuInd:

Inhibition of DNA relaxation activity:

Both metal complexes inhibit the supercoiled DNA relaxation activity of topo II. Ruind completely inhibits the DNA relaxation activity of topo II at a concentration of 250 μM , while RuIm inhibits the activity at a concentration of 300 μM **Figure 32** shows the dose dependent inhibition of topo II activity by these two drugs.

Inhibition of the DNA stimulated ATPase activity of topoisomerase II:

The ATPase assay shows that RuIm and Ruind significantly inhibit the DNA stimulated ATP hydrolysis activity of topo II. A comparison of ATPase inhibition by the two

complexes with RuSal is shown in **Figure 33**. These results correlate well with the inhibition of DNA relaxation activity by these complexes.

Formation of drug- induced, topoisomerase II mediated cleavage complex:

Consequent to the relaxation and ATPase inhibition by RuIm and RuInd, the next step was to check for the ability of the two complexes to freeze topo II and cleaved DNA in a cleavage complex. The results of this assay show that RuInd was very potent in poisoning the enzyme activity by formation of a cleavage complex (at a concentration of 150 μM), as evidenced by the appearance of linear DNA in the assay gels (**Figure 34**). RuIm also forms the cleavage complex, but at a much higher concentration of 300 μM . As shown earlier in *Chapter 3*, RuSal does not form the cleavage complex.

Anticancer activity assay:

The anticancer activity of the two drugs was analyzed through [^3H] thymidine incorporation assays on the two human cancer cell lines, colo-205 and ZR-75-1. The results of this assay agree with the previous reported findings that RuInd is a stronger anticancer agent compared to RuIm (**Figure 35**). The DNA intercalator was slightly more potent than RuInd, while RuSal showed the least effect on the cancer cell proliferation. The two drugs were more potent on the the breast carcinoma (ZR-75-1) compared to the colon carcinoma (colo-205).

Molecular modeling analysis:

An earlier study on Cobalt salicylaldoxime (CoSAL) and its derivatives showed that in these molecules, the cobalt atom and the salicylaldoxime ligands are in the same plane, 180° to each other (Ph.D. thesis of D. Jayaraju). But in case of RuSal, the large atomic size of ruthenium may sterically hinder this planar conformation, which orients the ligands at an angle of $\sim 40^\circ$ to each other. In RuIm and RuInd, the imidazole and indazole ligands are oriented in the same plane, giving the molecules a planar conformation, similar to that of CoSAL (**Figure 36**).

DISCUSSION

In order to investigate why RuSal does not poison topo II activity while CoSAL does, molecular modeling studies were carried out. The results of the modeling studies reveal that in CoSAL, planar conformation of the ligands along the horizontal axis of the molecule spatially orients the oxime groups to project out of the planar structure. This exposes the enzyme interacting oxime groups outside the plane of the molecule, thus facilitating a strong enzyme interaction. But in case of RuSal, the ruthenium atom induces a conformational change on the bidentate salicylaldoxime ligands and orients them at an angle of $\sim 40^\circ$ to each other along the horizontal axis. This orientation masks the oxime

groups from the outside environment. As a result of this steric interference by the ligand **orientation**, a proper interaction with the enzyme may be prevented. This could be **the** reason why **RuSal** partially inhibits the activity of topo II. Though the **salicylaldoxime** groups in CoSAL are also in a bidentate association with the metal atom, similar to RuSal, the cobalt atom is relatively smaller and may not induce any conformational stress on **the** ligands.

To investigate further if the abolition of topo II poisoning in RuSal is because of **the** spatial orientation of the ligands alone or possibly due to any other reason, two ruthenium coordination complexes which show excellent anticancer activity have been examined for topo II antagonism. The two complexes, RuIm and RuInd were selected due to two reasons. Firstly, they are similar to RuSal in being coordination complexes and possess two ligands on either side of the ruthenium atom. The second reason is that, the molecular modeling studies on their structures showed that the ligands are oriented in the same plane. 180° to each other, similar to CoSAL. Unlike RuSal, the ligands are monodentate, due to which they may not be under any conformational stress from the ruthenium atom, and are therefore in the same plane. Though these two molecules do not have the typical oxime interacting group, they have nitrogen atoms in the heterocyclic rings, at approximately the same positions as the oxime groups in CoSAL and RuSal. Hence, according to our reasoning, they would be able to antagonize topo II action at least to a small extent.

The topo II antagonism studies showed that these two compounds indeed poison **the** activity of topo II. The poisoning ability correlated well with their anticancer activity. This

shows that topoisomerase II antagonism may account for a significant amount of the anticancer activity attributed to these drugs.

Some studies have indicated putative structural and conformational requirements for topo II poisoning by drugs (MacDonald et. al., 1991, Capranico et. al., 1994, Zwelling et. al., 1992; Rene et. al., 1996). Though these conformations are not always a stringent requirement, such analysis on conformational requirements by structurally disparate topo II poisons will give an insight into the development of novel therapeutics directed against topo II. This is particularly important because, cancer cells regularly evolve mechanisms to resist the cytostatic action of anti-topo II drugs.

This case study about the effect of drug conformation on its molecular action merits a deeper investigation into the structure-activity relationship that drugs often possess. This would immensely help the cancer pharmacologist to develop rational drug molecules that attack a definite target.

FIGURE 32

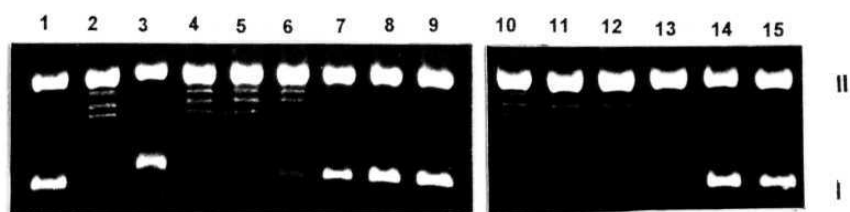


Figure 33: The ATPase inhibition assay shows that RuInd strongly inhibits the ATP hydrolysis reaction of topo II compared to RuIm. Both show a dose dependent action. The effect of RuSal on the ATPase action of topo II is also shown.

FIGURE 33

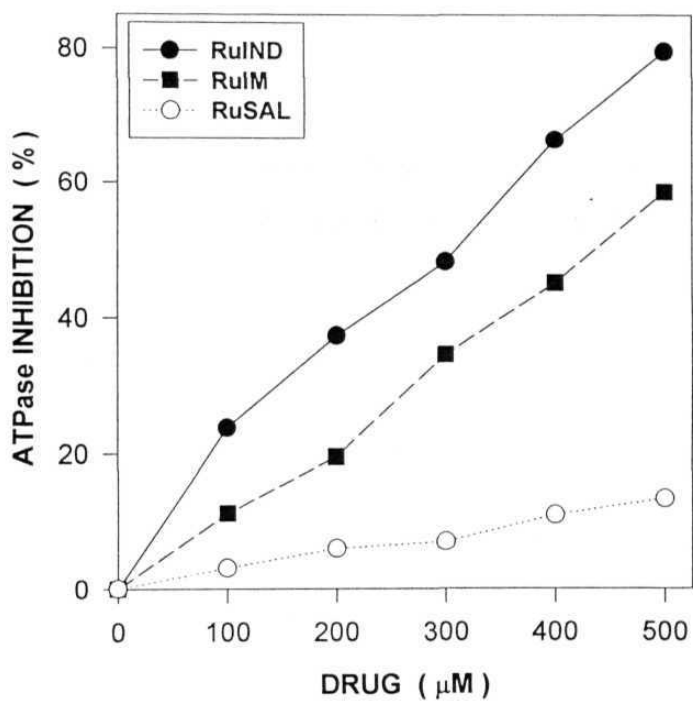


Figure 34: The cleavage assay on pBR322 DNA (lane 1) with topo II (lane 2) in the presence of 100 μ M m-AMSA (lane 3) and 100, 150, 200, 250, 300 and 350 μ M of RuInd (lanes 4 to 9) and the same concentrations of RuIm (lanes 10-15) shows that RuInd forms the cleavage complex at a concentration of 150 μ M and RuIm at 300 μ M.

FIGURE 34

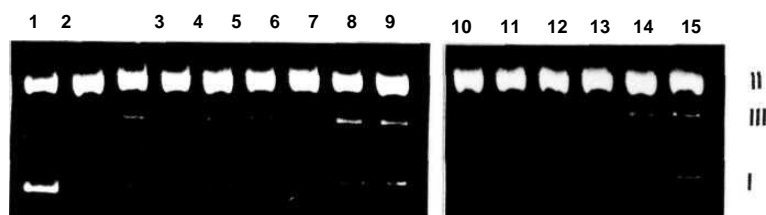


Figure 35: The anticancer activity assay on the two cancer cell lines shows that RuInd is a very potent anticancer agent, which almost matches the anticancer effect of m-AMSA. RuIm also showed a significant effect on the proliferation of the cancer cells. RuSal was the least effective. As observed in the earlier studies, the ZR-75-1 cells (B) were less responsive to the anti-proliferative action compared to the colo-205 cells (A).

FIGURE 35

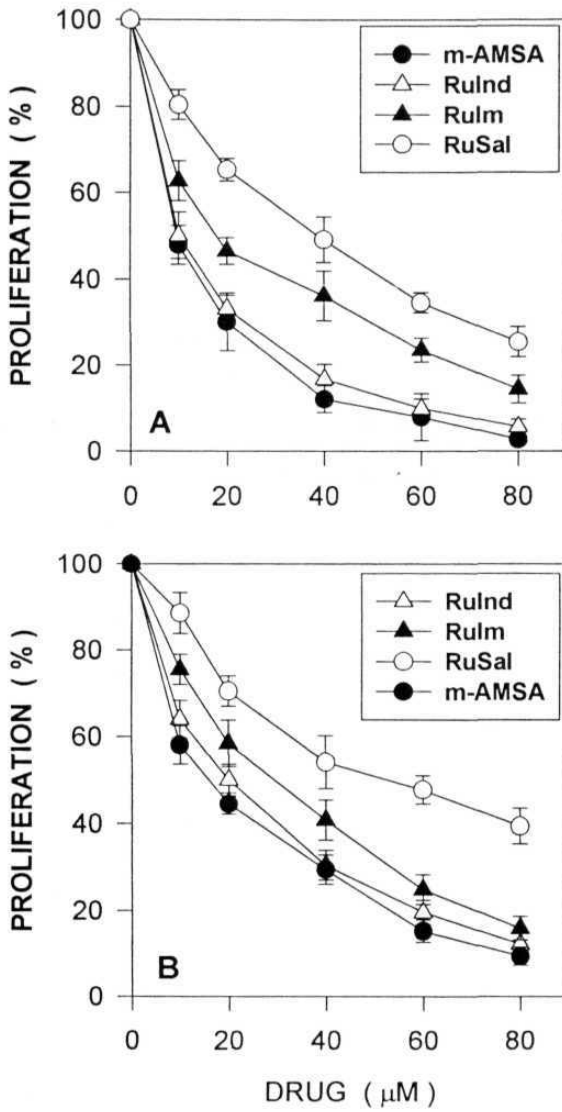
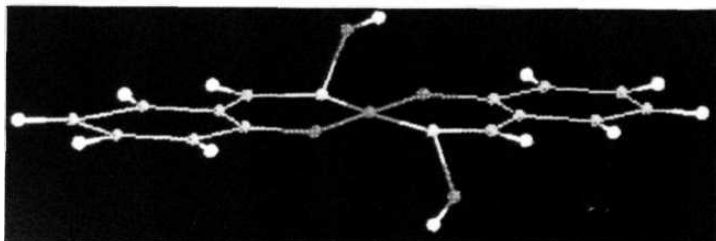


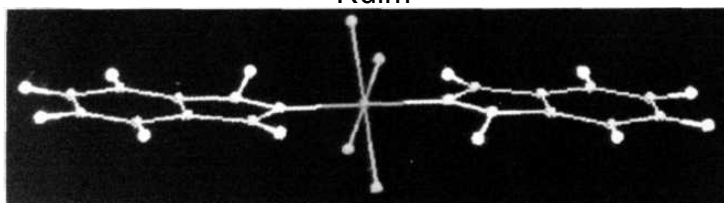
Figure 36: A comparison between the molecular models of CoSAL, RuSal, RuInd and RuIm shows that in CoSAL, RuInd and RuIm, the ligands attached to the metal atom are in the same plane with each other, while in RuSal, the ligands are oriented at an angle of 40° to each other along the horizontal plane of the molecule. The central metal atom in all the molecules is shown in green. In RuIm and RuInd, chlorides are shown in yellow and ring nitrogens are shown in white. In CoSAL and RuSal, the N-OH oxygens and the metal coordinating oxygens are shown in red. In CoSal, the OH groups (of N-OH) project out of the plane of the molecule, while in RuSal, the OH groups are in the same plane as the respective salicylaldoxime ligands.

FIGURE 36

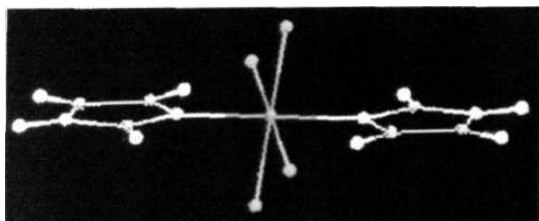
CoSAL



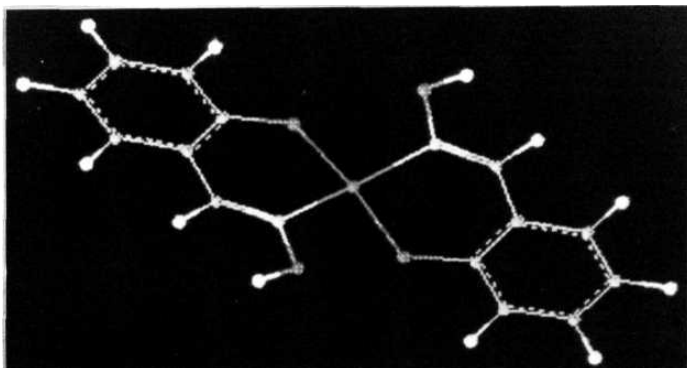
Rulm



Rulnd



RuSal



CONCLUSIONS

The work embodied in this thesis evaluates the functional significance of topoisomerase II antagonism by organometallic complexes of iron and ruthenium for anticancer therapy. The major conclusions of our study are enumerated below, which argue that these topoisomerase II targeting drugs have the potential to be exploited for cancer chemotherapy.

1. The molecular analysis of topoisomerase II poisoning suggests the requirement of N-donor, O-donor and S-donor groups on the ligands (attached to the iron or ruthenium atom) to interact with the enzyme. These electronegative centers may be involved in non-covalent interaction with the electropositive groups on the enzyme.
2. Unsubstituted ferrocene has no effect on topoisomerase II activity and also shows no anticancer action, while the mono-substituted acetyl and carboxaldoxime derivatives of ferrocene (AcFecp and FecpOx) inhibit the topoisomerase II-catalyzed relaxation of supercoiled DNA but do not poison the enzyme by cleavage complex formation. On the other hand, the di-substituted derivatives (DacFecp & FecpDox) effectively poison topoisomerase II by cleavage complex formation. This, coupled with the molecular modeling analysis suggests that though the iron atom and the cyclopentadiene rings do not directly involve in topoisomerase II poisoning, the structural conformation provided by this backbone to the double substitution (and not the single substitution) may be important for topoisomerase II poisoning by these compounds.

3. FecpDox was more potent than DacFecp suggesting that the N-donor interaction of the carboxaldoxime group with topoisomerase II may be more effective for poisoning the enzyme compared to the O-donor interaction of the acetyl group. The DNA non-binding nature of the ferrocene molecules and the organometallic linkages on the metal atom could minimize iron induced toxicity. These observations suggest that the di-substituted ferrocene compounds are attractive anticancer drug candidates, and merit further investigation.
4. Our work on the RuBen drugs introduces novel and effective topoisomerase II poisons, which poison the enzyme through formation of a ternary 'cleavage complex' The first compound in this class, RuBen(dmso), served as a good lead molecule for the design of new derivatives with enhanced anticancer action.
5. A noteworthy point in understanding the molecular mechanism of action of these compounds is that a pyridine ring in place of the dimethyl sulfoxide group (in RuBenPy) abolishes topoisomerase II poisoning. In RuBenPy, the electronegative center of the pyridine ring, the nitrogen atom, is already coordinated to the ruthenium atom and there is no other group on the ring for enzyme interaction. Introduction of a single amino group on the pyridine ring (RuBenAPy) greatly increased topoisomerase II poisoning and anticancer activity. This result and the molecular modeling analysis suggest that the coordinated ligands, 'dmso', 'aminopyridine', 'aminoguanidine' and 'aminobenzoic' acid may be major enzyme interacting domains on the RuBen drugs.

6. Based on the molecular analysis of topoisomerase II poisoning by the ferrocene and RuBen drugs, the following putative mechanism of action may be proposed -

" The di-substituted ferrocene drug binds to the topoisomerase II and following DNA interaction and cleavage by the enzyme, the drug freezes the enzyme and cleaved DNA in a 'closed clamp conformation' called the cleavage complex, thus abrogating the DNA religation step

The RuBen drugs follow a slightly different mechanism. They interact bi-directionally with both enzyme and DNA- the ruthenium atom interacts with DNA while the coordinated ligands interact with the enzyme, ultimately leading to the formation of the cleavage complex. "

7. The anticancer studies using the iron and ruthenium drugs correlate with their topoisomerase II poisoning ability, arguing that topoisomerase II poisoning may be the major mechanism involved in their anticancer action.

8. Our studies show that the spatial conformation of the organometallic iron and ruthenium molecules is an important determinant for topoisomerase II poisoning. The enzyme interacting groups must extend out of the molecular structure in order to interact strongly with the enzyme. This is especially true in the case of the coordination ruthenium complexes of RuIm and RuInd. A detailed X-ray crystallographic analysis on the topoisomerase II-drug association could determine the exact drug interacting

sites on the enzyme. This information could be immensely useful for understanding the molecular events leading to cleavage complex formation and in the development of superior organometallic therapeutics targeted to topoisomerase II.

- 9 Our studies on the transferrin mediated delivery of the RuBen drugs provides a methodology for targeting topoisomerase II antagonistic anticancer metal complexes to cancer cells. Because transferrin is a natural delivery system and has a good affinity for binding to ruthenium containing compounds, it is an attractive approach for delivery of such compounds. The results of this study show that apotransferrin holds promise as a potential delivery vehicle for ruthenium containing compounds

REFERENCES

- Adachi, Y, Luke, M., and Laemmli, U.K. (1991) *Cell* **64**, 137-148
- Adamson, R.H, Canellos, G.P., and Sieber, S.M., (1975) *Cancer Chemolther. Rep.* 59 (part 1), 599-610
- Anderson, R.D., and Berger, N.A. (1994) *Mutat. Res.* **309**, 109-142
- Barabas, K, Sizensky, J.A., and Faulk, W.P. (1992) *Biol. Chem.* **267**, 9437-42
- Bates, G.W., Workman, E.F., and Schlabach, M.R. (1973) *Biochem. Biophys. Res. Commun.* **50**, 84-90
- Beck, W.T., Kim, R., and Chen, M. (1994) *Cancer Chemolther. Pharmacol.* **34**, 14-18
- Bell, W.B. (1929) *Br. Med.* **7**, 431-437
- Bennet, M.A., and Smith, A.K., (1974) *J. Chem. Soc. (Dalton trans.)* 233-241
- Berger, J.M., Gamblin, S.J., Harrison, S C, and Wang, J.C. (1996) *Nature*, **379**, 225-232
- Blum, H, Beier, H., and Gross, H.J., (1987) *Electrophoresis* **8**, 93-97
- Bodley, A , Wu, H.Y., and Liu, L.F. (1987) *NCI Monogr* **4**, 31-35
- Bradford, M.M. (1976) *Anal. Biochem* **72**, 248-254
- Broadhead, G D, Osgerby, J. M, and Pauson, P. L. (1955) *J. Chem. Soc.* **77**, 650-656
- Capranico, G, Palumbo, M, Tinelli, S., Mabilia, M., Pozzan, A., and Zunino, F. (1994) *J.Mol. Biol.* **235**, 1218-1230
- Cardenas, ME., and Gasser, S.M., (1993) *Cell Sci.* **104**, 219-225
- Chen, A Y, and Liu, L.F. (1994) *Annu. Rev. Pharmacol. Toxicol.* **34**, 191-218
- Chen, G.L., Yang, L., Rowe, T.C., Halligan, B.D., Tewey, KM, and Liu, L.F. (1984) *Biol. Chem.* **259**, 13560-13566
- Christman, M.F., Dietrich, F.S., and Fink, G.R., (1988) *Cell* **55**, 413-425
- Clarke, M.J. (1989) *Prog. Clin. Biochem. Med.* **10**, 25-39

- Collier, W. A., and Krauss, F. (1981) *Orgmet. In Cancer Chemother.* 34, 526
- Corbett, AH., and Osheroﬀ, N. (1993) *Chem. Res. Toxicol.* 6, 585-597
- Courts, J., Plumb, J.A., Brown, R., and Keith, W.N., (1993) *Br. J. Cancer* **68**, 793-800
- D'Arpa, P., and Liu, L.F. (1989) *Biochem. Biophys. Acta* **989**, 163-177
- Devita, V.T., Hellman, S., Rosenberg, S.A. (eds) (1985) *Cancer, Principles and Practice of Oncology*. Lippincott, Philadelphia
- DiNardo, S., Voelkel, K., and Sternglanz, R., (1984) *Proc. Natl. Acad. Sci. U.S.A.* **81**, 2616-2620
- Downes, C.S., Clarke, D.J., Mullinger, A.M., Gimenez-Ablan, J.F., Greighton, A.M., Johnson, R.T. (1994) *Nature* **372**, 467-470
- Drake, F.H., Zimmerman, J.P., McCabe, F.L., Bartus, H.F., Per, S.R., Sullivan, D.M., Ross, W.E., Mattern, M.R., Johnson, R.K., and Crooke, S.T. (1987) *J. Biol. Chem.* **262**, 16739-16747
- Drlica, K., and Franco, R.J. (1988) *Biochemistry* 27, 2253-2259
- Earnshaw, W.C., and Heck, M.M (1985)./ *Cell Biol.* **100**, 1716-1725
- Ehrlich, P (1910) *Berl. Klin. Wochenschr* 43, 1996-1999
- Ferguson, L.R., and Baguley, B.C. (1994) *Environ. Mol. Mutagen.* 24, 245-261
- Froelich-Ammon, S.J., and Osheroﬀ, N. (1995) *J. Biol. Chem.* **270**, 21429-21432
- Fruhauf, S., and Zeller, W.J. (1991) *Cancer Res.* 51, 2943-8
- Galande, S., and Muniyappa, K. (1996) *Biochim Biophys. Acta* **1308**, 58-66
- Galbraith, G.M.P., Galbraith, R.M., and Faulk, W.P. (1980) *Cell Immunol.* 49, 215-222
- Gasser, S.M., and Laemmli, U.K. (1987) *Trends Genet.* 3, 16-22
- Giraldi, T., Sava, G., Bertoli, G., Mestroni, G., Zassinovich, G, and Stolfi, D. (1977) *Cancer Res.* **37**, 2662-2666

- Gupta, M, Fujimori, A., and Pommier, Y. (1995) *Biochem. Biophys. Acta* **1262**, 1-14
- Haiduc, I., and Silvestru, C. *Organomet. in Cancer Chemotherapy*, Vol II, 1994.
- Hertzberg, R. P., Caranfa, M. J., and Hecht, S. M. (1989) *Biochemistry* **28**, 4629-4638
- Hill, B.T., Whatley, S.A., Bellamy, A.S., Jenkins, L.Y., Whelan, R.D.H. (1982) *Cancer Res.* **42**, 2852-6
- Hirano, T., and Mitchison, T.J. (1993)./. *Cell. Biol.* **120**, 601-612
- Holm, C, Goto, T., Wang, J.C., and Botstein, D. (1985) *Cell* **41**,553-563
- Holm, C, Stearns, T., and Botstein, D (1989) *Mol. Cell Biol.* **9**, 159-168
- Hsiang, Y.H., Wu, J.Y., and Liu, L.F (1988) *Cancer Res.* **48**, 3230-3235
- Ishida, R., Sato, M., Narita, T., Utsumu, K.R., Nishimoto. T., Morita, T., Nagata, H., Andoh, T. (1994) *J. Cell. Biol* **126**, 1341-1351
- Jayaraju, D., Vashisht Gopal, Y.N., and Kondapi, A.K. (1999) *Arch. Biochem. Biophys.* **369**, 68-77
- Juliano, R.L., Alahari, S , Yoo, H., Kole, R., and Cho, M. (1999) *Pharm. Res.* **16**, 494-502
- Kelly, J.M., Tossi, A.B., McConnell, D J., and OhUigin, C. (1985) *Nucleic Acids Res.* **13**,6017-6033
- Keppler, B K., Berger, Berger, M.R., and Heim, M.E., (1990) *Cancer Treat. Rev.* **17**, 261-277
- Keppler, B.K., Henn, M, Juhl, U.M., Berger, M.R., Niebl, R., and Wagner, F.F. (1989) *Prog. Clin. Biochem. Med.* **10**, 41-69
- Keppler, B.K., Friesen, C, Moritz, H.G., Vongerichten, H., Vogel, E., (1991) *Struct. Bond.* **78**,97-127
- Keppler, B.K., Henn, M, Juhl, U.M., Berger, M.R., Niebl, R., and Wagner, F.F. (1989) *Prog. Clin. Biochem. Med.* **10**, 41-69
- Kim, R.A., and Wang, J.C. (1989) *J. Mol. Biol.* **208**, 257-267

- Kim, R.A., and Wang, J.C., (1989) *Cell* **51**, 975-985
- Kopf-Maier, P. (1989) *Cancer Chemother. Pharmacol* **23**, 225-230
- Kopf-Maier, P., and Kopf, H. (1988) *Structure and Bonding*, p. 103, Springer-Verlag, Berlin, Heidelberg.
- Kopf-Maier, P. (1994) *Eur. J. Clin. Pharmacol.* **147**, 1-16
- Kratz, F , Hartmann, M, Keppler, B.K., and Messori, L (1994) *J. Biol. Chem.* **269**, 2581-2588
- Laemmli, U.K. (1970) *Nature* **227**, 680-685
- Lippard, S J. (1993) *Robert A. Welch Foundation 37th Conference on Chem. Res.* Pp. 49-60
- Liu, L.F., and Wang, J.C. (1987) *Proc. Natl. Acad. Sci. U.S.A.* **84**, 7024-7027
- Liu, L.F (1989) *Annu Rev. Biochem.* **58**, 351-375
- Lockshon, D., and Morris, DR., (1983) *Nucleic Acids Res* **11**, 2999-3017
- Liu, L.F (ed) (1994) *Adv. Pharmacol.* **29**.
- Lu, Z.R., Kopeckova, P., and Kopecek, J. (1999) *Nat. Biotechnol.* **17**, 1101-1104
- Lumme, P., and Elo, H. (1984) *Inorg. Chim. Ada* **92**, 241-251
- Ma, X., Saitoh, N., and Curtis, P.J., (1993) *J. Biol. Chem.* **268**, 6182-6188
- MacDonald, T.T., Lehnert, E.K., Loper, J.T., Chow, K.C., and Ross, WE. (1991) *DNA Topoisomerases in Cancer* (Potmesil, M. and Kohn, K.W., eds.), P p 199-214, Oxford University Press, New York
- Maxwell, A. (1992) *J. Antimicrob. Chemother* **30**, 409-414
- Mayer, L.D. (1998) *Cancer Metastasis Rev.* **17**, 211-218
- McCord, J.M. (1996) *Nutr. Rev.* **54**, 85-88

Mestroni, G , Alessio, E., Calligaris, M., Attia, W.M., Quadrifoglio, F., Cauci, S., Sava, G., Zorzet, S., Pacor, S., Monti-Bragadin, C, Tamaro, M., and Ddolzani, L. (1989) *Prog. Clin. Biochem.* 10, 73-87

Nabiev, I., Chourpa, I., M. J., Riou, J. F., and Nguyen, C. H., Lavelle. F., and Manfait, M. (1994) *Biochemistry* 33, 9013-9023

Nelson, EM., Tewey, K.M., Liu, L.F. (1984) *Proc. Natl. Acad. Sci. U.S.A.* 81, 1361-1365

Nicolini, M (ed) (1988) *Platinum and other Metal Coordination Compounds in Cancer Chemotherapy* Nijhoff, Boston

Osheroff, N., Shelton, E. R., and Brutlag, D. L. (1983) *J. Biol. Chem.* **208**, 9536-9543

Pacor, S., Sava, G., Ceschia, V., Bregant, F., Mestroni, G , and Alessio, E. (1991) *Chem. Biol. Interact.* 78, 223-234

Pommier, Y. (1993) *Cancer Chemother. Pharmacol* 32, 103-108

Pommier, Y., Leteurtre, F., Fesen, M.R., Fujimori, A., Bertrand, R., Solary, E., Kohlhausen, G., and Kohn, K.W. (1994; *Cancer Invest* 12, 530-542

Potmesil, M., and Kohn, K.W (1991) *DNA Topoisomerases in Cancer*, Oxford University Press, New York.

Prus, G.J., and Drlica, K. (1986) *Proc. Natl. Acad. Sci. U.S.A.* 83, 8952-8956

Reece, R. J., and Maxwell, A. (1991) *Crit. Rev. Biochem. Mol. Biol.* 26, 335-375

Rene, B , Fosse, P., Khelifa, T., Jacquemin-sablon, A., and Bailly, C. (1996) *Mol. Pharmacol.* 49, 343-350

Rice, L.M., Slaik, M., Schein, P., (1977) *Clinical brochure: spirowgermanium* (NSC-192965) NCI, Bethesda, Md.

Robinson, M.J., and Osheroff, N. (1990) *Biochemistry* 29, 2511-2515

Roca, J. (1995) *Trends Biochem. Sci.* **20**, 156-160

Rosenberg, B., VanCamp, L., Trosko, J.E., and Mansour, V.H. (1969) *Nature* **222**, 385-386

- Saitoh, N , Goldberg, I.G., Wood, E.R., and Earnshaw, W.C. (1994) *J. Cell Biol.* **127**, 303-318
- Sava, G , Pacor, S., Bregant, F., and Ceschia, V. (1991) *Anticancer Res* **11**, 1103-1108
- Sava, G., Pacor, S., Zorzet, S., Alessio, E., and Mestroni, G , (1989) *Pharmacol. Res.* **21**, 617-628
- Sava, G., Zorzet, S., Giraldi, T., Mestroni, G., and Zassinovich, G. (1984) *Eur. J. Cancer Clin. Oncol.* **20**, 841-847
- Sinha, B.K., (1995) *Drugs* **49**, 11-19
- Singh, M. (1999) *Curr. Pharm. Des.* **5**, 443-51
- Singh, M , Atwal, H , and Micetich, R. (1998) *Anticancer Res.* **18**, 1423-7
- Slichenmyer, W.J., Rowinsky, E.K., Donehower, R C , and Kaufmann, S.H. (1993) *J. Natl. Cancer Inst.* **85**, 271-287
- Smith, P.J. (1990) *BioEssays* **12**, 167-172
- Srivastava, S C , Mausner, L.F , Clarke, M.J. (1989) *Prog Clin. Biochem.* **10**, 111-149
- Swedlow, J.R., Sedat, J.W., and Agard, D A , (1993) *Cell* **73**, 97-108
- Tan, K.B., Dorman, T.E., Falls, K.M., Chung, T.D.Y., Mirabelli, C.K., Crooke, ST., and Mao, J (1992) *Cancer Res.* **52**, 231-234
- Towbin, H., Stachelin, T., and Gordon, J. (1979) *Proc. Natl. Acad. Sci. U.S.A.* **76**, 4350-4354
- Tricoli, J.V., Sahai, B.M., McCormick, P.J., Jarlinski, S.J., Bertram, J.S., and Kowalski, D. (1985) *Exp. CellRes* **158**, 1-14
- Tsai-Pflugfelder, M., Liu, L.F , Liu, A.A., Tewey, K.M., Whang-Peng, J., Knutsen, T., Huebner, K., Croce, C.M., and Wang, J.C. (1988) *Proc. Natl. Acad. Sci. U.S.A.* **85**, 7177-7181
- Uemura, T., and Yanagida, M. (1986) *EMBO J.* **5**, 1003-1010
- Vashisht Gopal, Y.N., Jayaraju, D , and Kondapi, A.K., (1999) *Biochemistry* **38**, 4382-88

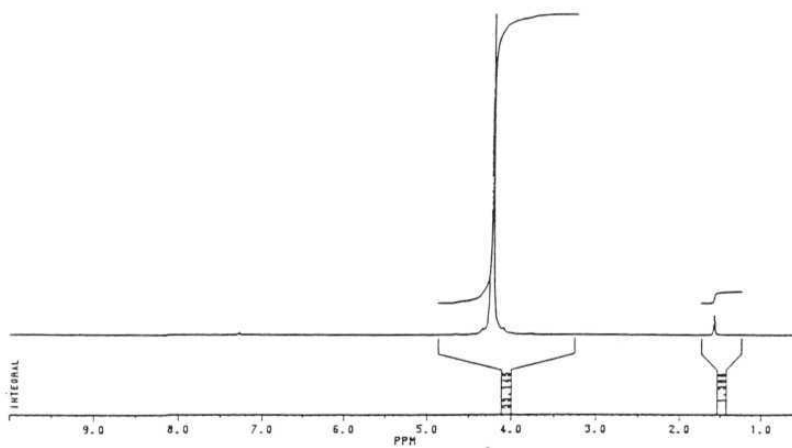
- Waalkes, T.P , Sanders, K., Smith, R.G., Adamson, R.H. (1974) *Cancer Res.* 34, 385-391
- Wang, J.C. (1985) *Annu. Rev. Biochem.* 54, 665-697
- Wang, J.C. (1991) *J. Biol. Chem.* **266**, 6659-6662
- Wang, J.C. (1996) *Annu. Rev. Biochem.* 65, 635-692
- Wang, Z , and Rossman, T. G. (1994) *BioTechniques* 16, 460-463
- Watt, P.M., and Hickson, ID. (1994) *Biochem. J.* **303**, 681-695
- Weinberg, E.D. (1999) *Emerging Infectious Diseases* 5, 346-352
- Weinberg, E.D , and Weinberg, G.A. (1995) *Curr. Opinion Infect. Diseases* 8, 164-169
- Wilkinson, G , Cotton, F. A., and Birmingham, J. M. (1956) *J. Inorg. Nucl. Chem.* 2, 95
- Woessner, R.D., Chung, T.D.Y., Hofmann, G.A., Mattern, M.R., Mirabelli, C.K., Drake, F.H., and Johnson, R.K. (1990) *Cancer Res.* 50, 2901-2908
- Woessner, R.D , Mattern, M.R., Mirabelli, C.K., Johnson, R.K., and Drake, F.H. (1991) *Cell Growth Differentiation.* 2, 209-214
- Wood, E.R., and Earnshaw, W.C. (1990) *J. Cell Biol.* **111**, 2839-2850
- Zecheidrich, E L , Christiansen, K., Anni, H , Ole, W., and Osheroff, N. (1989) *Biochemistry* 28, 6229-6236
- Zelonka, R.A., and Baird, M.C. (1972) *Canad. J. Chem.* 50, 3063-3072
- Zwelling, L.A., Mitchell, M.J., Satitpunwaycha, P., Mayes, J., Altschuler, E., Hinds, M., and Baguley, B.C. (1992) *Cancer Res.* 52, 209-217

SPECTRAL DATA OF THE SYNTHESIZED COMPLEXES

SPECTRA 1

Ferrocene : $Di-\pi$ -cyclopentadiene iron (II)

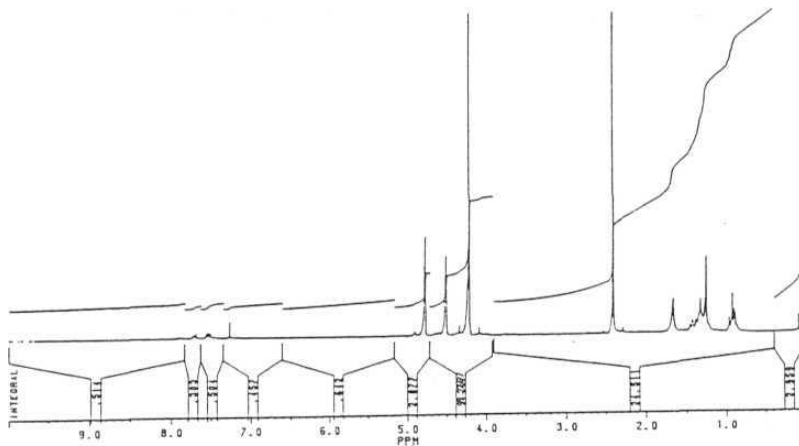
Proton NMR spectra: Singlet peak at 4.18 PPM, corresponding to the cyclopentadiene ring hydrogens.



SPECTRA 2

Acetyl Ferrocene: 1-acetyl di- π -cyclopentadiene iron (II)

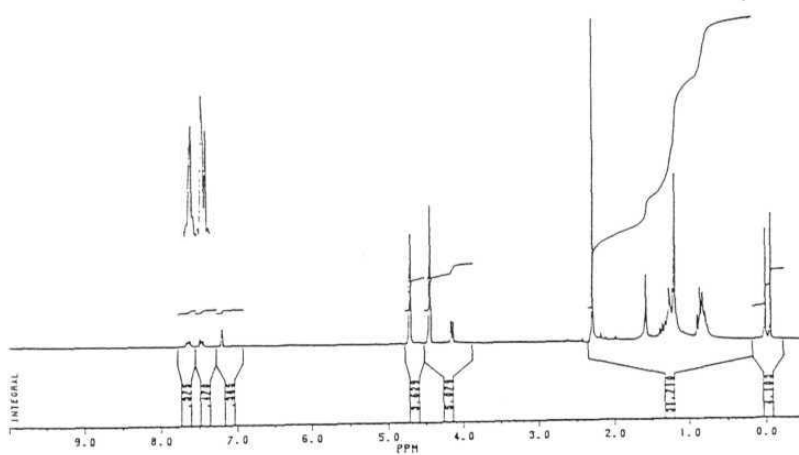
Proton NMR spectra: 4.2 PPM corresponding to the un-substituted lower ring hydrogens, 2.42 PPM corresponding to methyl group hydrogens, 4.5 and 4.8 PPM corresponding to the shifted hydrogens in the acetyl substituted ring.



SPECTRA 3

Diacetyl ferrocene: 1,1'-diacetyl- π -cyclopentadiene iron (II)

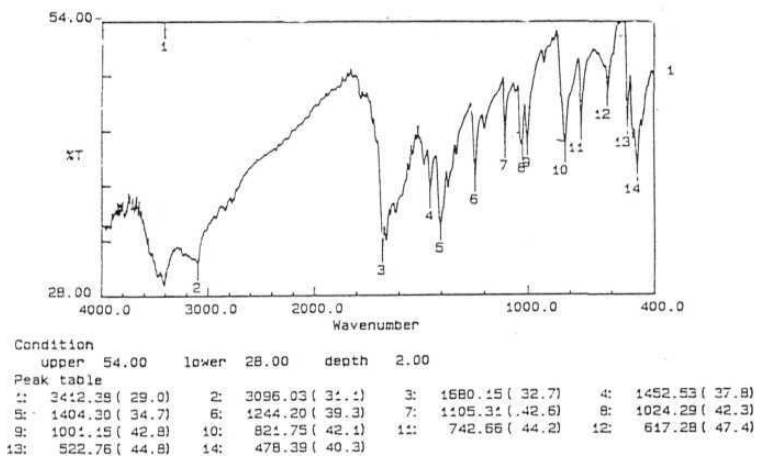
Proton NMR spectra: 2.3 PPM corresponding to the methyl group hydrogens. 4.48 and 4.7 PPM corresponding to the hydrogens on the acetyl substituted ring.



SPECTRA 4

Ferrocene Carboxaldoxime: 1-carboxaldoxime di- π -cyclopentadiene iron (II)

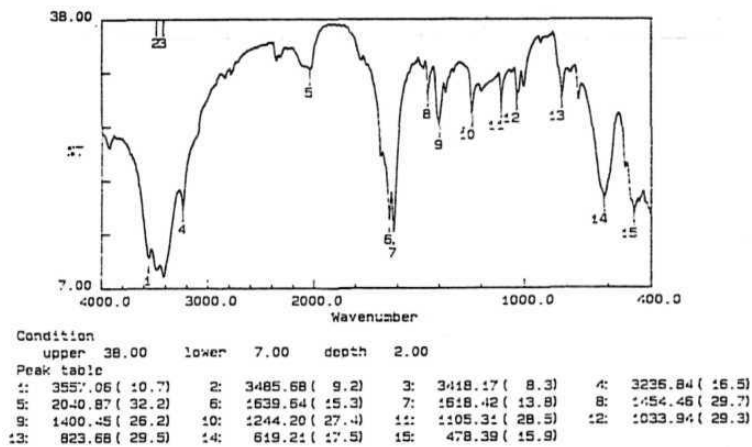
FT-IR spectra: IR band at 3412 cm⁻¹ confirms the presence of carboxaldoxime group in ferrocene.



SPECTRA 5

Ferrocene dicarboxaldoxime: 1,1'-di-carboxaldoximdi- π -cyclopentadiene iron (II)

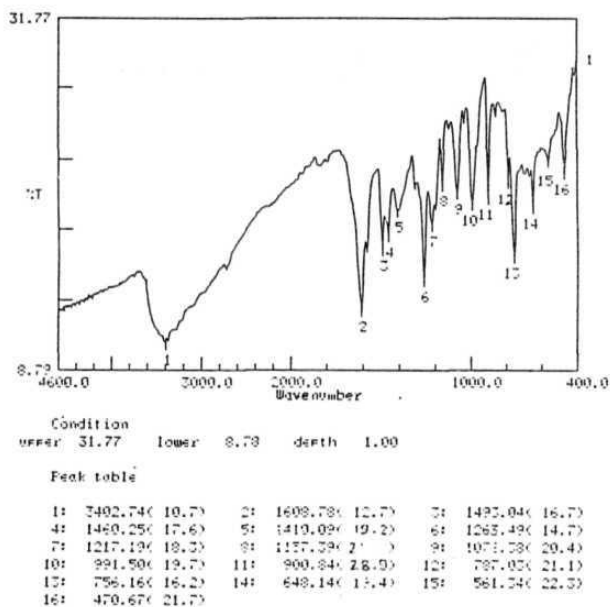
FT-IR spectra: IR band at 3557 cm^{-1} confirms the formation of the dicarboxaldoxime.



SPECTRA 6

RuSAL: *Trans his salicylaldoximate ruthenium (IT)*

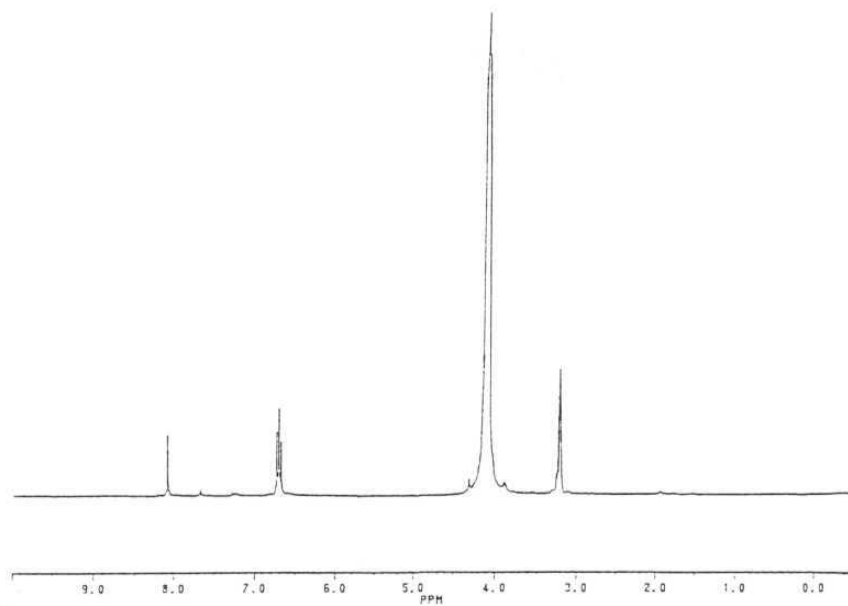
FT-IRspectra: Band at 1608 cm^{-1} confirms the formation of a coordination bond between imine nitrogen and metal atom; band at 1493 cm^{-1} confirms the metal- oxygen bond



SPECTRA 7

RuBen(dmsO):(η^6 -benzene)dichloro sulfinyl bis(methane)-O-ruthenium(II) /

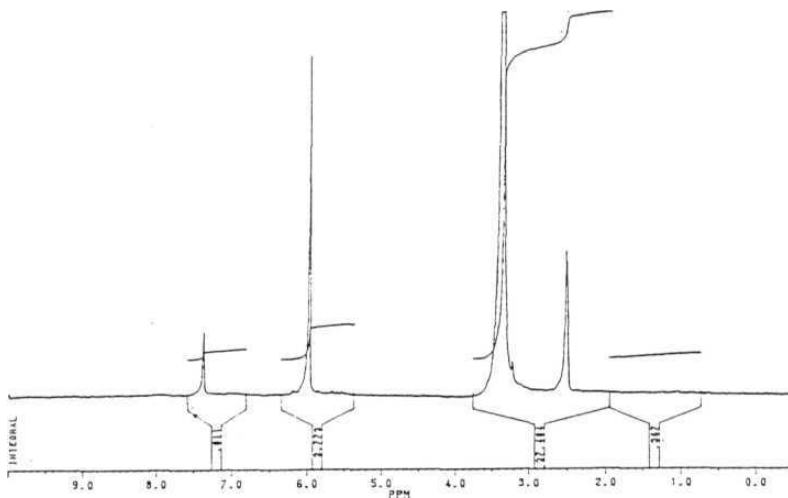
Proton NMR spectra in *d*₆- DMSO (the '*dmsO*' ligand is also *d*₆-DMSO):5 4.07 PPM
corresponding to the organometallic bonded benzene ring hydrogens.



SPECTRA 8

RuBenPv: η^6 -benzene(pyridine)-N-ruthenium(II)

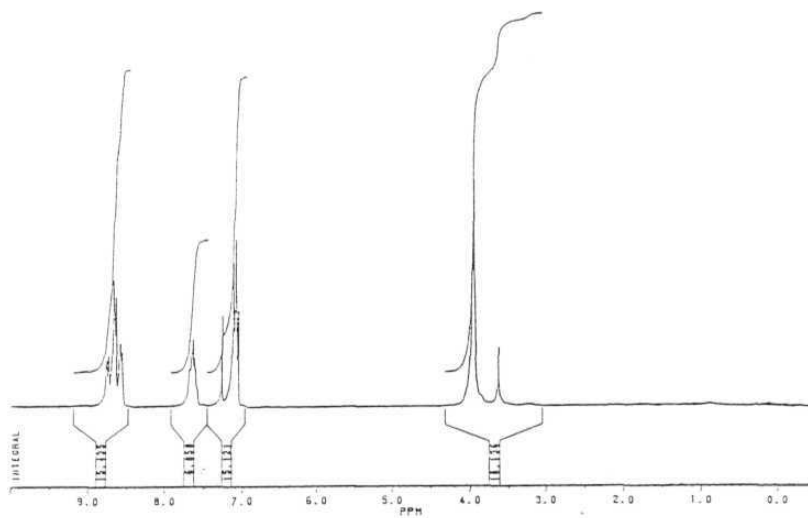
Proton NMR spectra in *d*₆-DMSO: 5.6 and 7.4 PPM corresponding to the shifted pyridine hydrogens, 5.3 and 3.4 PPM corresponding to the benzene ring hydrogens.



SPECTRA 9

RuBenAPy: η^0 -benzene (3-amino pyridine)-N1-ruthenium(II) /

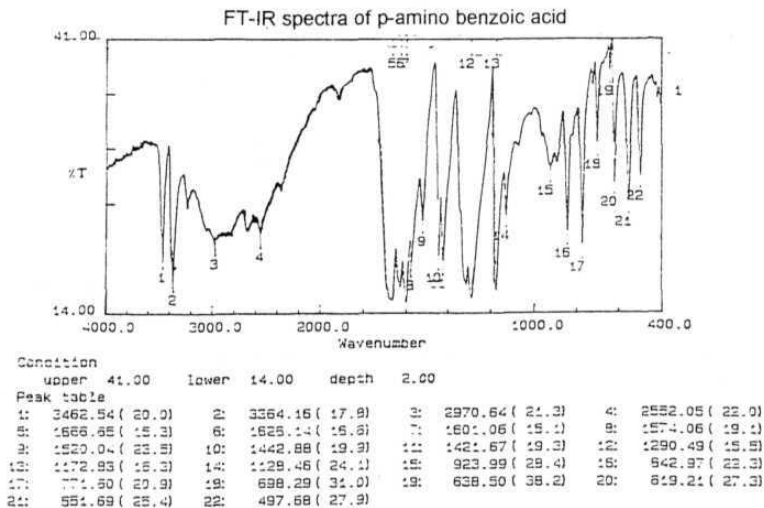
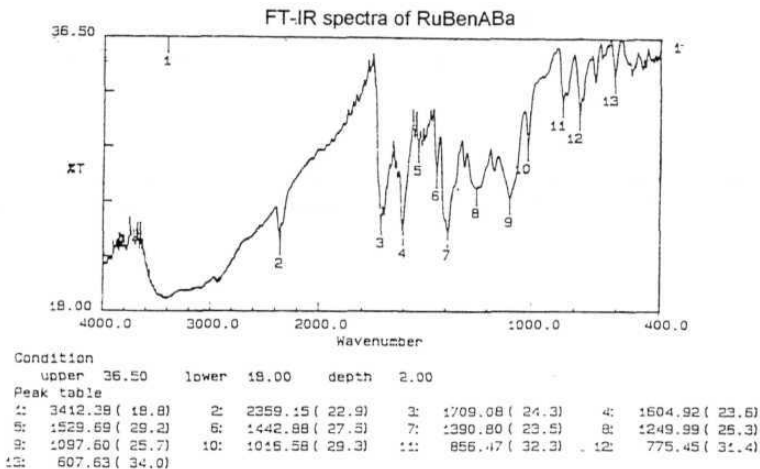
Proton NMR spectra in *d*6-DMSO: 5 7.1, 7.65 and 8.7 PPM corresponding to the shifted pyridine ring hydrogens, 5 3 9 PPM corresponding to the benzene ring hydrogens.



SPECTRA 10

RuBenABa: I (η^6 -benzene)(p-amino benzoic)-O-ruthenium (II) I

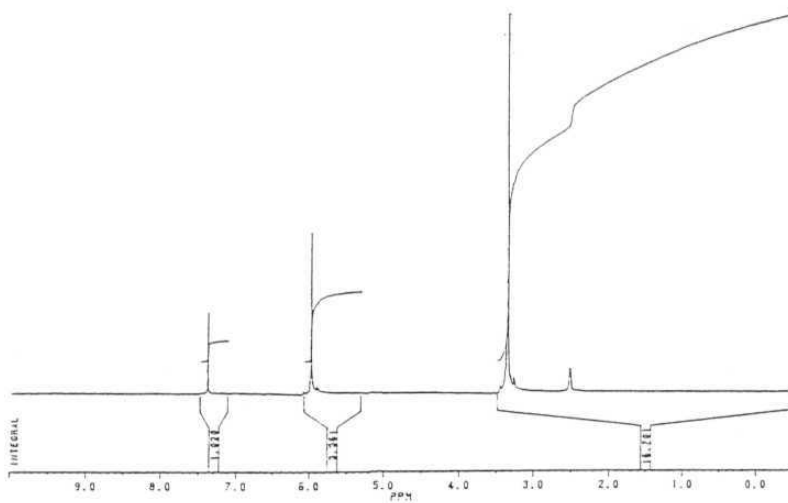
FT-IR Spectra: Bands at 3462 cm^{-1} and 3364 cm^{-1} correspond to the anti-bonding stretching by the hydroxyl oxygen upon coordination with the ruthenium atom.



SPECTRA 11

RuBenAGu: f (η^6 -benzene) (amino guanidine)-N1-ruthenium D 1

Proton NMR spectra in **d6-DMSO**: 5.59 and 7.3 PPM corresponding to the amino hydrogens of the amino guanidine group, 5.33 PPM.



List of Publications

1. *Inhibition of Topoisomerase II Catalytic Activity by two Ruthenium Compounds: A Tigand Dependent Mode of Action*

Y. N. Vashisht Gopal, D. Jayaraju and Anand K. Kondapi
Biochemistry (1999) 38, 4382-4388

2. *Topoisomerase II Poisoning and Aitineoplastic action by DNA non binding Diacetyl and Dicarboxaldoxime derivatives of Ferrocene.*

Y. N. Vashisht Gopal, D. Jayaraju and Anand K. Kondapi
Archives of Biochemistry and Biophysics (2000) TN PRESS

- 3 *Topoisomerase II Antagonism by Coordinated Derivatives of $[RuCl_2(C_6H_6)(dmsO)]$: Potential use of Apotransferin in Mediated Delivery for Anticancer Action.*

Y. N. Vashisht Gopal and Anand K. Kondapi
Communicated to the Journal of Biological Chemistry (2000)

Publications associated with:

Topoisomerase II is a Cellular Target for the Anti-proliferative Cobalt Salicylaldoxime Complex.

D. Jayaraju, Y. N. Vashisht Gopal and Anand K. Kondapi
Archives of Biochemistry and Biophysics (1999) 369, 68-77

Single Strand DNA Cleavage by Topoisomerase II in Presence of Anticancer Copper Salicylaldoxime Complex.

D. Jayaraju, Y. N. Vashisht Gopal and Anand K. Kondapi
Communicated to Journal of Bioscience (2000)

Inhibition of Topoisomerase II Catalytic Activity by Two Ruthenium Compounds: A Ligand-Dependent Mode of Action[†]

Y. N. Vashisht Gopal, D. Jayaraju, and Anand K. Kondapi*

Department of Biochemistry, School of Life Sciences, University of Hyderabad, Hyderabad-46, India

Received August 18, 1998; Revised Manuscript Received January 7, 1999

ABSTRACT: The ability of two structurally different ruthenium complexes to interfere with the catalytic activity of topoisomerase II was studied to elucidate their molecular mechanism of action and relative antineoplastic activity. The first complex, $[\text{RuCl}_2(\text{C}_6\text{H}_6)(\text{dmsO})]$, could completely inhibit DNA relaxation activity of topoisomerase II and form a drug-induced cleavage complex. This strongly suggests that the drug interferes with topoisomerase II activity by cleavage complex formation. The bi-directional binding of $[\text{RuCl}_2(\text{C}_6\text{H}_6)(\text{dmsO})]$ to DNA and topoisomerase II was verified by immunoprecipitation experiments which confirmed the presence of DNA and ruthenium in the cleavage complex. The second complex, Ruthenium Salicylaldehyde, could not inhibit topoisomerase II relaxation activity appreciably and also could not induce cleavage complex formation, though its DNA-binding characteristics and antiproliferation activity were almost comparable to those of $[\text{RuCl}_2(\text{C}_6\text{H}_6)(\text{dmsO})]$. The results suggest that the difference in ligands and their orientation around a metal atom may be responsible for topoisomerase II poisoning by the first complex and not by the second. A probable mechanism is proposed for $[\text{RuCl}_2(\text{C}_6\text{H}_6)(\text{dmsO})]$, where the ruthenium atom interacts with DNA and ligands of the metal atom form cross-links with topoisomerase II. This may facilitate the formation of a drug-induced cleavage complex.

Type II topoisomerases are a class of ubiquitous enzymes essential for maintaining genome organization in the dense nuclear milieu of eukaryotic cells (1, 2). Topoisomerase II (topo II)¹ plays an important role in replication, transcription, recombination, and segregation of chromosome pairs during cell division (3, 4). It is also involved in maintaining the structural organization of the mitotic chromosomal scaffold (5–7). The enzyme assists in these functions by altering the topological properties of DNA, which it catalyzes by creating transient double strand breaks, transporting an intact segment of DNA through the gap and finally religating the cleaved strands (8–11). Topo II is present as a major enzyme in the nuclei of rapidly dividing cells, especially in neoplastic conditions (2). During the past decade, numerous studies have indicated that selective poisoning of this enzyme leads to effective inhibition of neoplastic cell proliferation (8, 12, 13). A number of clinically prescribed anticancer drugs are now known to be topo II poisons. Topo II poisons are broadly classified into two types: (1) cleavable complex-forming compounds (DNA intercalating, e.g., m-AMSA, nonintercalating e.g., Etoposide) and (2) Noncleavable complex-forming compounds (e.g. ICRF-193) (8, 14, 15). Cleavage complex-forming compounds are of particular interest because they shift the enzyme's cleavage/religation cycle toward DNA cleavage and form a stable drug-mediated enzyme-cleaved DNA complex (16).

Metal complexes gained immense importance with the discovery of cisplatin as an anticancer agent in 1969. Since then, numerous complexes of metals of the main group, early transition, and late transition series of the periodic table have been vigorously tested for anticancer activity. However, very few of them have qualified for phase I and phase II clinical trials (18). Among the metal atoms used in anticancer metal complexes, ruthenium is most unique. It is a rare noble metal unknown to living systems and has a strong complex-forming ability with numerous ligands. In vitro and in vivo studies reveal that most ruthenium complexes bind covalently to DNA via the N-7 atom of purines and cause cytotoxicity by possibly inhibiting cellular DNA synthesis (18, 19). Ruthenium complexes have a stronger affinity for cancer tissues than normal tissues. This is because ruthenium binds readily to transferrin molecules in plasma and is transported to the tumor tissues. Here, the ruthenium-transferrin complex is internalized into tumor cells through transferrin receptors which are abundantly expressed on the surface of tumor cells (20). Ruthenium(III) complexes have been hypothesized to function as pro-drugs which are reduced to the more reactive ruthenium(II). In this state, they coordinate with biological macromolecules and induce toxicity (20).

In the present study, we have examined and compared two structurally different ruthenium(II) complexes for their antiproliferation activity and molecular action on topo II to determine their efficacy as anticancer agents and their molecular mechanism of action.

MATERIALS AND METHODS

Materials. Topo II was purified from rat liver following the procedure of Galand et al. (21). The enzyme concentration was determined using Bradford colorimetric assay (22). The negatively supercoiled pBR322 plasmid DNA was

* This work was supported by the Council of Scientific and Industrial Research, India, Sanction number: 37 (0854)/93/EMR-II.

† To whom correspondence should be addressed. Tel: 91-40-3010 500, ext. 4571. Fax: 91-40-3010 120 or 145. E-mail: akksl@uohyd.ernet.in.

¹ Abbreviations: RuBen, $[\text{RuCl}_2(\text{C}_6\text{H}_6)(\text{dmsO})]$; RuSal, ruthenium salicylaldehyde; m-AMSA, 4-[9-acridinylamino]-N-[methanesulfonyl]-m-aminidine; topo II, topoisomerase II; SDS, sodium dodecyl sulfate; DTT, dithiothreitol.

purified as described by Wang and Rossman (23). Anti-topoisomerase II antibody was from Topogen Inc.; RPMI-1640 medium, m-AMSA, and calf thymus DNA were from Sigma Chemical Co.; protein A agarose, fetal calf serum, and antibiotics were from Gibco-BRL; PEI (polyethyleneimine) Cellulose-F TLC sheets were from Merck; Proteinase K and ATP were from Boehringer-Mannheim; and $\gamma^{32}\text{P}$ -ATP and ^3H -labeled thymidine were supplied by BRIT, India. Other chemicals and biochemicals were of analytical grade.

Synthesis of the Ruthenium Complexes. (a) *RuBen* ($[\text{RuCl}_2(\text{C}_6\text{H}_6)(\text{dmsO})]$). This was synthesized following the procedure of Zelonka and Baird (24). Freshly synthesized 1,3-hexadiene (6 mL) was added to $\text{RuCl}_3 \cdot 3\text{H}_2\text{O}$ (1.7 g) in 100 mL of 90% aqueous ethanol. The solution was heated at 45 °C for 3 h to form a red precipitate, which was washed in ethanol and dried in vacuo to give the dimeric complex $[\text{RuCl}_2(\text{C}_6\text{H}_6)]_2$. To this dimer, DMSO was added to form the monomeric DMSO complex $[\text{RuCl}_2(\text{C}_6\text{H}_6)(\text{dmsO})]$ and vacuum-dried. *NMR spectra in d_6 -DMSO*: < 4.07 ppm (identical with that reported by Zelonka and Baird).

(b) *RuSal* (Trans bis salicylaldoximate ruthenium (II)). This was synthesized following a slightly modified procedure of Lumme et al. (25) for the synthesis of copper salicylaldoxime. Dry salicylaldoxime (10 mmol) was dissolved in dry methanol, and anhydrous ruthenium trichloride (5 mmol) was added in the presence of dry nitrogen gas. The constituents were refluxed at 70 °C for about 1 h until a green solution formed. This was vacuum-dried and crystallized to form dark green complex of ruthenium (II) salicylaldoxime. *IR spectra*: Band at 1608 cm^{-1} confirms the formation of a coordination bond between imine nitrogen and metal atom; band at 1493 cm^{-1} confirms the metal-oxygen bond.

Molecular Modeling and Energy Minimization. The atomic coordinates for RuBen and RuSal were generated employing standard geometry and then refined using the energy minimization procedure of Vinter et al. (35) at all atom levels on Desktop Molecular Modeler software (distributed by Oxford University Press) (Figure 1). In RuBen, the organo-metallic bond between the ruthenium atom and benzene was simulated on the basis of the information obtained from literature (36).

Solubilization of Complexes. The ruthenium complexes and m-AMSA were dissolved in DMSO and diluted with deionized water prior to use in the biological assays. All of the DNA and topo II controls in our experiments contained 1% DMSO, which was equivalent to the maximum amount of DMSO present in the drug-containing assay samples. DMSO at this concentration had no effect on the assays.

In vitro Antiproliferation Activity. ^3H -Thymidine incorporation assays were performed to analyze the effect of the ruthenium complexes on the proliferative response of cancer cells. Crit-2 (nonhodkins human lymphoma) cells were grown in RPMI-1640 medium supplemented with 10% fetal calf serum. Cells ($0.2 \times 10^6/200\mu\text{L}$) were distributed in triplicates in a 96-well microtiter tissue culture plate. The cultures were incubated for 16 h at 37 °C in a CO_2 incubator maintaining 5% CO_2 atmosphere. The two ruthenium drugs were added to the cells at increasing concentrations (negative controls contained an equivalent amount of DMSO present in the drug-treated samples). After further incubation for 8 h, the cultures were pulsed with $0.5\text{ }\mu\text{Ci}$ of ^3H -thymidine.

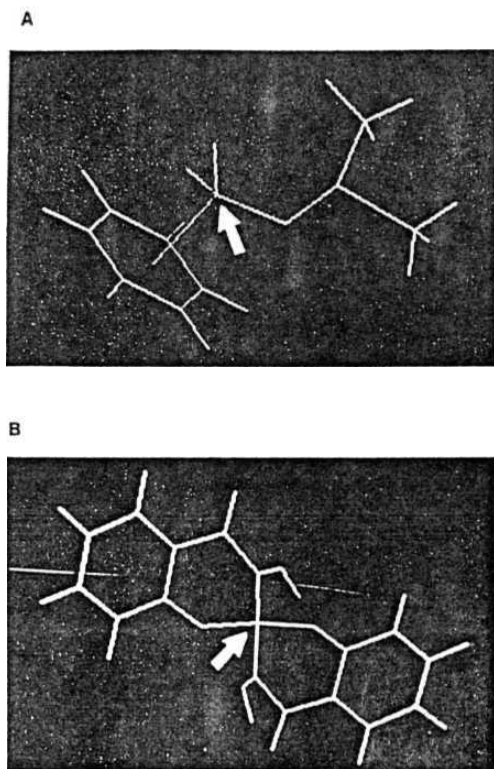


FIGURE 1: Three-dimensional chemical structures of RuBen (A) and RuSal (B) represented as line diagrams. The arrows point toward the ruthenium atom.

Incubation was continued for 4 h to allow thymidine incorporation by cells. The cells were harvested on glass microfiber strips using a Skatron automated cell harvester. Radioactivity was measured in a Wallac liquid scintillation counter.

Relaxation Assay. This assay was performed following the procedure of Osheroff et al. (26). The reaction mixture (20 μL) contained relaxation buffer (50 mM Tris-HCl (pH 8.0), 120 mM KCl, 0.5 mM EDTA, 0.5 mM DTT, 10 mM MgCl_2 , 30 $\mu\text{g/mL}$ BSA, 1 mM ATP), 0.6 μg of negatively supercoiled pBR322 plasmid DNA (>95% supercoiled), and increasing concentrations of the ruthenium drugs. The reaction was initiated by adding 2 units (~8 nM) of topo II, and the mixture was incubated at 30 °C for 15 min. The reaction was stopped by the addition of 2 μL of 10% SDS. To this, 3 μL of loading dye (0.5% bromo-phenol blue, 0.5% xylene cyanol, 60% sucrose, 10 mM Tris-HCl, pH 8.0) was added, and the products were separated on a 1% agarose gel in 0.5 x TAE buffer (20 mM Tris-acetate, 0.5 mM EDTA) at 50 V for 12 h. The gel was stained with ethidium bromide, visualized in a Photodyne UV transilluminator, and photographed.

Cleavage Assay. The formation of the cleavage complex was assayed following the procedure of Zechiedrich et al. (27). The 20 μL reaction mixture contained relaxation buffer (minus ATP), 0.6 μg of pBR322 supercoiled DNA (70%

supercoiled, 30% nicked circular), and increasing concentrations of drugs. The reaction was initiated by adding 10 units (40 nM) of topoisomerase II and incubated at 30 °C for 15 min. The reaction was stopped with 2 μ L of 10% SDS. The DNA-bound protein was degraded by incubating the reaction mixture with 2 μ L of 1 mg/mL Proteinase K at 45 °C for 1 h. The products were separated on 1% agarose gel for 8 h at 50 V in 1 x TAE buffer (40 mM tris-acetate, 1 mM EDTA), stained, and photographed. The linear DNA band was quantified as a percentage of total DNA in a UVP gel documentation system.

ATPase Activity Assay. This assay is a modified procedure of Osheroff et al. (26). The 20 μ L reaction mixture contained relaxation buffer (the 1 mM ATP component contained 0.025 μ Ci γ - 32 P-ATP), 0.6 μ g of pBR322 DNA, and increasing concentrations of drugs. The reaction was initiated with 2 units of topo II and incubated at 30 °C for 15 min. The reaction was stopped with 2 μ L of 250 mM EDTA. The reaction mixture was spotted on PEI cellulose-F TLC sheets, and the sheets were subjected to thin-layer chromatography in 1 M lithium chloride solution. In these conditions, γ - 32 P_i migrates first followed by ADP and γ - 32 P-ATP. After resolution, the bands were monitored under reflected UV light at 366 nm in a Photodyne transilluminator. The illuminated bands of ATP, ADP, and P_i (inorganic phosphate) were cut and counted for 32 P in a liquid scintillation counter.

Assay for Ruthenium and DNA in Cleavage Complex. The cleavage assay was performed in the presence of 500 μ M ruthenium drugs. After the reaction, topo II in the cleavage complex and in free form was immunoprecipitated with 0.04 units of anti-topo II antibody. The antibody-antigen complex was trapped in 20 μ L of protein A agarose. This was washed twice with 1 x relaxation buffer at 1000 rpm to remove unbound reactants. Topo II in the immunoprecipitate was released by adding 20 μ L of 1% trichloroacetic acid (TCA). To this was added 10 μ L of 1 N HCl, and the samples were boiled in steam to dryness. Samples were then analyzed for parts per million of ruthenium metal by atomic absorption spectroscopy in an ECIL-AAS4129 atomic absorption spectrometer. The same assay was performed with 3 H-thymidine-labeled DNA. After TCA treatment, the samples were spotted on filter paper strips and the radioactivity was measured.

Drug-DNA Interaction. (a) Thermal Denaturation. Calf thymus DNA (sodium salt) was dissolved in 1 mM sodium phosphate buffer containing 1 mM sodium chloride. The DNA concentration was adjusted to give an absorbance of 1.0 in 1 mL at 260 nm. The ruthenium drugs were added to DNA at concentrations which gave drug-to-nucleotide ratios of 1:20, 1:10, 1:5, 1:2, and 1:1, respectively. The samples were incubated in 1 mL quartz cuvettes for 2 min to allow drug-DNA binding. A Hitachi 150-20 spectrophotometer was set to give a 1 °C rise in temperature per minute with a KPC-6 thermo-programmer and SPR-7 temperature controller. The increase in absorbance at 260 nm was recorded from 40 to 90 °C. T_m was determined from the denaturation curves. The curve width of the individual melting curves was calculated by the procedure of Kelly et al. (28). Curve width is the temperature range between which 10–90% of the absorbance increase occurs. The data were plotted and analyzed.

(b) 1D Gel Mobility Assay. pBR322 DNA (0.6 μ g) was incubated in increasing concentrations of the drugs in

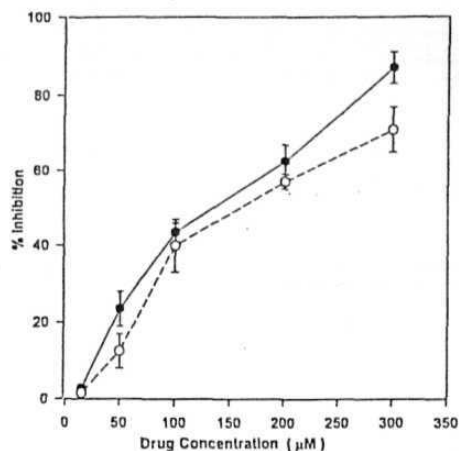


FIGURE 2: Crit-2 cells were incubated with increasing concentrations of RuBen and RuSal. 3 H thymidine incorporation during the last 4 h of incubation was measured as described in methods. Values are presented as means of three independent experiments. Data are graphically expressed as a percentage increase in inhibition versus concentration of RuBen (○) and RuSal (●) in micromolar units.

relaxation buffer at 30 °C for 15 min. Loading dye was added and the products were run on a 0.8% agarose gel for 15 h at 25 V in 0.5x TAE buffer.

2D Gel Mobility Assay. pBR322 DNA (0.6 μ g) was incubated as above in 500 μ M ruthenium drugs. The samples were loaded on 0.7% agarose gels and run in the first dimension at 30 V for 10 h in 0.5 x TAE buffer. The second dimension was run in similar conditions in the presence of Chloroquine diphosphate (0.5 μ g/mL). The gels were documented as in relaxation assay.

(c) CD Spectra. Circular dichroic spectra of pBR322 DNA in the presence of RuBen or RuSal was measured in a Jasco J-715 spectropolarimeter. The DNA and drug concentrations corresponded to 0.6 μ g of DNA and 500 μ M drug as used in the topoisomerase II catalytic assays. m-AMSA (corresponding to 100 μ M concentration in the catalytic assays) was included as a positive control. The spectra were measured in a quartz cuvette of 1 cm path length. Data were represented graphically as molar ellipticity [$[\theta] \times 10^{-3}$ deg cm²/dmol) versus wavelength (nanometers).

RESULTS

Antiproliferation Activity. Antiproliferation activity of the ruthenium drugs was measured by thymidine incorporation assays. The results show a dose-dependent inhibition of the Crit-2 cell proliferation. At the highest concentration of 300 μ M, RuBen inhibited 87% of cell growth, while RuSal showed a marginally less inhibition of 71% (Figure 2).

Relaxation Assay. DNA relaxation activity of topo II in the presence of increasing concentrations of RuBen was significantly inhibited, and at 500 μ M, the drug could completely inhibit topo II-catalyzed relaxation of supercoiled pBR322 DNA (Figure 3A). RuSal could partially inhibit the relaxation activity with no significant increase in inhibition up to 500 μ M (Figure 3B).

Cleavage Assay. The ability of RuBen and RuSal to cause drug-induced stabilization of DNA-topo II complex was

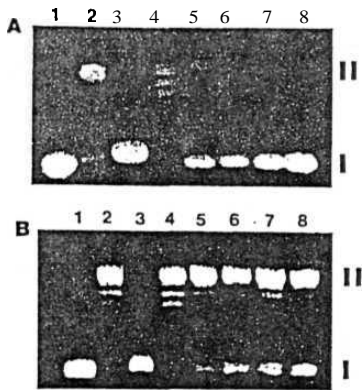


FIGURE 3: Effect of RuBen(A) and RuSal (B) on topo II-catalyzed DNA relaxation activity. Supercoiled pBR322 DNA (lane 1) was incubated with lopo II in the absence (lane 2) or presence of 100 μ M m-AMSA (lane 3) and 100, 200, 300, 400, and 500 μ M ruthenium drugs (lanes 4-8). The positions of supercoiled (form I) and nicked circular (form 2) DNA are indicated by I and II.

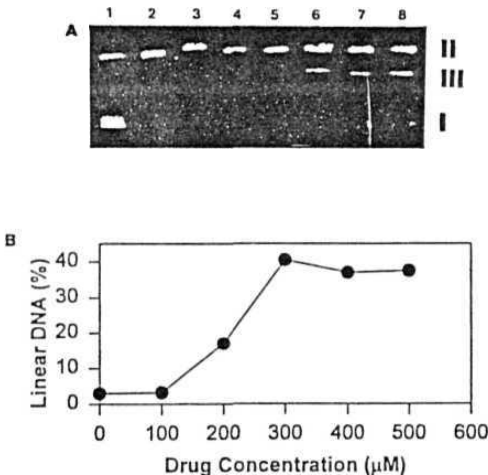


FIGURE 4: (A) The cleavage reaction was conducted by incubating pBR322 DNA (lane 1) with topo II (lane 2) in the presence of 100 μ M m-AMSA (lane 3) and 100, 200, 300, 400, and 500 μ M of RuBen (lanes 4-8). The positions of supercoiled, nicked circular, and linear (form 3) DNA are indicated by I, II, and III. (B) The plot shows the percentage of linear DNA formed with increasing concentrations of RuBen.

studied. The formation of the enzyme–drug–DNA complex can be seen by the appearance of linear DNA which results from DNA strand breaks caused by dissociation of the topo II homodimer by SDS (29). RuBen stabilized the enzyme–DNA cleavable complex at a concentration of 200 μ M, as seen by the appearance of linear DNA equivalent to 17% of the total DNA. At 300 μ M, the linear DNA increased to 40.5% and then decreased to ~37% for the higher drug concentrations (Figure 4). RuSal did not induce cleavage complex formation even at 500 μ M concentration (data not shown).

Presence of Ruthenium and DNA in Cleavage Complex. The immunoprecipitation assay was performed to get a direct

Table 1: Presence of Ruthenium and DNA in Cleavage Complex"

	RuBen (%)	RuSal (%)
(A) Ruthenium		
DNA + Topo II	0	0
Drug	<2	<2
DNA + Drug	<2	<2
Topo II + Drug	8 \pm 0.82	<2
DNA + Topo II + Drug	46 \pm 3.05	9 \pm 1.63
(B) DNA		
DNA + Topo II	3.0 \pm 0.5	3.0 \pm 0.5
DNA	0.5	0.5
DNA + Drug	1.0 \pm 0.5	1 \pm 0.7
Topo II + Drug	0	0
DNA + Topo II + Drug	21 \pm 1.63	3 \pm 0.82

" Data are presented as a percentage mean of three independent experiments conducted in triplicates, and standard deviations are given against each value.

evidence for the involvement of RuBen in the drug-induced cleavage complex. The cleavage assay was conducted in the presence of 500 μ M concentrations of the ruthenium drugs. After incubation, the enzyme in the cleavage complex as well as the free enzyme was immunoprecipitated with anti-lopo II antibody. The antigen–antibody complex was then trapped in protein A agarose. Samples were washed to remove unbound components, and the bound enzyme was released from protein A agarose by 1% TCA and analyzed for the presence of ruthenium by atomic absorption spectroscopy. The results presented in Table 1A show that, while 46% of 500 μ M RuBen is present in the cleavage complex, only 9% of RuSal is present in the same. Concentrations less than 2% (20 ng) could not be determined accurately by the instrument used and they were expressed as such.

The presence of DNA in the cleavage complex was confirmed by repeating the same assay in the presence of 3 H-labeled DNA. After TCA treatment, the products were spotted on filter paper strips and the radioactivity was measured. The results presented in Table 1B show that 21% of 0.6 μ g of DNA is present in the RuBen-induced cleavage complex, as compared to 3% in the RuSal-induced complex. All of the controls correlate well with the atomic absorption spectral data. These results confirm the bidirectional interaction of RuBen with DNA and lopo II. RuSal shows such a bidirectional binding to a very small extent.

Effect on ATPase Activity of Topoisomerase II. This assay was performed to examine the effect of ruthenium drugs on the ATPase activity of topo II. The relaxation assay was performed with increasing concentrations of the drugs in the presence of γ - 32 PATP and products were resolved on PEI Cellulose-F TLC sheets. The results show that RuBen inhibited ATP hydrolysis in a dose-dependent manner. At 500 μ M concentration, it could inhibit 50% of the total ATPase activity while RuSal could inhibit 13.5% of the ATPase activity (Figure 5).

Drug–DNA Interactions. The melting of calfthymus DNA was studied in the presence of increasing concentrations of drugs. The melting temperature curves showed a gradual increase in T_m with increasing concentrations of RuBen and RuSal (Figure 6A,B). Figure 6D shows that RuBen and RuSal exert a minor increase in the curve width of melting curves plotted against drug/nucleotide (D/N). The DNA intercalator m-AMSA, caused a major change in this curve width. In Figure 6C, D/N was plotted against the T_m values,

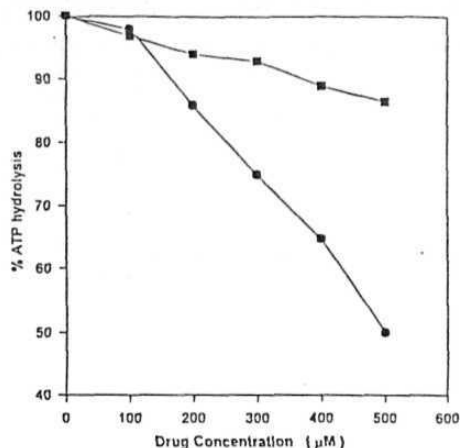


FIGURE 5: Inhibition of ATPase activity of topo II by RuBen (●) and RuSal (■). ATP hydrolysis in the control sample was taken as 100% and values in the presence of increasing concentration of the drugs are presented as mean of three experiments; data is plotted as the percentage of ATP hydrolyzed versus the concentration of drug in micromolar units.

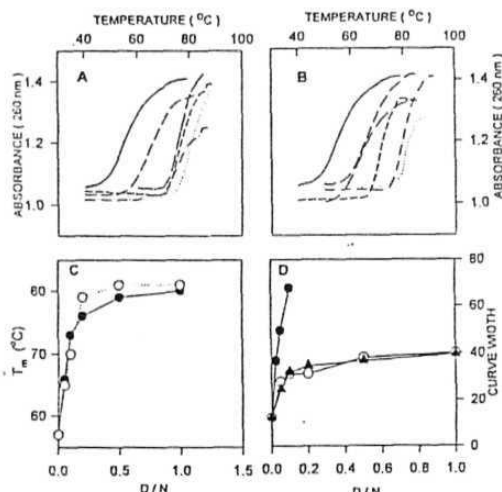


FIGURE 6: Drug-DNA-binding studies. (A) RuBen increases the T_m of calf thymus DNA from 57 °C for UNA control (—) to 66, 73, 76, 78, and 80 °C for DNA nucleotide-to-drug ratios of 20:1 (—), 10:1 (---), 5:1 (- - -), 2:1 (- · -), and 1:1 (···), respectively. (B) RuSal shows an increase in T_m of 65, 70, 79, 81, and 81 °C for the same drug to DNA ratios. (C) D/N (drug/nucleotide) plotted against the increase in T_m by RuBen (●) and RuSal (○) to determine specific drug binding to DNA nucleotides from the slopes of the curves. (D) D/N plotted against curve width shows a characteristic increase in curve width by m-AMSA (●) and a very small increase by RuBen (A) and RuSal (○).

and the slopes of the curves were calculated to determine the stoichiometric binding of drug to DNA. RuBen showed a DNA-binding stoichiometry of 4 nucleotides and a weak binding stoichiometry of 7 nucleotides per drug molecule, while RuSal showed a stoichiometry of 4 nucleotides per molecule.

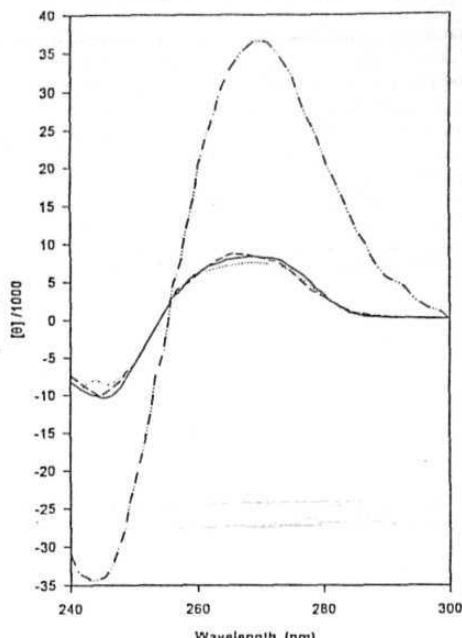


FIGURE 7: The circular dichroism spectra of pBR322 DNA (—) in the presence of RuBen (···) and RuSal (---) shows a small change in the molar ellipticity of DNA while m-AMSA (- · -) shows a very prominent change at a concentration less than 5 times that of the ruthenium drugs.

In the ID and 2D gel mobility assays, it was observed that neither RuBen nor RuSal could change the DNA mobility or DNA conformation (data not shown).

Circular dichro spectra of pBR322 DNA showed that RuBen and RuSal marginally affected the DNA conformation at the concentration which showed maximum inhibition of topo II relaxation activity. In comparison, m-AMSA caused a significant change in the DNA conformation (Figure 7).

DISCUSSION

Though DNA is implicated as the main target for anticancer ruthenium compounds (30), our data suggests that, apart from DNA, topo II poisoning may also be an effective mode of antineoplastic activity for one of the ruthenium compounds tested. We have compared an organometallic complex (RuBen) with a coordinated covalent complex (RuSal) for antiproliferative action and poisoning of topo II. Both compounds show good antiproliferative action; that of RuBen is 16% more than RuSal at the highest concentration tested. The relaxation, cleavage, and immunoprecipitation assays clearly show that RuBen can poison topo II through a drug-induced cleavage complex formation. RuSal, on the other hand, causes partial inhibition of relaxation activity and does not form a cleavage complex.

Analysis of the curve width of DNA melting curves is a useful way to distinguish between intercalative and external binding (28). Intercalators substantially increase the width of melting curves, while external binders have a smaller effect on this parameter. m-AMSA shows a curve width

typical of a DNA intercalator while RuBen and RuSal seem to fit into the group of compounds which bind externally to DNA like 2,2'-bipyridyl and feripyridyl complexes of ruthenium (28). Since both RuBen and RuSal show similar DNA binding, the metal atom in them may directly interact with DNA. The ruthenium atom could bind outside the DNA helix through ionic interactions or by covalent bonding with the nucleotide bases. In RuBen, an intercalative mode of DNA binding is not possible because the benzene ring forms an organometallic bond with the ruthenium atom, which prevents π -orbital stacking interaction of the aromatic ring with DNA bases. In RuSal, since there are no organometallic bonds, the π -stacking orbitals in the salicylaldehyde ligand are not affected. But the compound does not intercalate to DNA. Whether the orientation of the salicylaldehyde ligands or the presence of the metal atom absolve an intercalative mode of binding, it cannot be explained at present. RuBen and RuSal bind similarly to DNA but show different sensitivity for topo II poisoning. This points toward ligand involvement in topo II poisoning.

The strong DNA-binding ability of the ruthenium drugs prompted us to examine if these compounds produce conformational changes in DNA which could block enzyme activity. The gel mobility assays showed no change in DNA migration or conformation. This was confirmed by CD spectral analysis, which showed an inconsequential change in DNA conformation in the presence of RuBen and RuSal. Farther, the ATPase assay shows that RuBen inhibits the DNA-stimulated ATPase activity of topo II. This is possible only if the drug induces the formation of the enzyme-drug-DNA cleavage complex or if the drug directly interacts with the enzyme at the ATPase domain. The first possibility seems true, which is supported by the cleavage reaction.

On the basis of molecular modeling analyses and superimposition of drug structures, a putative structure was proposed for topo II cleavage complex-forming drugs, which shows that these drugs have three distinct domains in them; the first is a planar ring system, the second is a pendant ring, and the third is a pendant moiety of heterogeneous structure (37). Though studies have shown that this structure is not an absolute requirement for topo II poisoning (17), most poisons do have large planar aromatic domains for DNA binding and substituents for enzyme interaction. It is interesting that a simple and small molecule like RuBen, with only one aromatic ring, could poison topo II by cleavage complex formation. RuBen has an octahedral geometry (37) which may facilitate the spatial orientation of its ligands to form interactions with enzyme. This interaction by the benzene, chloride, and DMSO ligands of RuBen may play an important role in poisoning the enzyme.

Prior to enzyme action, RuBen bound to DNA may interact with the catalytic domain of one or both monomers of topo II through the chloride atoms and the methyl groups of DMSO. The benzene ring may fit into some pocket in the enzyme and sterically hinder the conformation changes in the enzyme required for DNA religation. Whatever the mode of action, RuBen traps the cleaved DNA and topo II in the cleavage complex and prevents DNA religation action of the enzyme. The cleavage assay confirms that RuBen indeed shifts the enzyme's cleavage/religation equilibrium toward DNA cleavage.

In RuSal, the planar salicylaldehyde ligands are attached to the metal atom and oriented with an angle of $\sim 40^\circ$ to each other along the planar axis. This orientation may block enzyme action to a certain extent when the DNA-bound drug approaches the catalytic domain of topo II but may not allow a strong interaction with the enzyme. Even if an interaction does take place, the coordinated metal-ligand bonds may not provide a strong interface for cleavage complex formation. This could explain RuSal's ability to partially inhibit the relaxation activity of topo II, but not induce cleavage complex formation.

DNA intercalating topo II poisons intercalate to DNA through π -stacking interactions of their planar rings with DNA bases. The side chains of these drugs are involved in enzyme interaction. Such an interaction is important in facilitating the formation of the drug-enzyme-DNA ternary complex. Though RuBen binds externally to DNA nucleotides, it may still form a similar ternary complex in which the metal atom binds to DNA and ligands on the metal atom interact with topo II.

These findings allow us to propose a probable mode of topo II poisoning by RuBen. The metal atom interacts covalently or noncovalently with DNA nucleotides and the ligands form cross-links with the enzyme and prevent the DNA religation step, leading to the formation of a stable drug-induced cleavage complex, which is the hallmark of most topo II poisons. Such topo II poisons increase the steady state concentration of cleavage complexes which harbor topo II-associated double strand breaks. These become permanent double strand fractures following traversal by replication complexes. The accumulation of such DNA breaks in cells ultimately results in cell death by apoptosis or necrosis (26, 27). RuBen could be categorized as a topo II poison which is a cleavable complex-forming, DNA-binding but nonintercalating agent.

Similar DNA interaction and effective antiproliferative action of RuBen and RuSal indicate that inhibition of the lymphoma cell proliferation may in part be due to a topo II-independent mechanism, probably at the DNA level. In RuSal, the salicylaldehyde ligand may also cause antiproliferative action. As an analogue of pyridoxal, salicylaldehyde is known to inhibit pyridoxal kinase activity and hinder transamination and decarboxylation processes leading to inhibition of protein synthesis, causing appreciable cytotoxicity (28). The marginally higher antiproliferation activity of RuBen in comparison with RuSal may possibly be due to topo II poisoning.

Studies indicate that antitumor activity of DNA-binding drugs in most cases depends on their capacity to interfere with catalytic activity of topo II (25, 27). We have limited the scope of this work to topo II targeting, though ruthenium drugs, being DNA-binding agents, may interact with other DNA-binding proteins (e.g., DNA polymerases) and other biomolecules in the cell leading to toxicity generally associated with chemotherapy.

A better understanding of the molecular action of RuBen and the inherent advantage of ruthenium compounds (in lieu of their selectivity for entering tumor tissues) can aid in designing novel ruthenium compounds which poison topo II with higher potency and show substantial anticancer action, while mitigating the toxic side effects to a certain degree.

We have demonstrated, for the first time, topo II poisoning by a ruthenium compound and its relative antiproliferation activity.

ACKNOWLEDGMENT

We acknowledge CSIR for financial support. YNVG and DJ thank UCC and CSIR respectively for providing fellowships. We are thankful to Dr. M. Ramanadham for extending his laboratory facilities and for a thorough reading of the manuscript. We thank Ms. C. Subbalaxmi and the Director of CCMB for helping with the CD spectral analysis. We thank Dr. Robin Mukhopadhyaya of Cancer Research Institute, Mumbai, for the gift of Crit-2 cell line. We thank Bioinformatics center, I.I.Sc., Bangalore for providing the facility for molecular modeling.

SUPPORTING INFORMATION AVAILABLE

Characterization of ruthenium complexes and 1D and 2D gel mobility assays. This material is available free of charge via the Internet at <http://pubs.acs.org>.

REFERENCES

- Wang, J. C. (1985) *Annu. Rev. Biochem.* 54, 665-697.
- Watt, P. M., and Hickson, I. D. (1994) *Biochem. J.* 303, 681-695.
- Holm, C. (1994) *Cell* 77, 955-957.
- Hirano, T., and Mitchison, T. J. (1993) *J. Cell Biol.* 120, 601-612.
- Earnshaw, W. C., and Heck, M. M. S. (1985) *J. Cell Biol.* 100, 1716-1725.
- Earnshaw, W. C., Halligan, B., Cooke, C. A., Heck, M. M. S., and Liu, L. F. (1985) *J. Cell Biol.* 100, 1706-1715.
- Gasser, S., and Laemmli, U. K. (1986) *EMBO J.* 5, 511-518.
- Liu, L. F. (1989) *Annu. Rev. Biochem.* 58, 351-375.
- Osheroff, N., Zechiedrich, E. L., and Gale, K. C. (1991) *BioEssays* 13, 269-275.
- Roca, J. (1995) *Trends Biochem. Sci.* 20, 156-160.
- Berger, J. M., Gamblin, S. J., Harrison, S. C., and Wang, J. C. (1996) *Nature* 381, 225-232.
- Zwellig, L. A. (1985) *Cancer Metastasis Rev.* 4, 263-276.
- Glisson, B. S., and Ross, W. E. (1987) *Pharmacol. Ther.* 32, 89-106.
- Pommier, Y., Capranico, G., Orr, A., and Kohn, K. W. (1991) *Nucleic Acids Res.* 19, 5973-5980.
- Roca, J., and Wang, J. C. (1994) *Cell* 77, 609-616.
- Robinson, M. J., and Osheroff, N. (1990) *Biochemistry* 29, 2511-2515.
- Capranico, G., Palumbo, M., Tinelli, S., Mabilia, M., Pozzan, A., and Zunino, F. (1994) *J. Mol. Biol.* 235, 1218-1230.
- Kopf-Maier, P. (1994) *Eur. J. Clin. Pharmacol.* 147, 1-16.
- Haiduc, I., and Silvestru, C. *Organometallics in Cancer Chemotherapy*. Vol II, CRC Press LLC, FL.
- Sava, G., Pacor, S., Bregant, F., and Ceschia, V. (1991) *Anticancer Res.* 11, 1103-1105.
- Galande, S., and Muniyappa, K. (1996) *Biochim. Biophys. Acta* 1308, 58-66.
- Bradford, M. M. (1976) *Anal. Biochem.* 72, 248-254.
- Wang, Z., and Rossman, T. G. (1994) *BioTechniques* 16, 460-463.
- Zelonka, R. A., and Baird, M. C. (1972) *Can. J. Chem.* 50, 3063-3072.
- Lumme, P., and Elo, H. (1984) *Inorg. Chim. Acta* 92, 241-251.
- Osheroff, N., Shelton, E. R., and Brutlag, D. L. (1983) *J. Biol. Chem.* 258, 9536-9543.
- Zechiedrich, E. L., Christiansen, K., Anni, H., Ole, W., and Osheroff, N. (1989) *Biochemistry* 28, 6229-6236.
- Kelly, J. M., Tossi, A. B., McConnell, D. J., and OhUigin, C. (1985) *Nucleic Acids Res.* 13, 6017-6033.
- Rene, B., Fosse, P., Khalifa, T., Alain, J., and Bailly, C. (1996) *Mol. Pharmacol.* 49, 343-350.
- Clarke, M. J. (1989) *Prog. Clin. Biochem. Med.* 10, 25-39.
- MacDonald, T. T., Lehnert, E. K., Loper, J. T., Chow, K. C., and Ross, W. E. (1991) *DNA Topoisomerases in Cancer* (Pomesil, M.; and Kohli, K. W., Eds.) pp 199-214, Oxford University Press, New York.
- Froelich-Ammon, S. J., and Osheroff, N. (1995) *J. Biol. Chem.* 270, 21429-21432.
- Chen, A. Y., and Liu, L. F. (1994) *Annu. Rev. Pharmacol. Toxicol.* 34, 191-218.
- Martin, D. W., Jr. (1983) *Harper's Review of Biochemistry*, p 97. Lange Medical Pub., Los Altos, CA.
- Vinter, J. G., Davis, A., and Saunders, M. R. (1987) *J. Commit.-Aided Mot. Des.* 1, 31-51.
- Elschenbroich, Ch., and Salzer, A. (1992) *Organometallics - A Concise Introduction*, p 252-385, VCH Publications.
- Bennet, M. A., and Smith, A. K. (1974) *J. Chem. Soc., Dalton Trans.* 233-241.

B1981990S